Results from the search for neutrinoless double beta decay of ^{130}Te with CUORE-0

Lucia Canonica
INFN-LNGS

for the CUORE Collaboration

LNGS, April 9th 2015

The CUORE collaboration

UNIVERSITA' DEGLI STUDI DI MILANO BICOCCA

UNIVERSITA DEGLI STUDI DI CASSINO E DEL LAZIO MERIDIONALE – SOL PER NOCTEM

SINAP

LUX ET VERITAS

INFN Istituto Nazionale di Fisica Nucleare

CAL POLY SAN LUIS OBISPO

Lawrence Livermore National Laboratory

ALMA MATER STUDIORUM UNIVERSITA DI BOLOGNA A.D. 1088

Massachusetts Institute of Technology

UCLA

SAPIENZA UNIVERSITÀ DI ROMA

CSNSM

BERKELEY LAB

UNIVERSITY OF SOUTH CAROLINA

THE UNIVERSITY OF CALIFORNIA 1868

UNIVERSITAS STUDII PADUANI

CUORE

The CUORE Collaborators

C. Alduino [1], K. Alfonso [2], D. R. Artusa [1,3], F. T. Avignone III [1], O. Azzolini [4], M. Balata [3], T. I. Banks [5,6], G. Bari [7], J.W. Beeman [8], F. Bellini [9,10], A. Bersani [11], M. Biassoni [12,13], C. Brofferio [12,13], C. Bucci [3], A. Camacho [4], A. Caminata [11], L. Canonica [3], X. G. Cao [14], S. Capelli [12,13], L. Cappelli [3,15], L. Carbone [13], L. Cardani [9,10], N. Casali [3,16], L. Cassina [12,13], D. Chiesa [12,13], N. Chott [1], M. Clemenza [12,13], S. Copello [17], C. Cosmelli [9,10], O. Cremonesi [13], R. J. Creswick [1], J. S. Cushman [18], I. Dafinei [10], A. Dally [19], S. Dell'Oro [3,20], M. M. Deninno [7], S. Di Domizio [17,11], M. L. Di Vacri [3,16], A. Drobizhev [5,6], L. Ejzak [19], D. Q. Fang [14], M. Faverzani [12,13], G. Fernandes [17,11], E. Ferri [12,13], F. Ferroni [9,10], E. Fiorini [13,12], M. A. Franceschi [21], S. J. Freedman [6,5], B. K. Fujikawa [6], A. Giachero [12,13], L. Gironi [12,13], A. Giuliani [22], P. Gorla [3], C. Gotti [12,13], T. D. Gutierrez [23], E. E. Haller [8,24], K. Han [18,6], E. Hansen [25,2], K. M. Heeger [18], R. Hennings-Yeomans [5,6], K. P. Hickerson [2], H. Z. Huang [2], R. Kadel [26], G. Keppel [4], Yu. G. Kolomensky [5,26], C. Ligi [21], K. E. Lim [18], X. Liu [2], Y. G. Ma [14], M. Maino [12,13], M. Martinez [27], R. H. Maruyama [18], Y. Mei [6], N. Moggi [28,7], S. Morganti [10], T. Napolitano [21], S. Nisi [3], C. Nones [29], E. B. Norman [30,31], A. Nucciotti [12,13], T. O'Donnell [5,6], F. Orio [10], D. Orlandi [3], J. L. Ouellet [5,6], C. E. Pagliarone [3,15], M. Pallavicini [17,11], V. Palmieri [4], L. Pattavina [3], M. Pavan [12,13], G. Pessina [13], V. Pettinacci [10], G. Piperno [9,10], C. Pira [4], S. Pirro [3], S. Pozzi [12,13], E. Previtali [13], C. Rosenfeld [1], C. Rusconi [13], E. Sala [12,13], S. Sangiorgio [30], D. Santone [3,16], N. D. Scielzo [30], M. Sisti [12,13], A. R. Smith [6], L. Taffarello [32], M. Tenconi [22], F. Terranova [12,13], C. Tomei [10], S. Trentalange [2], G. Ventura [33,34], M. Vignati [10], S. L. Wagaarachchi [5,6], B. S. Wang [30,31], H. W. Wang [14], L. Wielgus [19], J. Wilson [1], L. A. Winslow [25], T. Wise [18,19], A. Woodcraft [35], L. Zanotti [12,13], C. Zarra [3], G. Q. Zhang [14], B. X. Zhu [2], S. Zucchelli [36,7]

- 19 groups
  - 8 Italy
  - 6 USA
  - 5 associate groups

- 157 collaborators
  - 120 researchers/authors
    - Italy: 71
    - USA: 38
    - Associated Institutions: 11

[1] Department of Physics and Astronomy, University of South Carolina, Columbia, SC 29208 - USA
[2] Department of Physics and Astronomy, University of California, Los Angeles, CA 90095 - USA
[3] INFN - Laboratori Nazionali del Gran Sasso, Assergi (L'Aquila) I-67010 - Italy
[4] INFN - Laboratori Nazionali di Legnaro, Legnaro (Padova) I-35020 - Italy
[5] Department of Physics, University of California, Berkeley, CA 94720 - USA
[6] Nuclear Science Division, Lawrence Berkeley National Laboratory, Berkeley, CA 94720 - USA
[7] INFN - Sezione di Bologna, Bologna I-40127 - Italy
[8] Materials Science Division, Lawrence Berkeley National Laboratory, Berkeley, CA 94720 - USA
[9] Dipartimento di Fisica, Sapienza Università di Roma, Roma I-00185 - Italy
[10] INFN - Sezione di Roma, Roma I-00185 - Italy
[11] INFN - Sezione di Genova, Genova I-16146 - Italy
[12] Dipartimento di Fisica, Università di Milano-Bicocca, Milano I-20126 - Italy
[13] INFN - Sezione di Milano Bicocca, Milano I-20126 - Italy
[14] Shanghai Institute of Applied Physics, Chinese Academy of Sciences, Shanghai 201800 - China
[15] Dipartimento di Ingegneria Civile e Meccanica, Università degli Studi di Cassino e del Lazio Meridionale, Cassino I-03043 - Italy
[16] Dipartimento di Scienze Fisiche e Chimiche, Università dell'Aquila, L'Aquila I-67100 - Italy
[17] Dipartimento di Fisica, Università di Genova, Genova I-16146 - Italy
[18] Department of Physics, Yale University, New Haven, CT 06520 - USA
[19] Department of Physics, University of Wisconsin, Madison, WI 53706 - USA
[20] INFN - Gran Sasso Science Institute, L'Aquila I-67100 - Italy
[21] INFN - Laboratori Nazionali di Frascati, Frascati (Roma) I-00044 - Italy
[22] Centre de Spectrométrie Nucléaire et de Spectrométrie de Masse, 91405 Orsay Campus - France
[23] Physics Department, California Polytechnic State University, San Luis Obispo, CA 93407 - USA
[24] Department of Materials Science and Engineering, University of California, Berkeley, CA 94720 - USA
[25] Massachusetts Institute of Technology, Cambridge, MA 02139 - USA
[26] Physics Division, Lawrence Berkeley National Laboratory, Berkeley, CA 94720 - USA
[27] Laboratorio de Fisica Nuclear y Astroparticulas, Universidad de Zaragoza, Zaragoza 50009 - Spain
[28] Dipartimento di Scienze per la Qualità della Vita, Alma Mater Studiorum - Università di Bologna, Bologna I-47921 - Italy
[29] Service de Physique des Particules, CEA / Saclay, 91191 Gif-sur-Yvette - France
[30] Lawrence Livermore National Laboratory, Livermore, CA 94550 - USA
[31] Department of Nuclear Engineering, University of California, Berkeley, CA 94720 - USA
[32] INFN - Sezione di Padova, Padova I-35131 - Italy
[33] Dipartimento di Fisica, Università di Firenze, Firenze I-50125 - Italy
[34] INFN - Sezione di Firenze, Firenze I-50125 - Italy
[35] SUPA, Institute for Astronomy, University of Edinburgh, Blackford Hill, Edinburgh EH9 3HJ - UK
[36] Dipartimento di Fisica e Astronomia, Alma Mater Studiorum - Università di Bologna, Bologna I-40127 - Italy

Outline

- Double beta decay physics
- Thermal detectors
- History of ^{130}Te double beta decay experiments
- CUORE-0 results
    - Detector performance
    - Neutrinoless double beta decay analysis

Outline

- **Double beta decay physics**
- Thermal detectors
- History of ^{130}Te double beta decay experiments
- CUORE-0 results
    - Detector performance
    - Neutrinoless double beta decay analysis

Double beta decay

Double beta decay is a very rare nuclear decay (N,Z) → (N-2, Z+2)

$$(A,Z) \rightarrow (A,Z+2) + 2e^- + 2\overline{\nu}$$

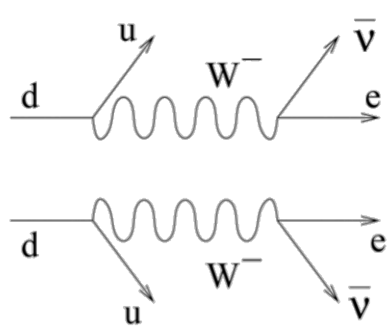

2νDBD:
- 2nd order process allowed in SM
- observed in several nuclei
- $\tau \sim 10^{19\text{-}21}$ y

$$(A,Z) \rightarrow (A,Z+2) + 2e^-$$

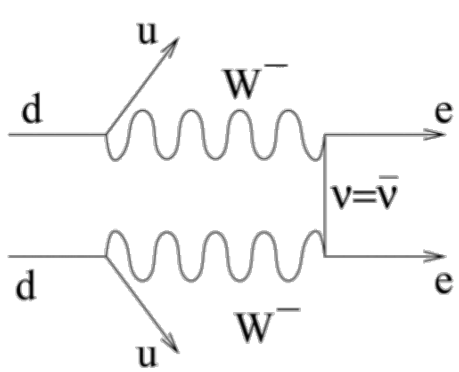

0νDBD:
- Lepton number violation ΔL=2
- exists for Majorana neutrinos $\nu = \bar{\nu}$
- $\tau > 10^{24\text{-}25}$ y

ββ summed e^- energy spectrum

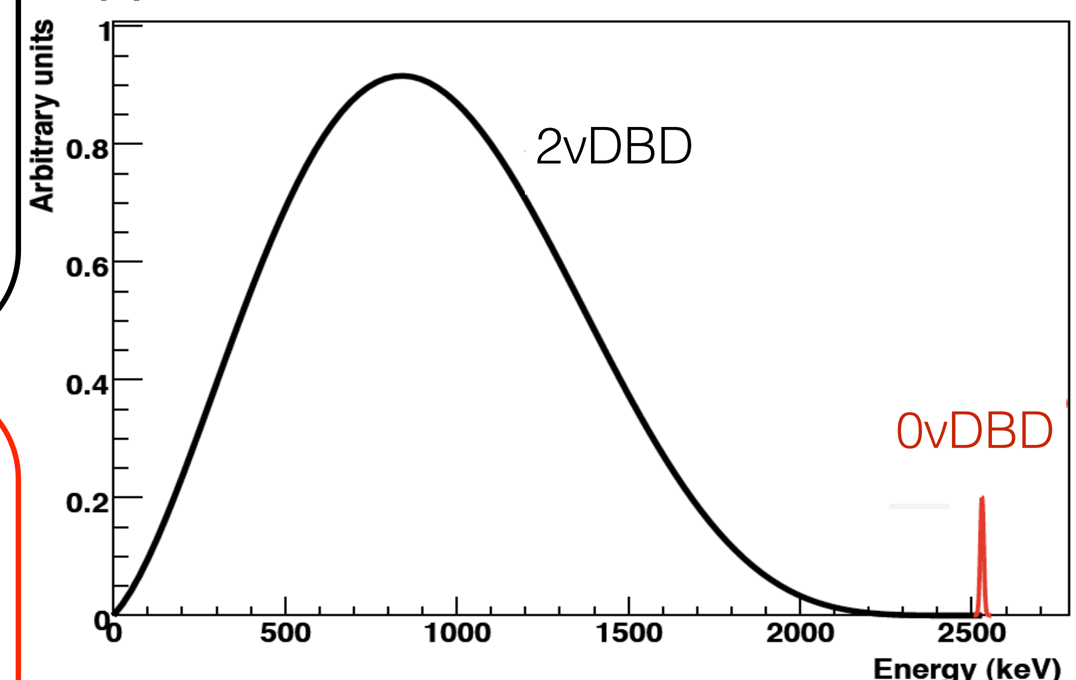

0vDBD and neutrino mass

$$T^{0\nu}_{1/2} = \frac{m_e^2}{G_{0\nu} \cdot M^2_{nucl} \cdot m^2_{\beta\beta}}$$

$G_{0\nu}$: Phase space integral ~Q^5
M_{nucl}: Nuclear Matrix Elements
$m_{\beta\beta}$: effective neutrino mass

$$m_{\beta\beta} = |\sum_i m_{\nu_i} U^2_{ei}|$$

- The observation of 0vDBD:
  - proof of the Majorana nature of neutrino
  - constraints on neutrino mass hierarchy and scale

F. Vissani, JHEP 06 022 (1999)

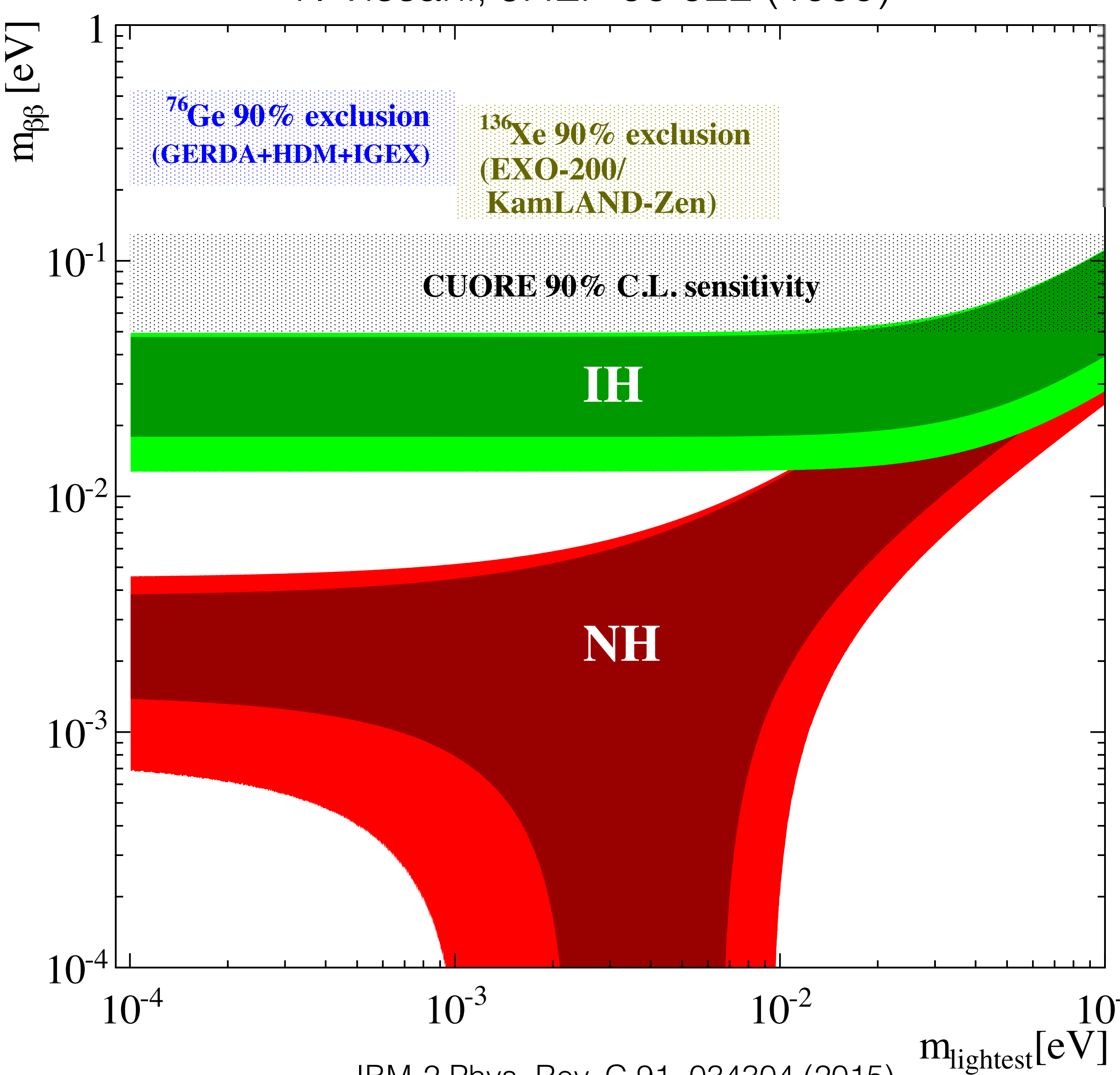

IBM-2 Phys. Rev. C 91, 034304 (2015)
QRPA-TU Phys. Rev. C 87, 045501 (2013)
pnQRPA Phys. Rev. C 91, 024613 (2015)
ISM Nucl. Phys. A 818, 139 (2009)
EDF Phys. Rev. Lett. 105, 252503 (2010)

Sensitivity

- Half-life corresponding to the minimum number of detectable signal events above background at a given C.L.

$$T_{0\nu} \propto i.a. \sqrt{\frac{M \cdot T}{\Delta E \cdot b}}$$

high natural i.a. among 0vDBD candidates or enrichment

i.a: isotopic abundance

M: detector mass

Large mass array

T: measuring time

Stable over long time (~y)

ΔE: energy resolution

Extremely good energy resolution

b: background

- Deep underground location
- Material selection

Outline

- Double beta decay physics
- **Thermal detectors**
- History of ^{130}Te double beta decay experiments
- CUORE-0 results
  - Detector performance
  - Neutrinoless double beta decay analysis

Thermal detectors

The working principle is very simple:

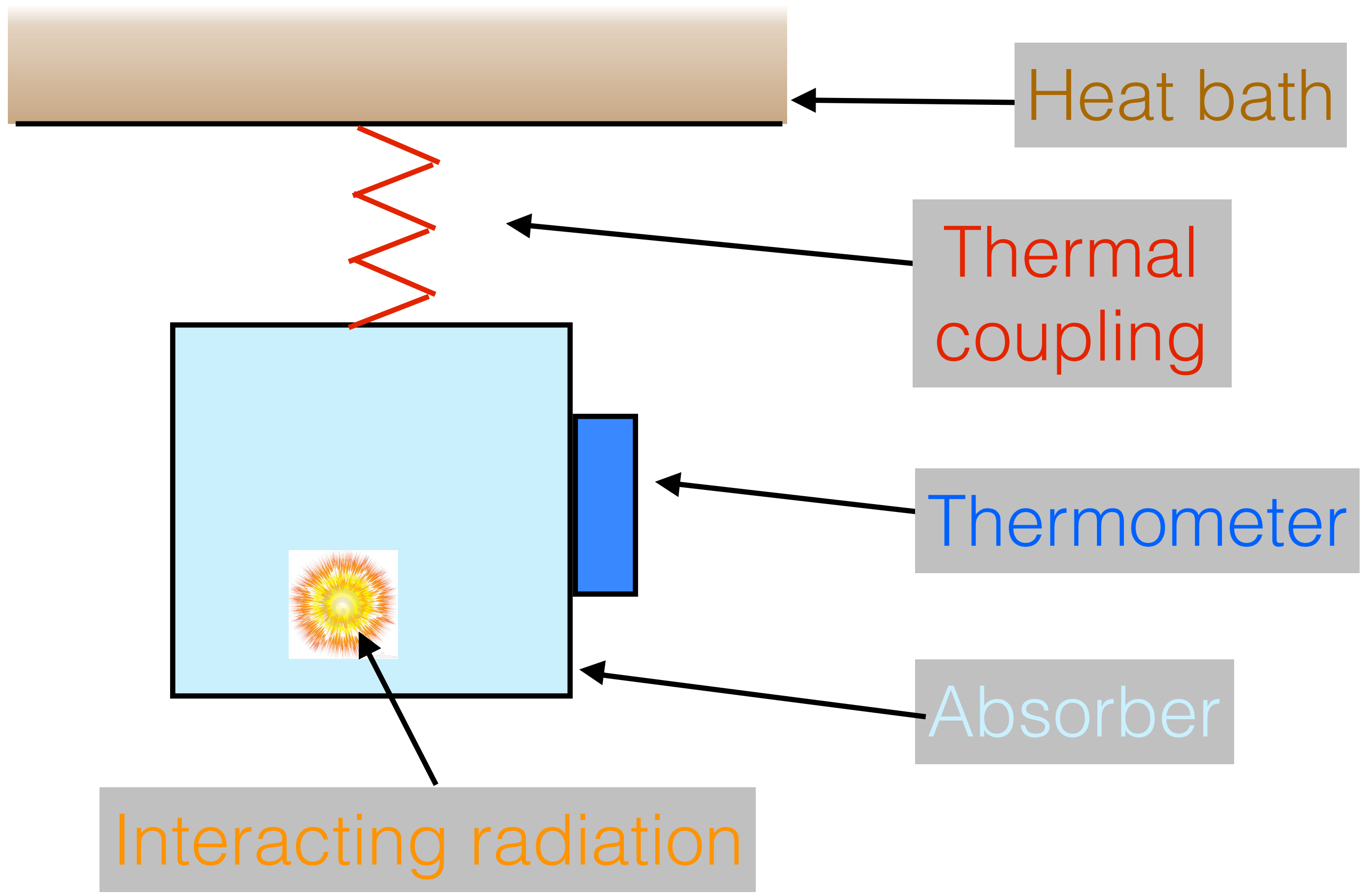

The energy deposited by a particle interaction in the absorber is converted to a measurable temperature variation.

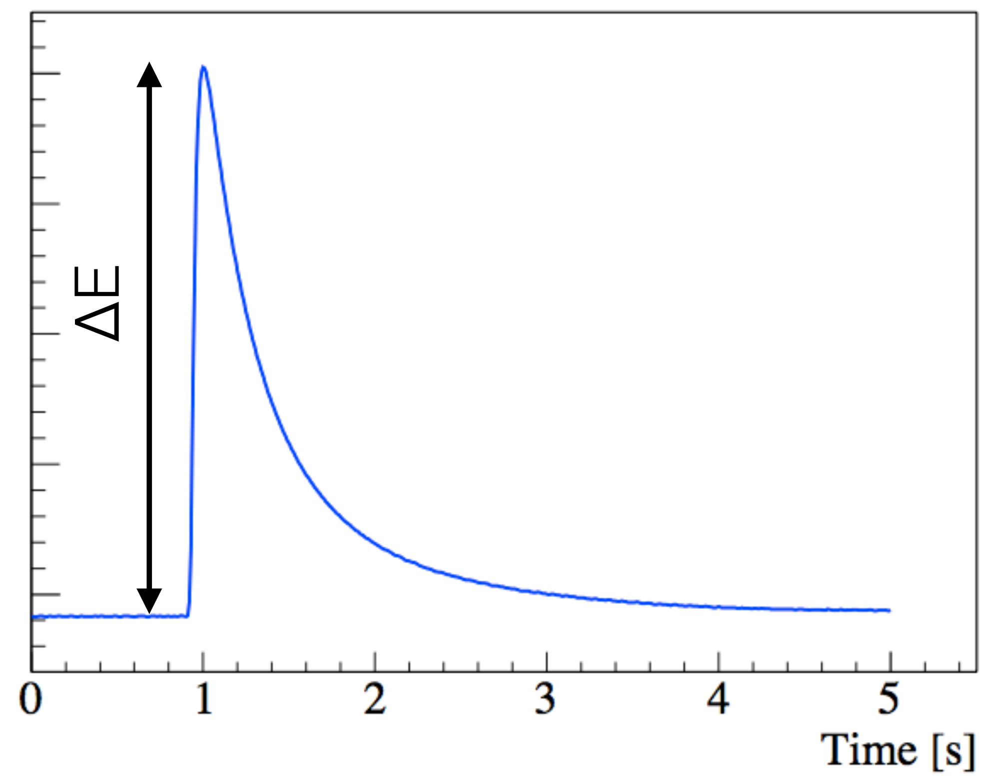

- wide choice of detector materials
- source embedded in the detector
- excellent energy resolution

^{130}Te for 0vDBD

- Q-value (2528 keV)
- Highest natural isotopic abundance (~34%)
- Favourable calculation of NME

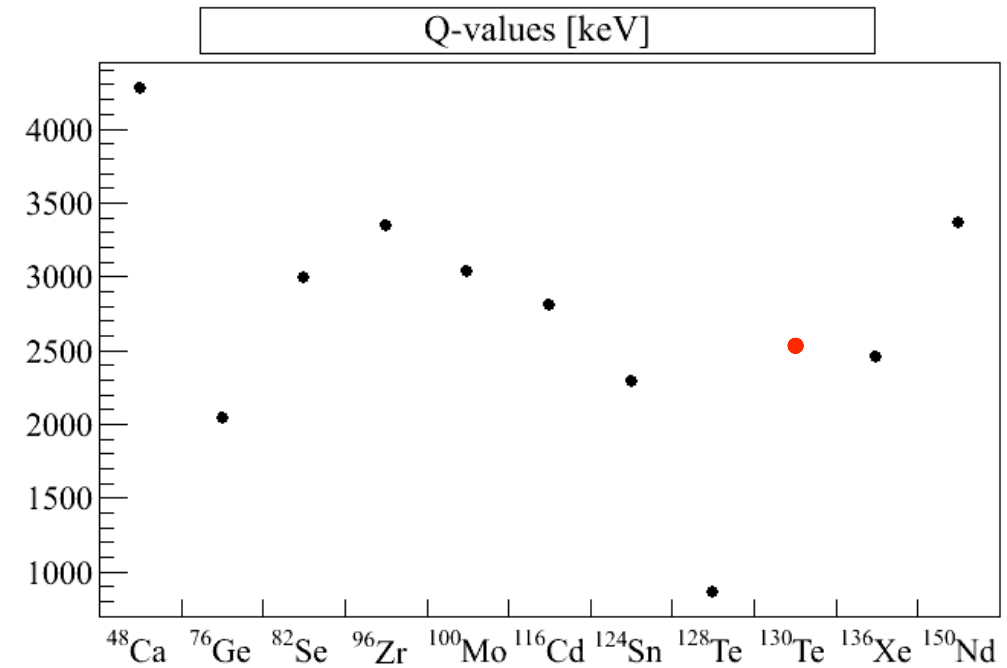

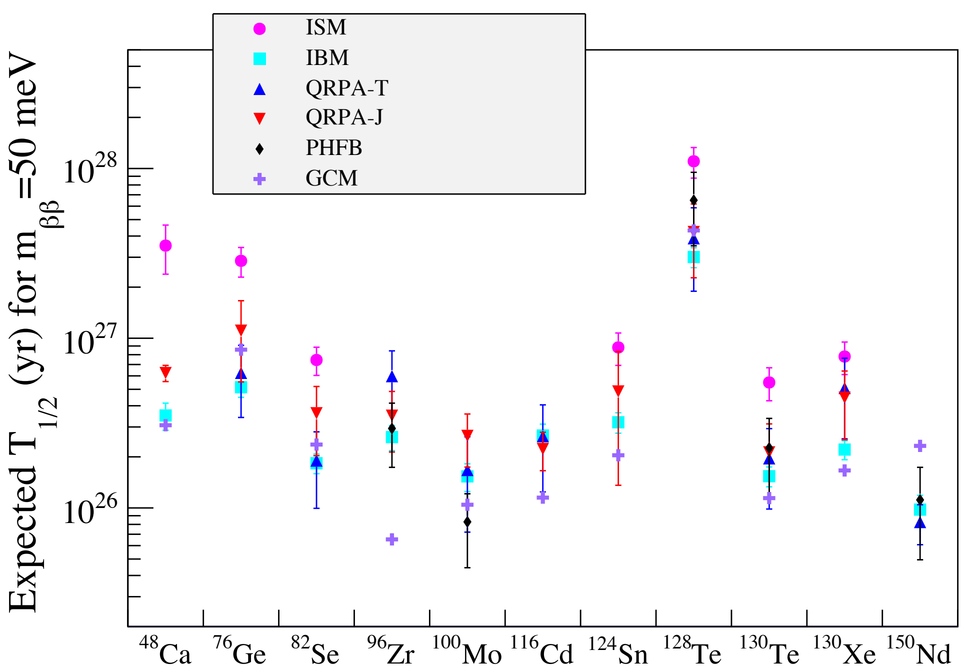

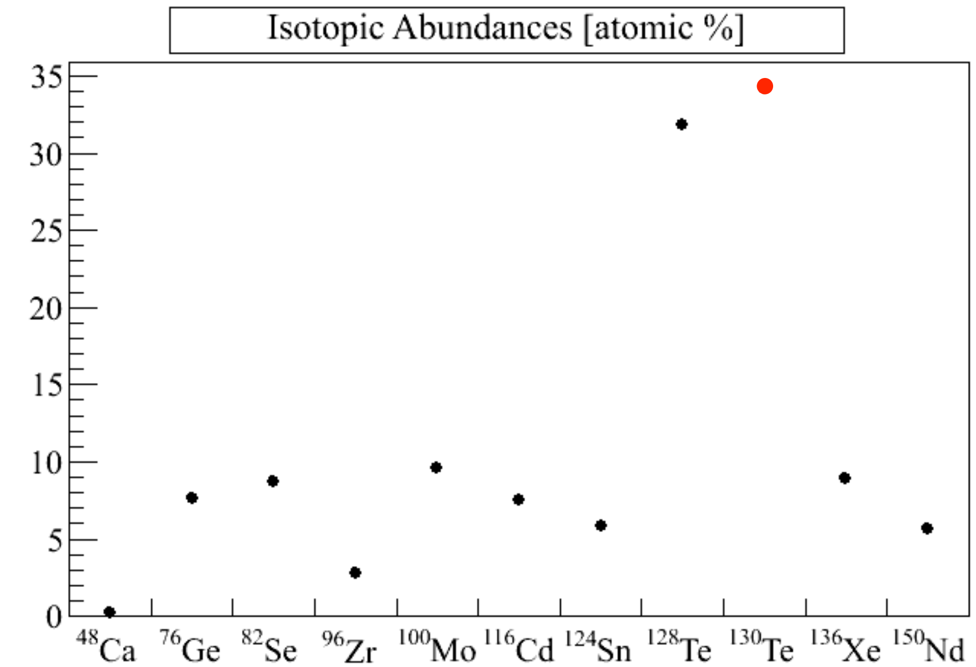

The CUORE bolometers

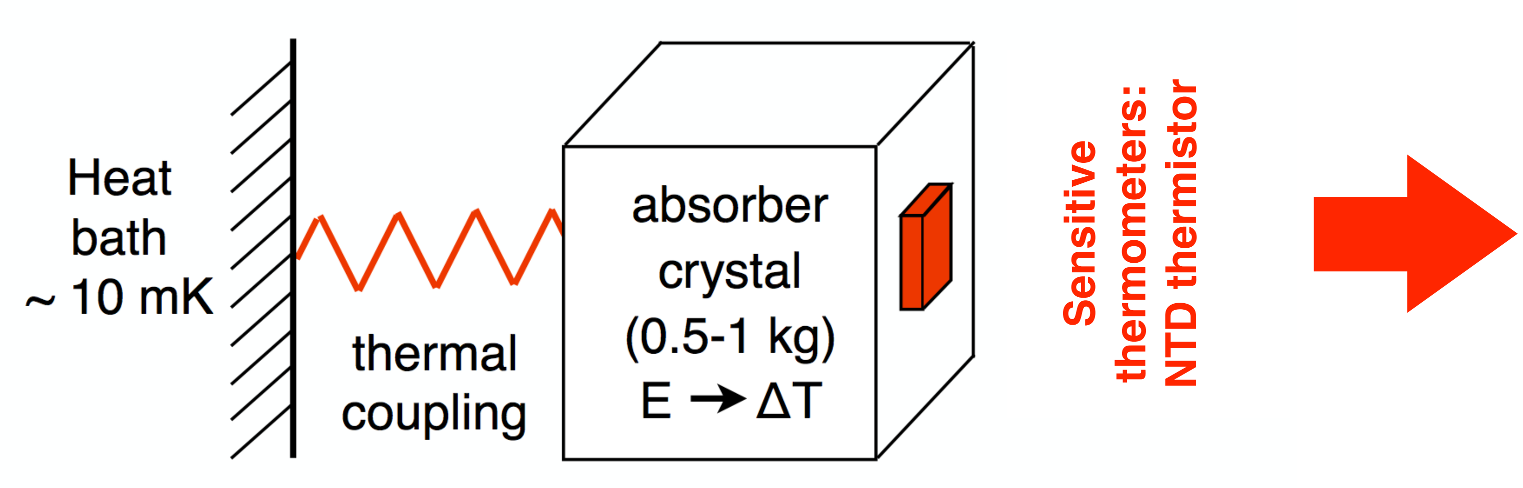

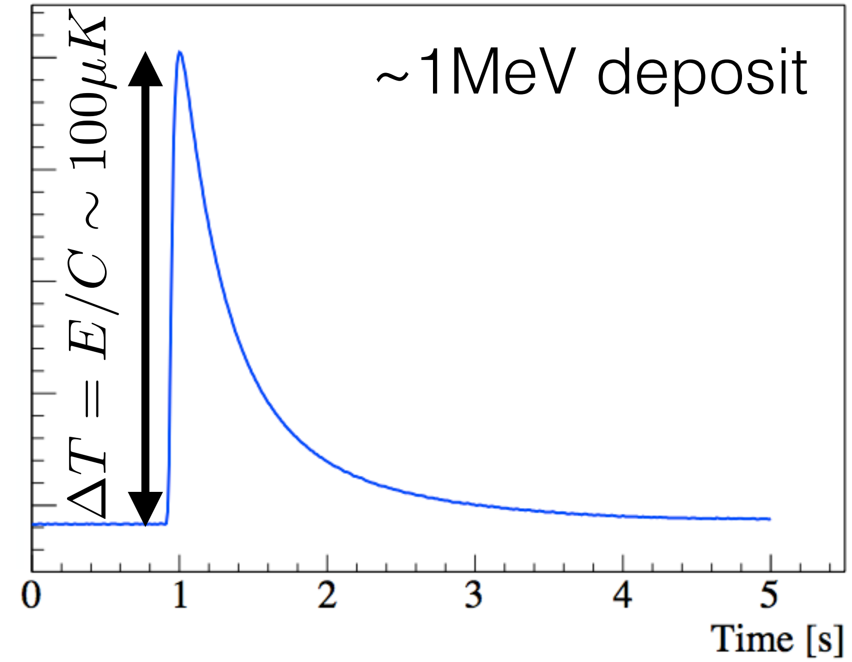

- $^{nat}TeO_2$ crystals
- NTD-Ge thermistor (R ~ 50MΩ)

$$R(T) = R_0 \exp\left[\frac{T_0}{T}\right]^{1/2}$$

- Resolution @0vDBD energy (2528 keV):

  ΔE= 5-7 keV FWHM

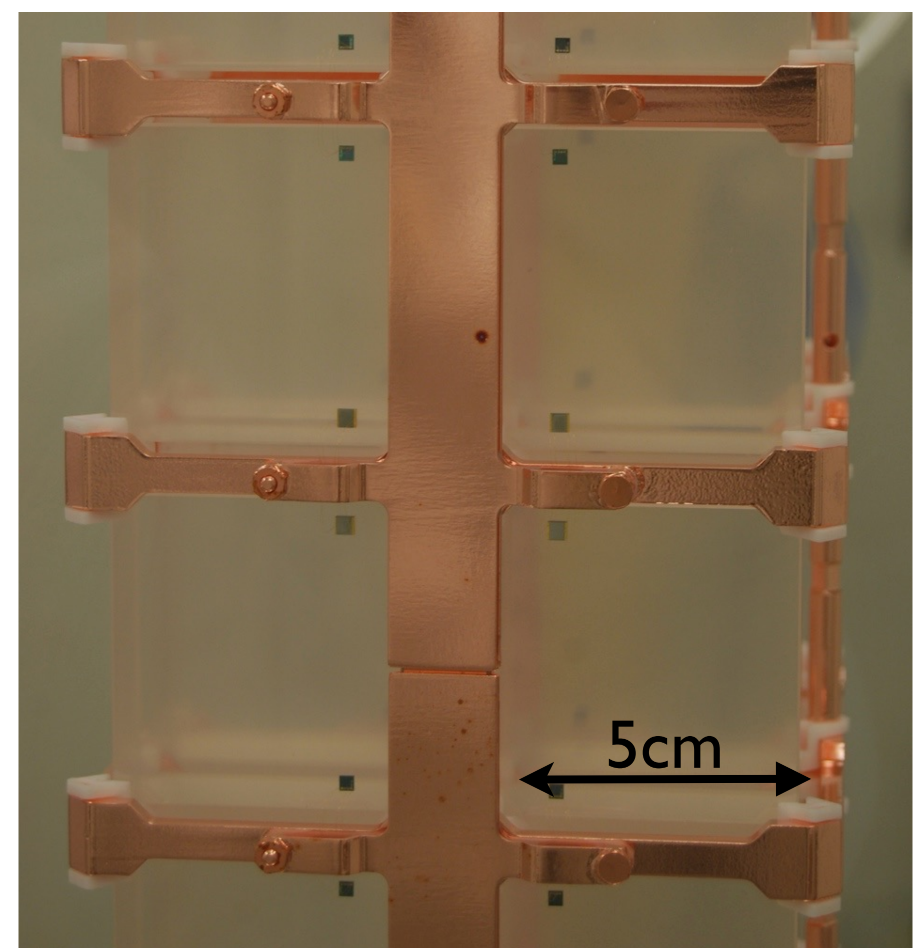

Outline

- Double beta decay physics
- Thermal detectors
- **History of ^{130}Te double beta decay experiments**
- CUORE-0 results
  - Detector performance
  - Neutrinoless double beta decay analysis

TeO_2 arrays

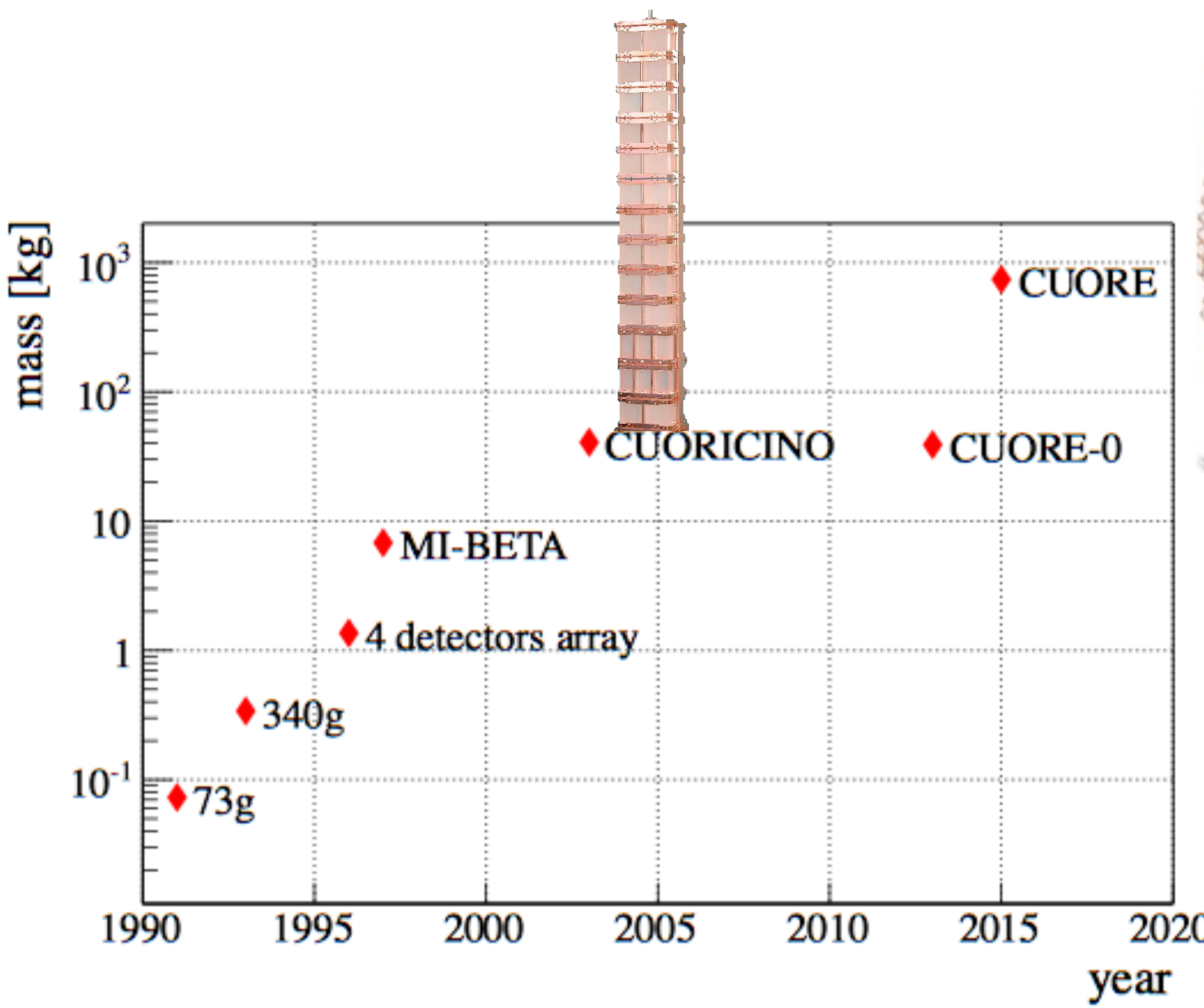
mass [kg]
10^3
10^2
10
1
10^{-1}
CUORE
CUORICINO
CUORE-0
MI-BETA
4 detectors array
340g
73g
1990
1995
2000
2005
2010
2015
2020
year

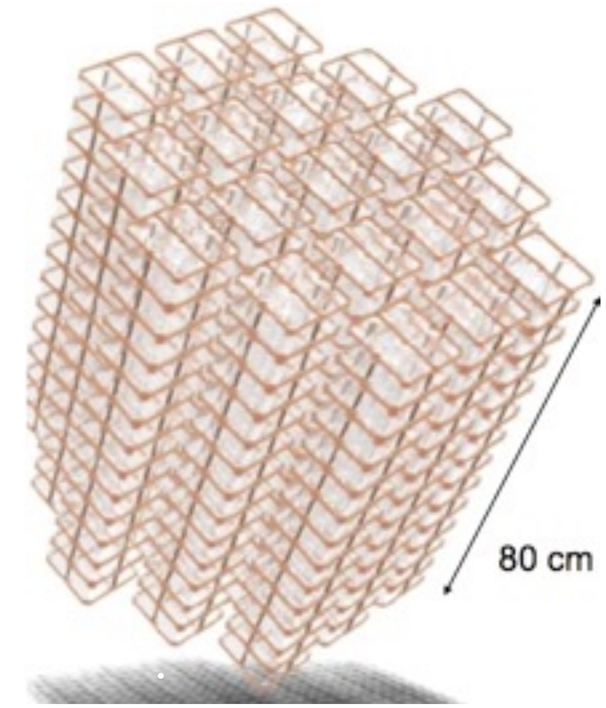
80 cm

The CUORE challenge

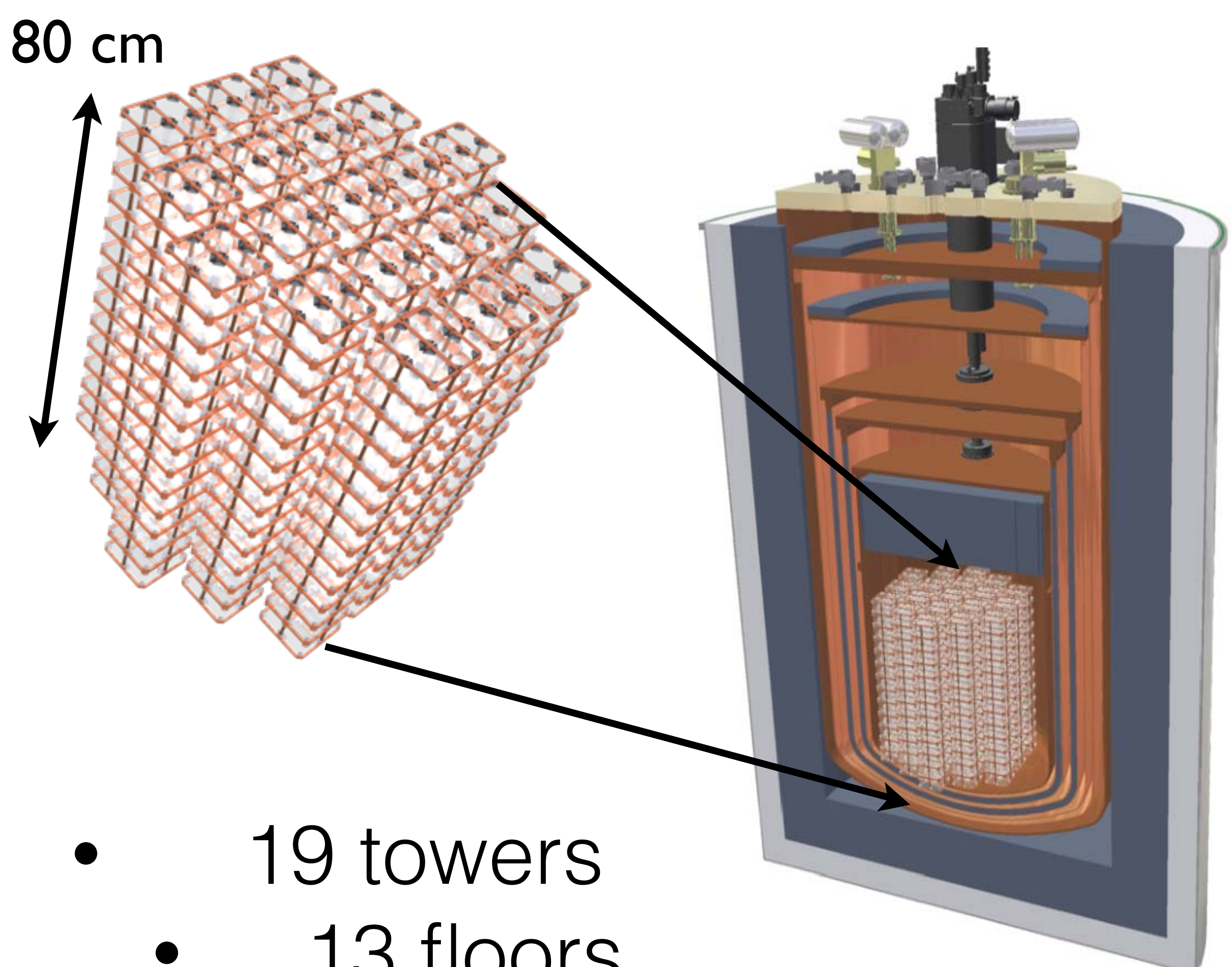

- 19 towers
  - 13 floors
    - 4 crystals

- Tightly packed array of 988 bolometric detectors.
- M = 741 kg of TeO_2 (206 kg ^{130}Te) to look for 0vDBD of ^{130}Te.

Energy resolution @ ROI: 5 keV

Background goal: 0.01 c/(keV kg y)

Sensitivity 90% C.L. (5 y):

$T_{1/2}$ = 9.5 x 10^{25} y

$m_{\beta\beta}$ = 50-130 meV

IBM-2 Phys. Rev. C 91, 034304 (2015)
QRPA-TU Phys. Rev. C 87, 045501 (2013)
pnQRPA Phys. Rev. C 91, 024613 (2015)
ISM Nucl. Phys. A 818, 139 (2009)
EDF Phys. Rev. Lett. 105, 252503 (2010)

Cuoricino

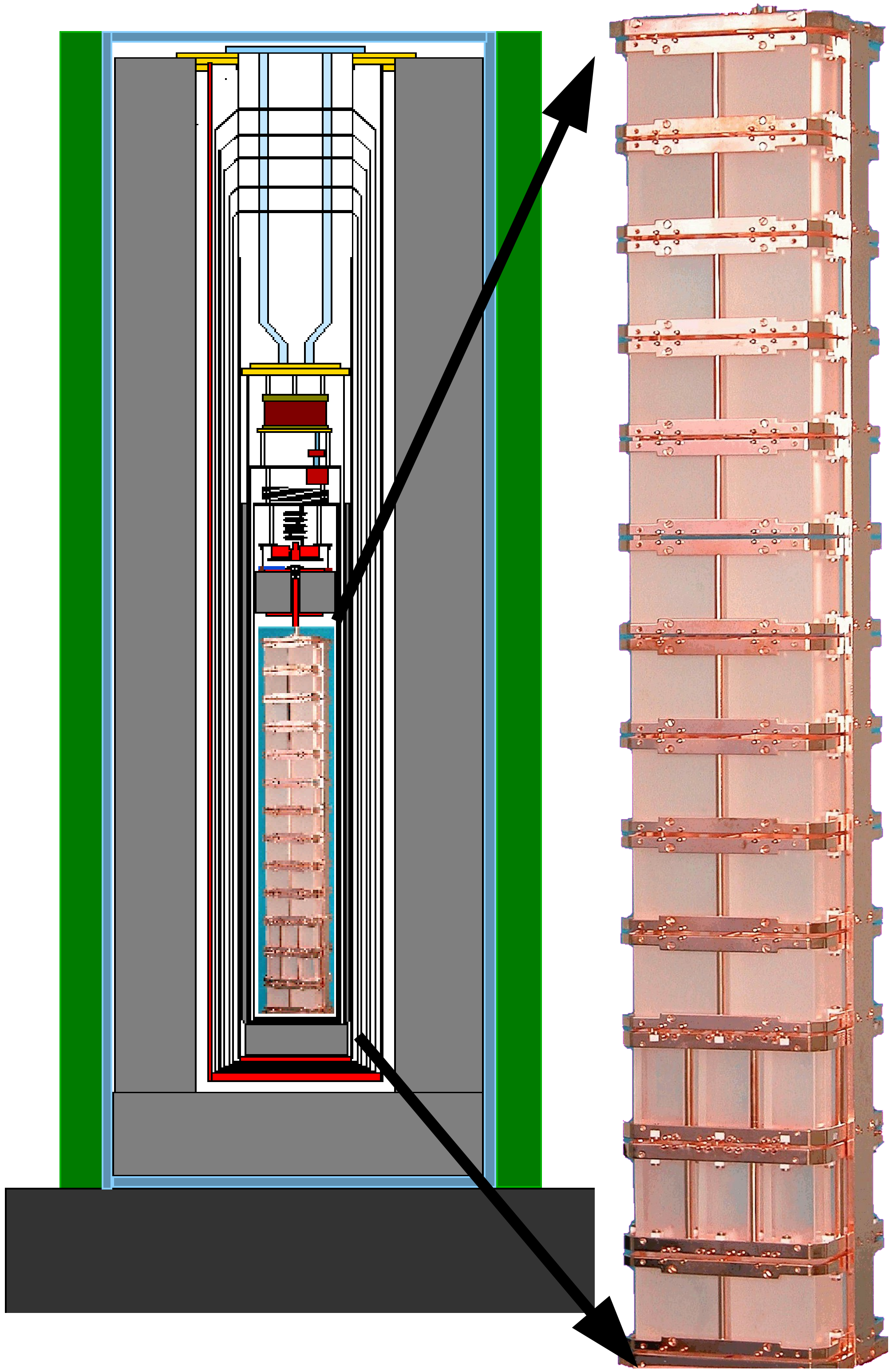

- 62 TeO_2 crystals, for a total mass of 40.7 kg.
- 19.75 kg · yr of ^{130}Te
- Run between 2003 and 2008

$$T_{1/2} > 2.8 \cdot 10^{24} y$$
$$m_{\beta\beta} < 0.3 \div 0.7 eV$$

Astropart. Phys. (2011), doi:10.1016/j.astropartphys.2011.02.002

Cuoricino final energy spectrum

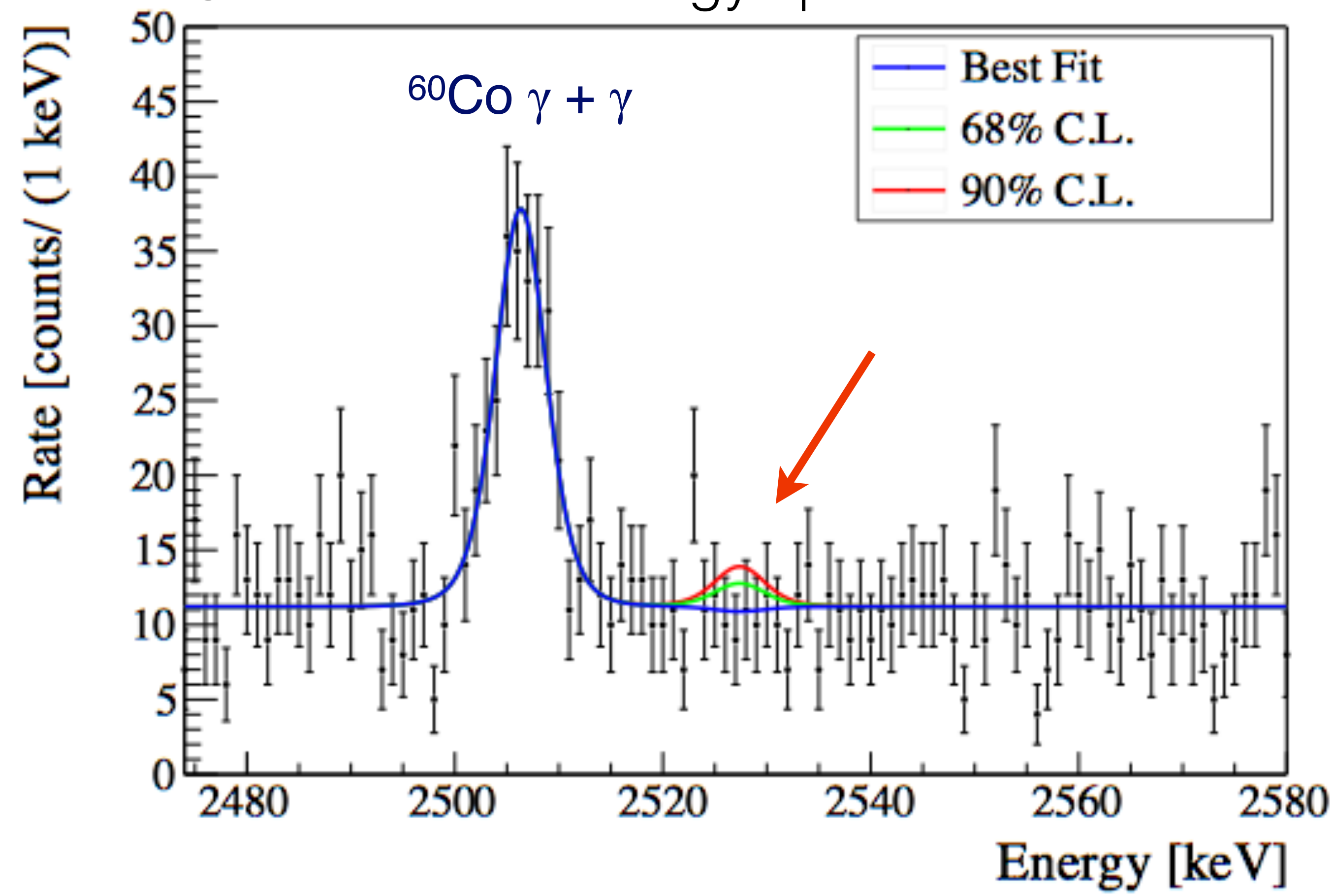

The Cuoricino background

Cuoricino final energy spectrum

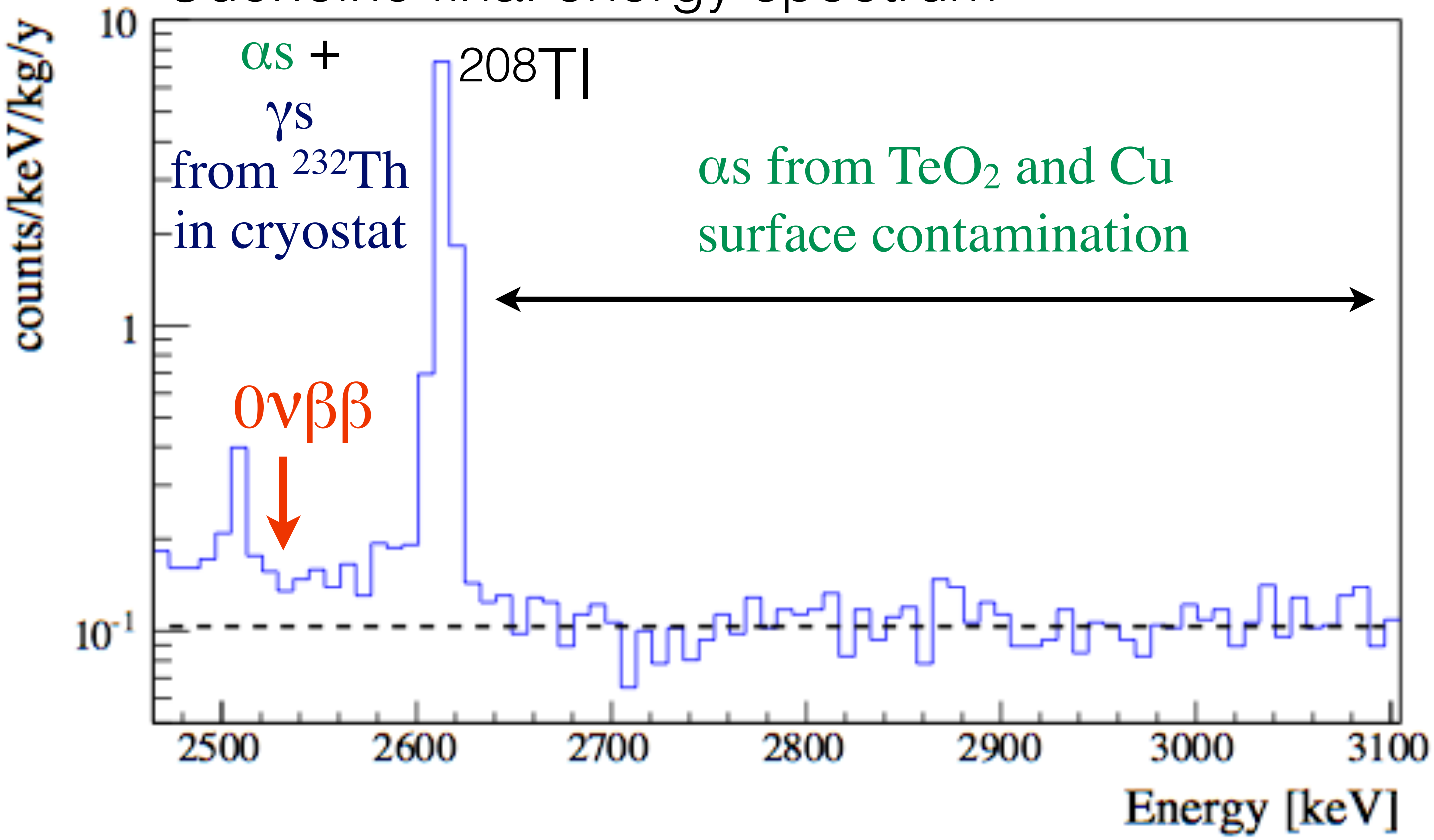

Background @ Q-value 0vDBD: 0.15 c/(keV· kg· y)

From MC simulations:

- ^{232}Th contaminations in cryostat shield: (~30%)
- Degraded alphas from crystal surfaces (~10%)
- Degraded alphas from Cu holders surfaces (~60%)

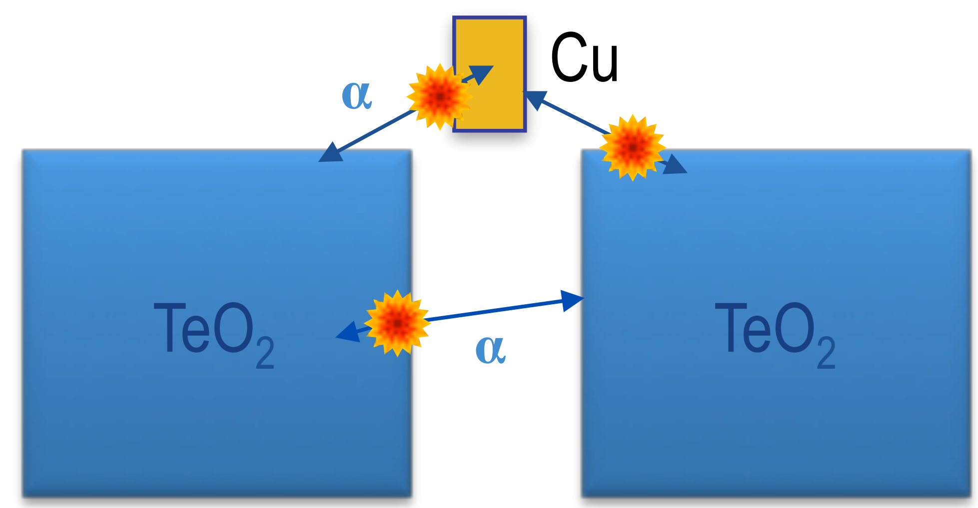

From Cuoricino to CUORE

- **Background suppression**
  - New (lighter) detector design structure
  - Reduced overall detector surfaces by a factor ~2
  - New surface cleaning technique
  - Strict production protocols for TeO_2 surface contamination
  - Minimization of Rn exposure (Glove Box assembly)
  - Strict material selection (e.g. raw materials)

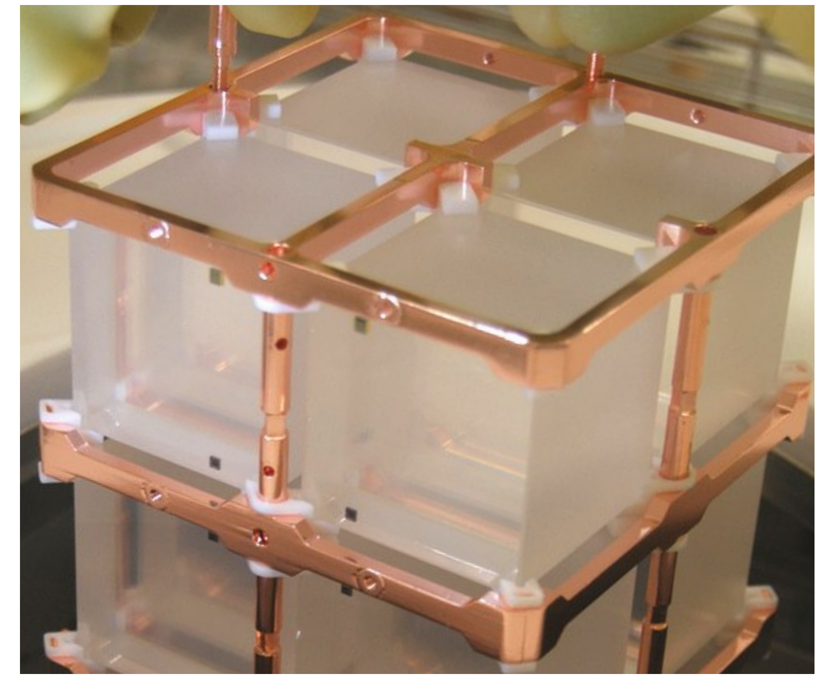

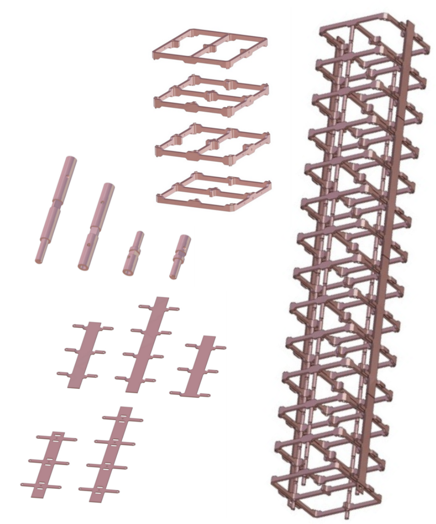

CUORE-0

CUORE-0 is the first tower produced out of the CUORE assembly line.

- 52 TeO_2 5x5x5 cm^3 crystals (~750 g each)
- 13 floors of 4 crystals each
- total detector mass: 39 kg TeO_2 (10.9 kg of ^{130}Te)

CUORE-0 has been taking data since March 2013 in the 25 year old Cuoricino cryostat.

- Proof of concept of CUORE detector in all stages
- Test and debug of the CUORE tower assembly line
- Test of the CUORE DAQ and analysis framework
- Extend the physics reach beyond Cuoricino while CUORE is being assembled

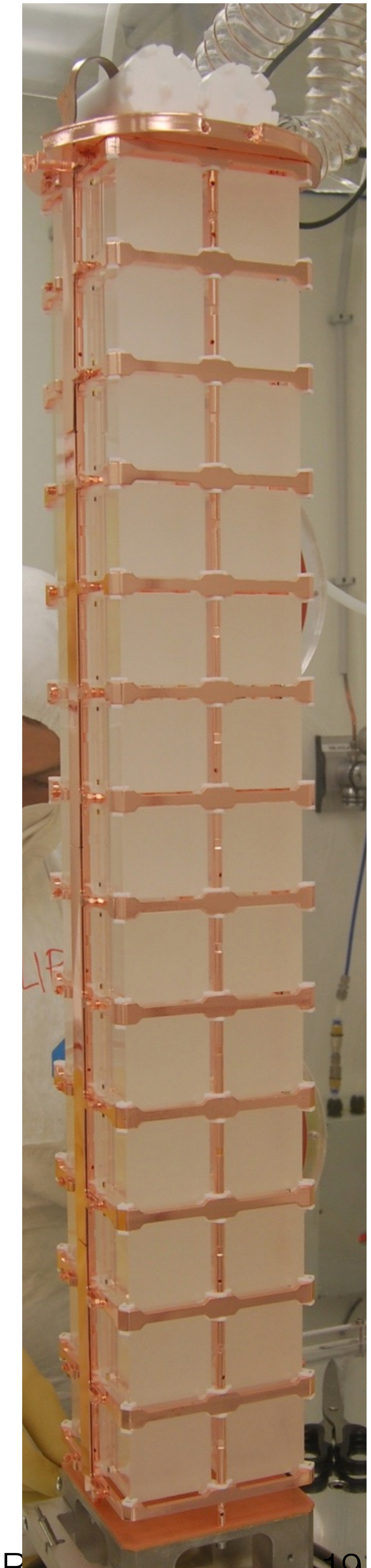

Tower assembly

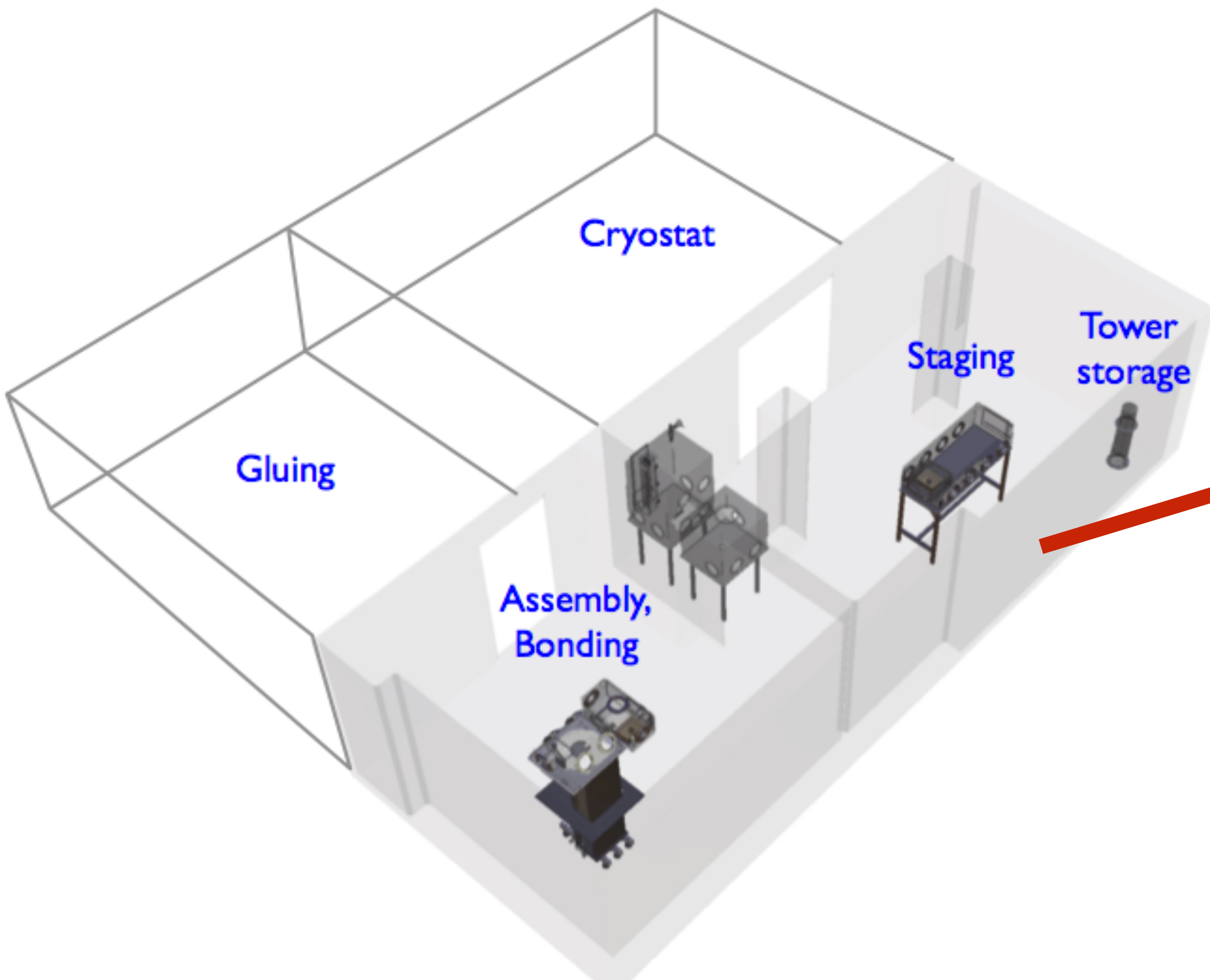

Sensors coupling

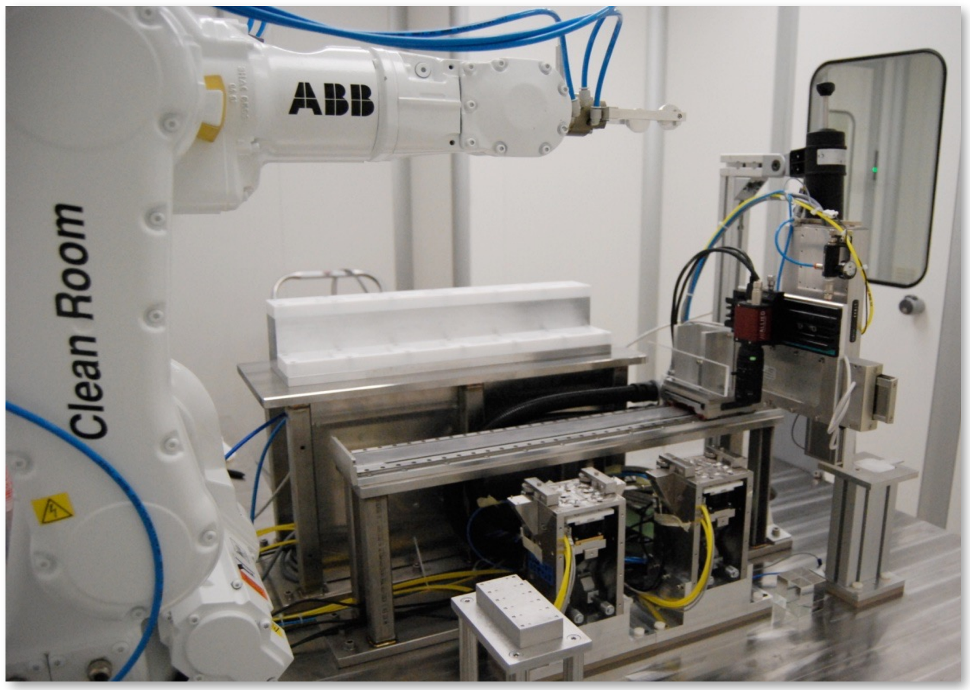

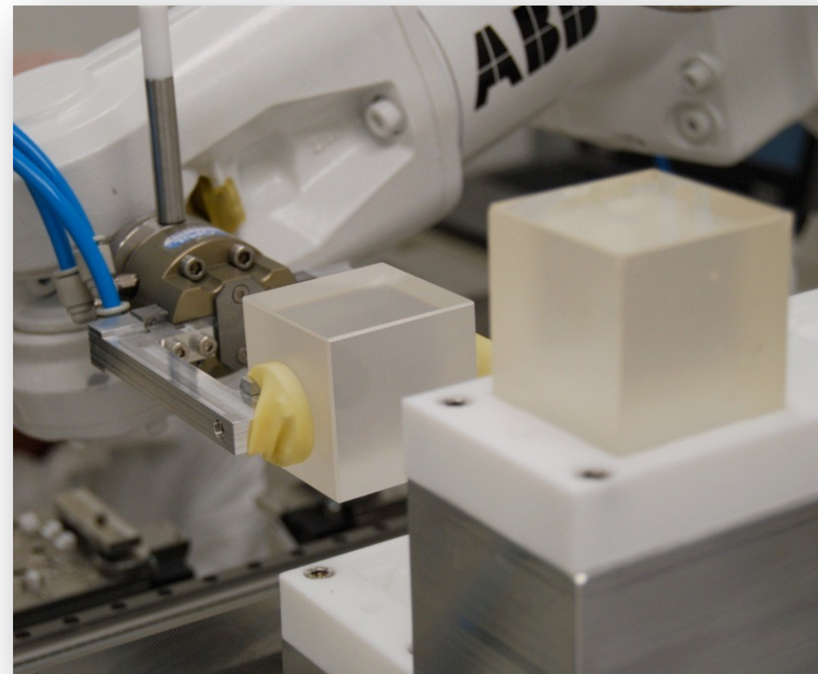

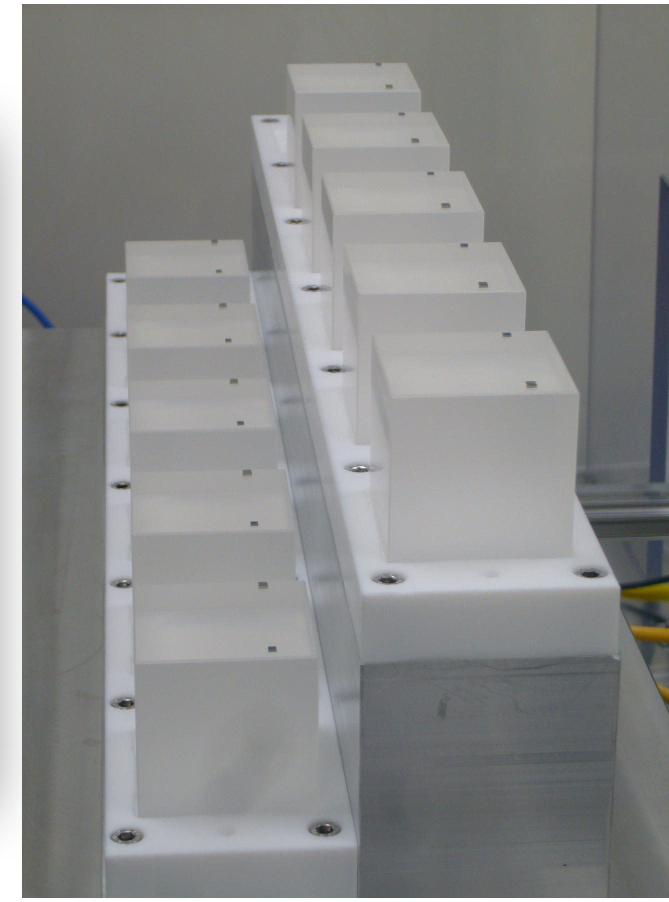

- The detector performance (e.g. energy resolution) are driven by the sensor-to-crystal coupling (glue spots).
- Features:
    - new semi-automatic system
    - highly-reproducible
    - minimize radioactive recontamination.

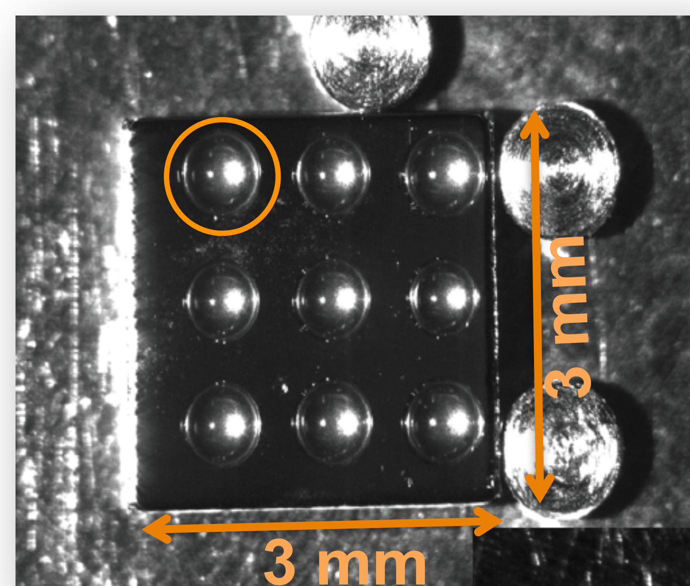

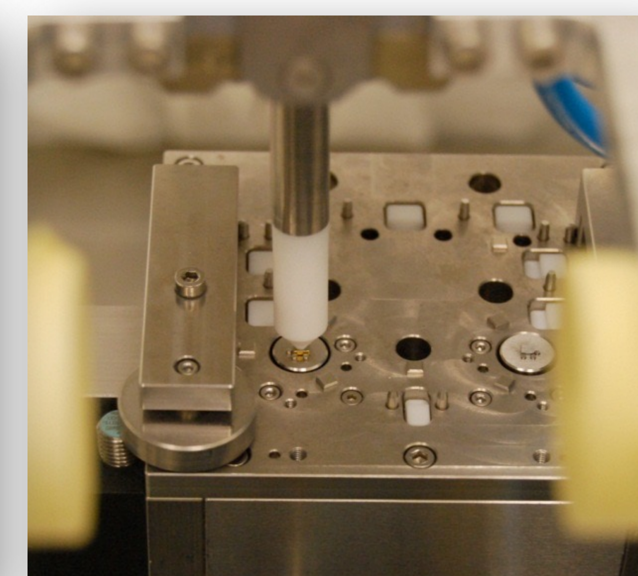

Tower assembly

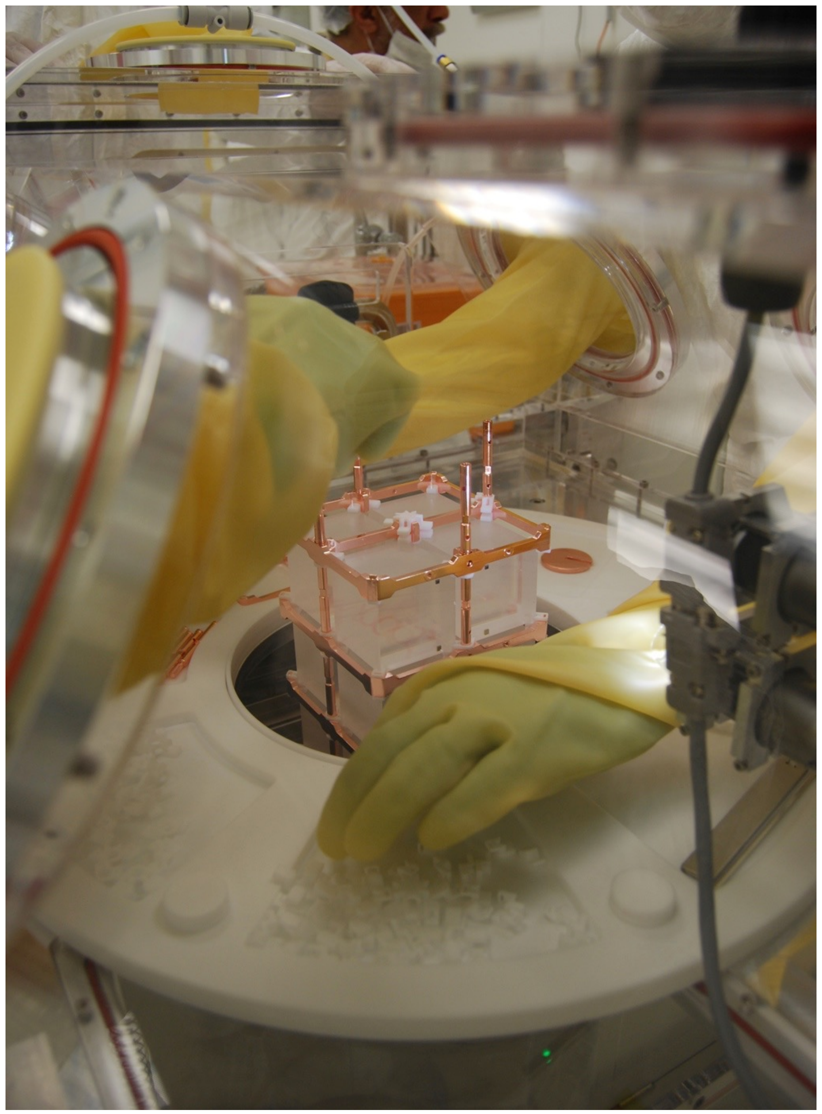

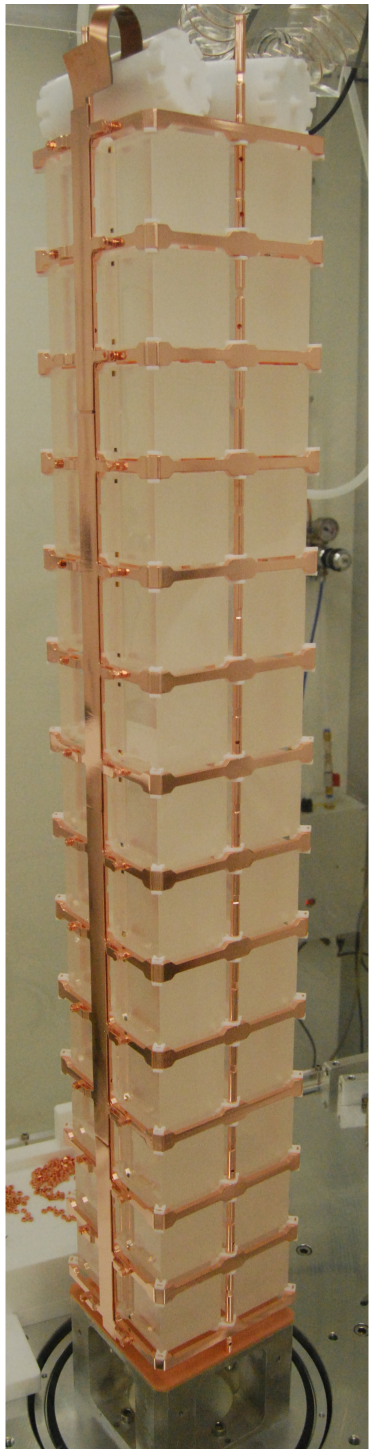

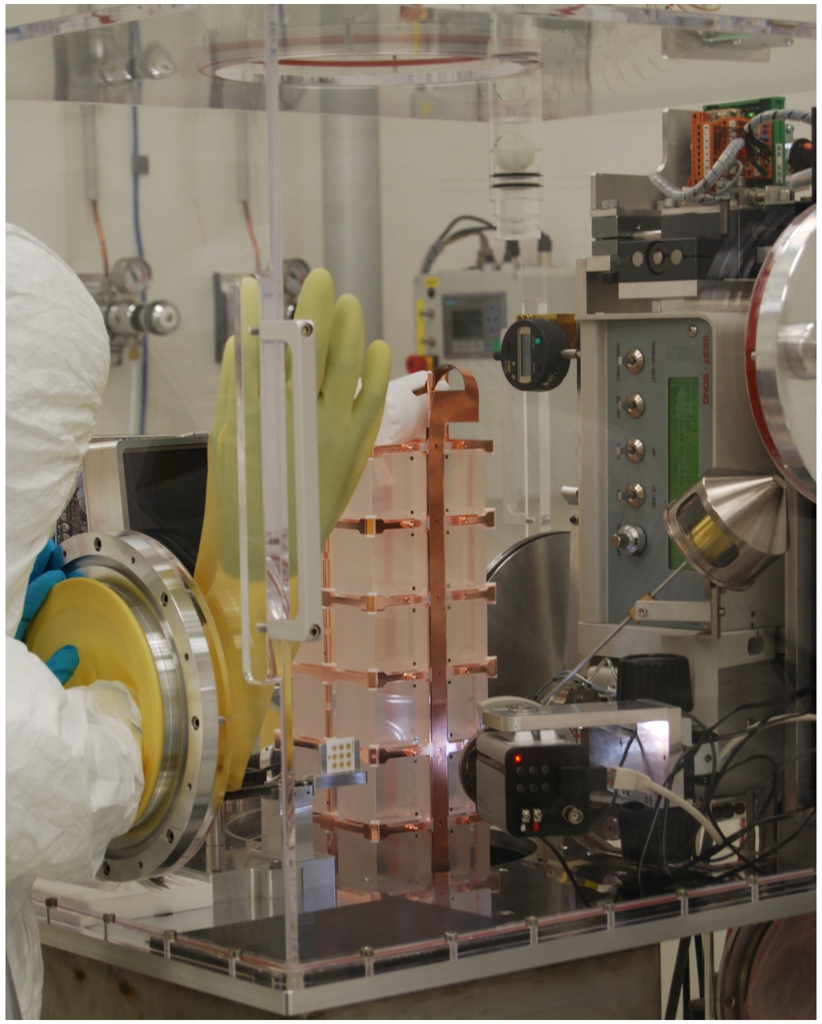

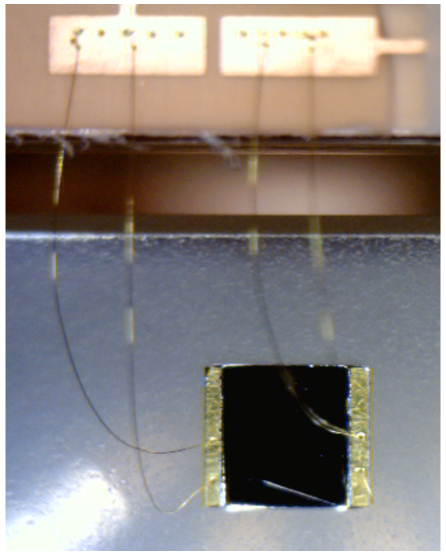

CUORE-0

51/52 NTD connected

51/52 heaters connected

Tower assembly

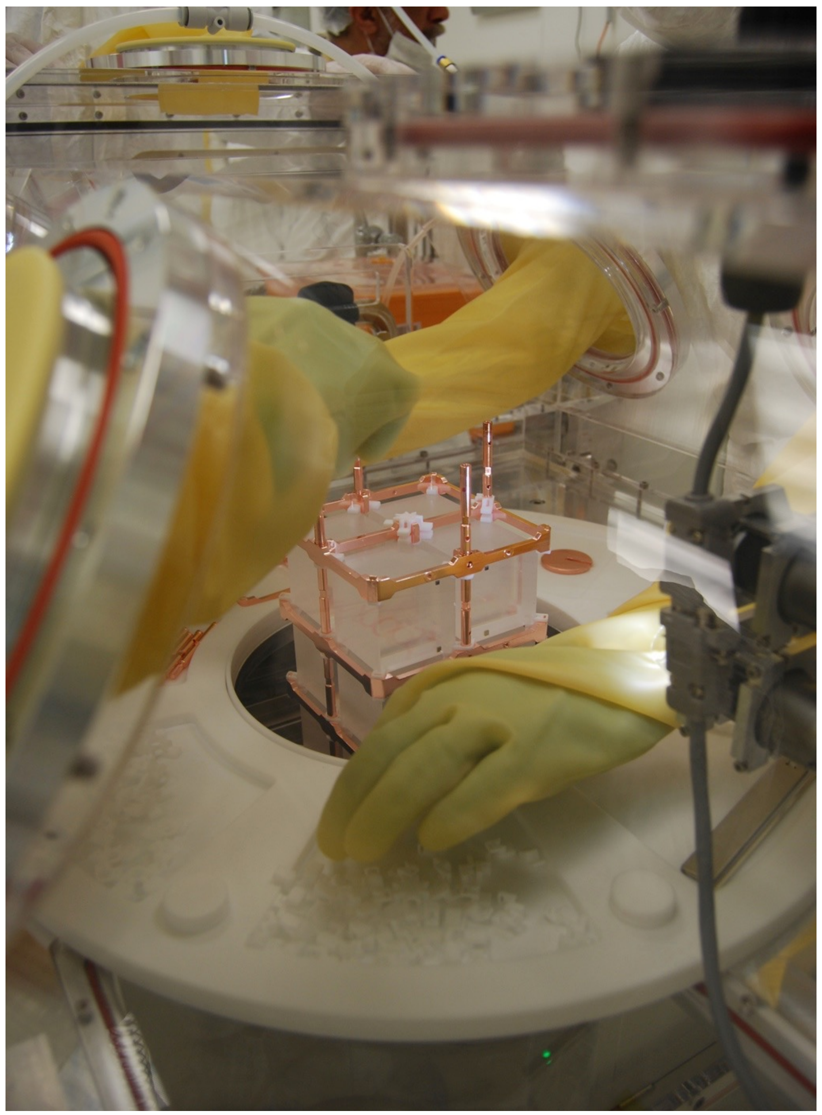

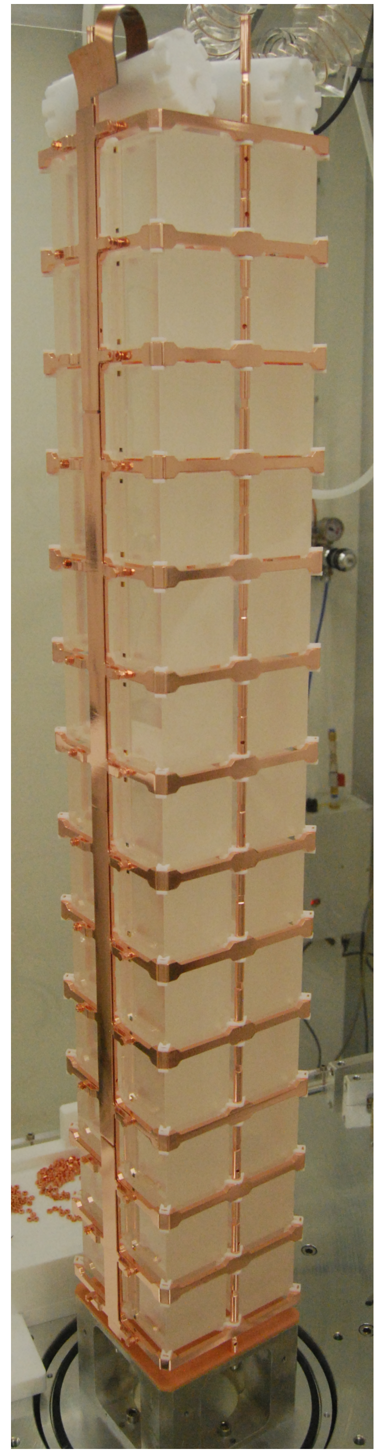

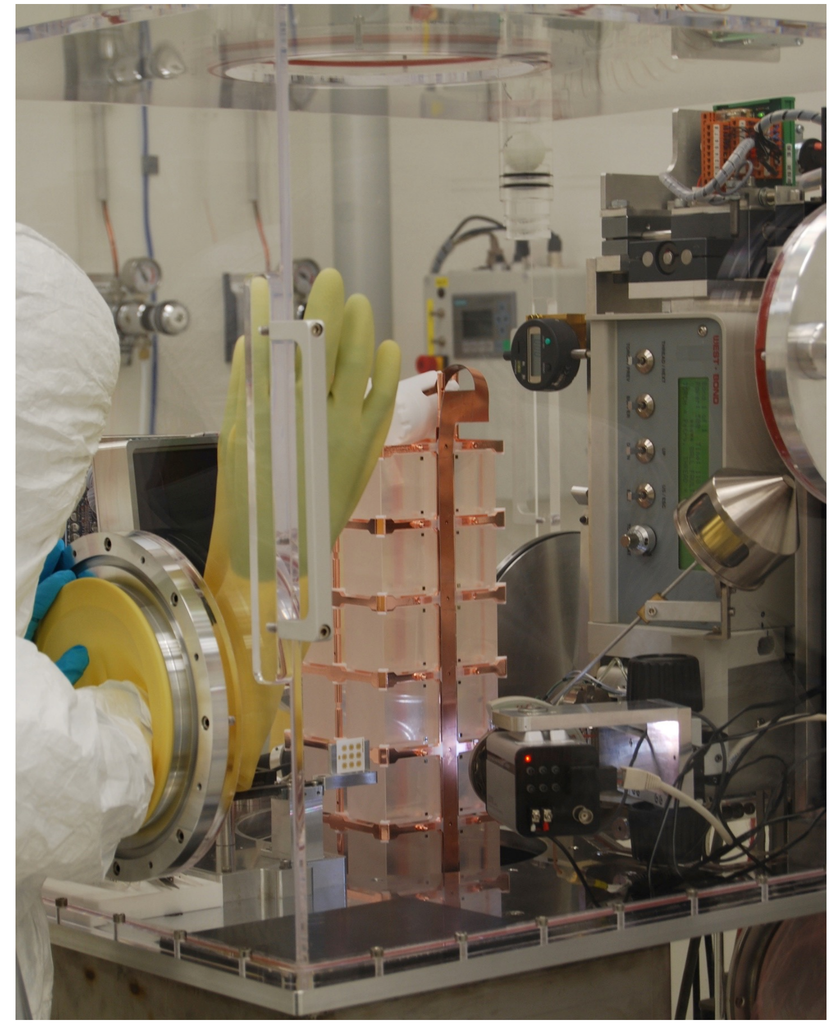

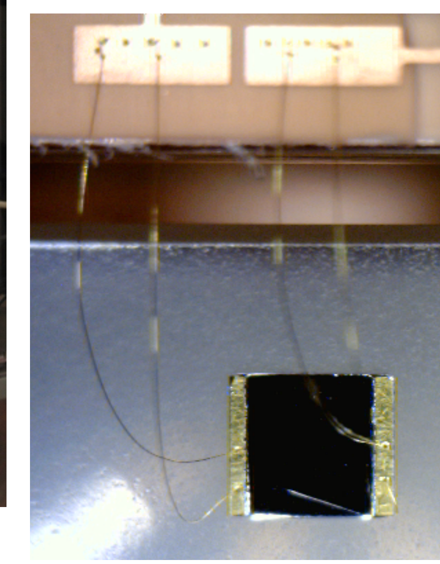

CUORE-0

51/52 NTD connected

51/52 heaters connected

CUORE

988/988 NTD connected

988/988 heaters connected

Tower installation

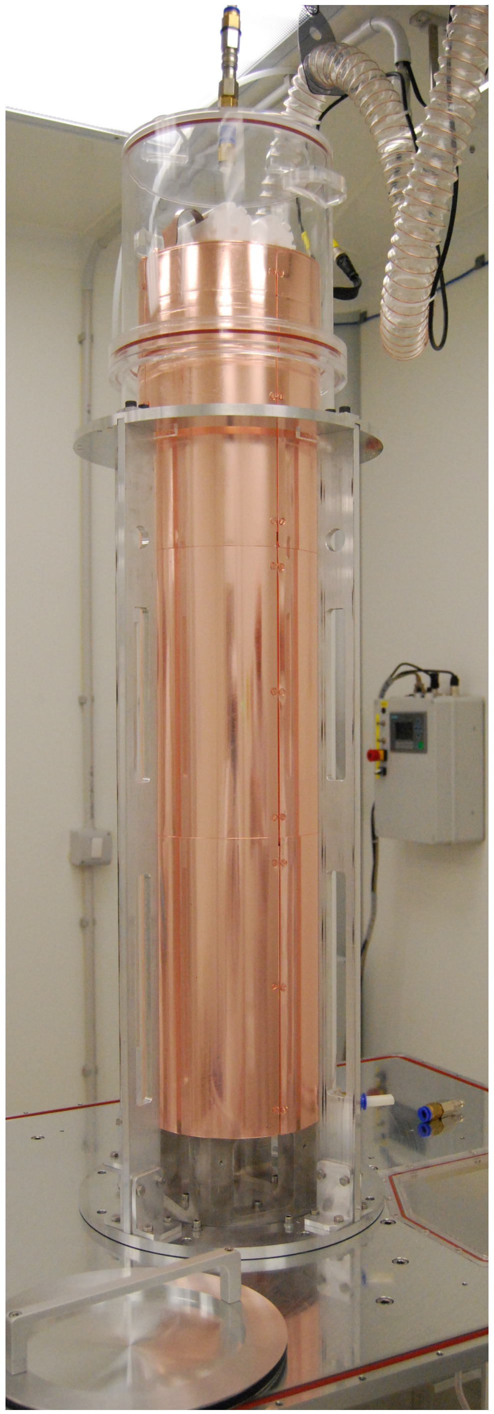

From the CUORE assembly clean room, to the Cuoricino dilution refrigerator

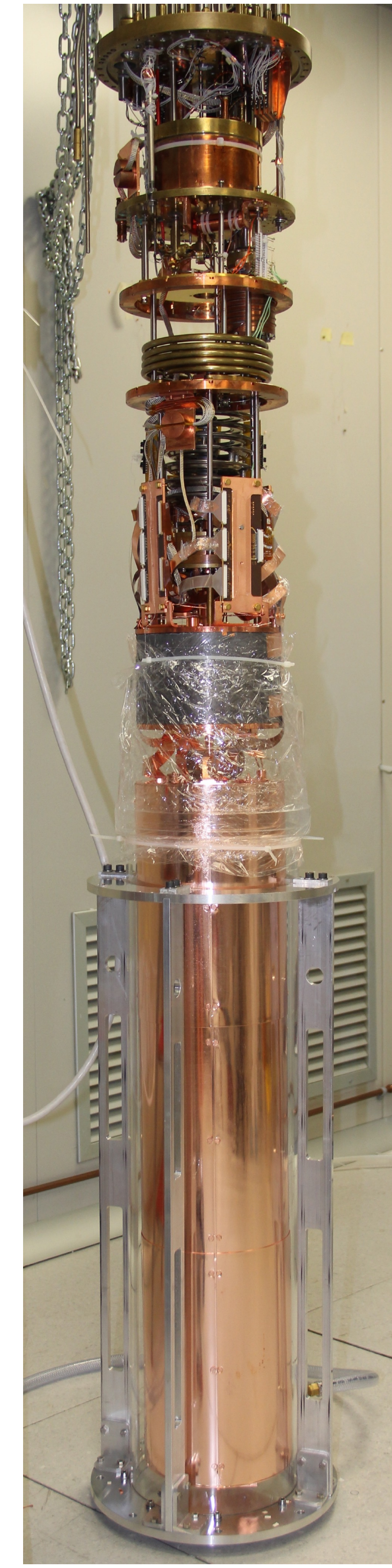

Experimental setup

- Same cryostat as Cuoricino:
  - inner shield: 1 cm of Roman Lead (A < 4 Bq/kg).
  - External shield: 20 cm of Modern Lead.
  - nitrogen flushing
- **gamma background from cryostat shields not expected to change** (test of alpha background)

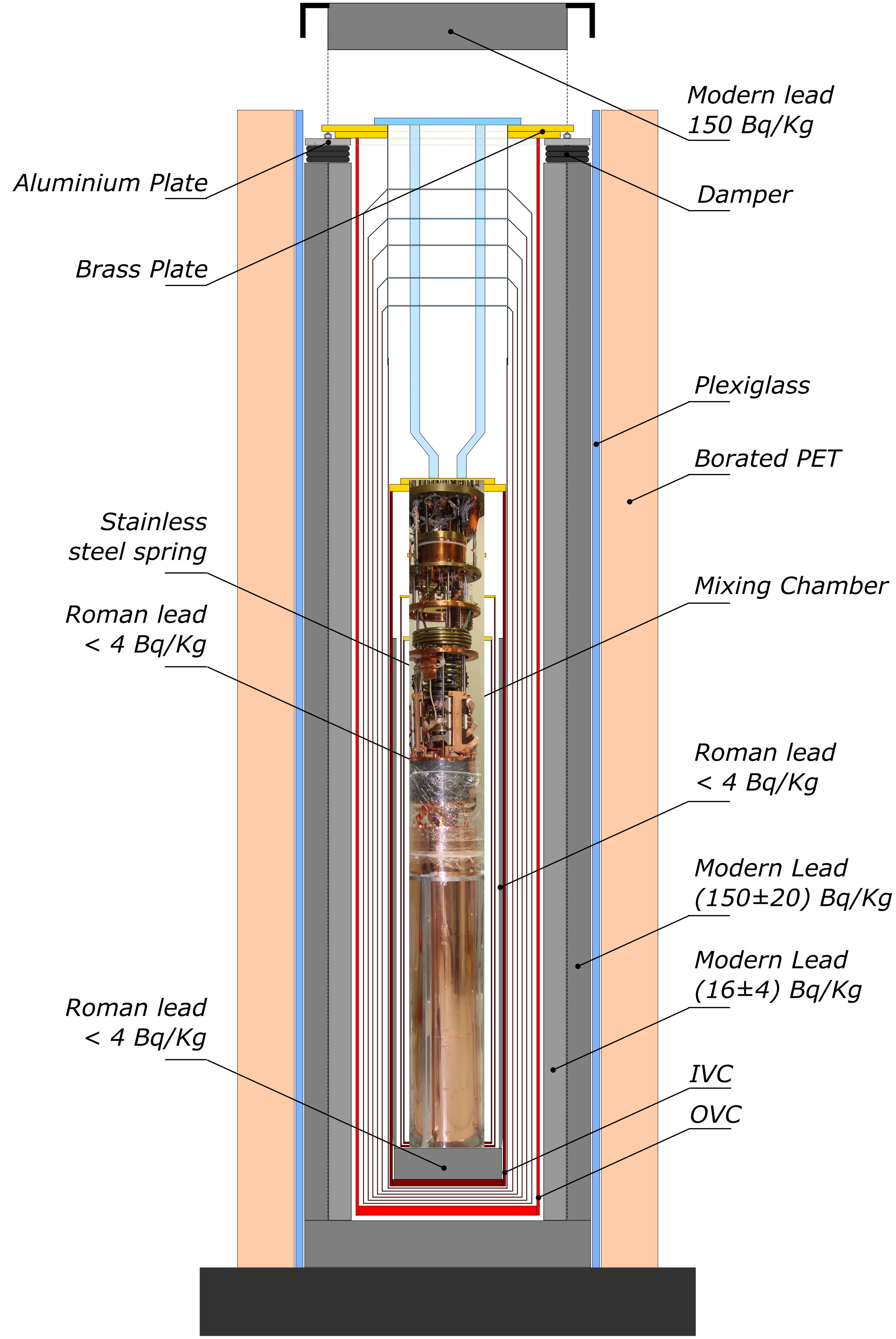

Outline

- Double beta decay physics
- Thermal detectors
- History of ^{130}Te double beta decay experiments
- **CUORE-0 results**
    - **Detector performance**
    - Neutrinoless double beta decay analysis

Data taking

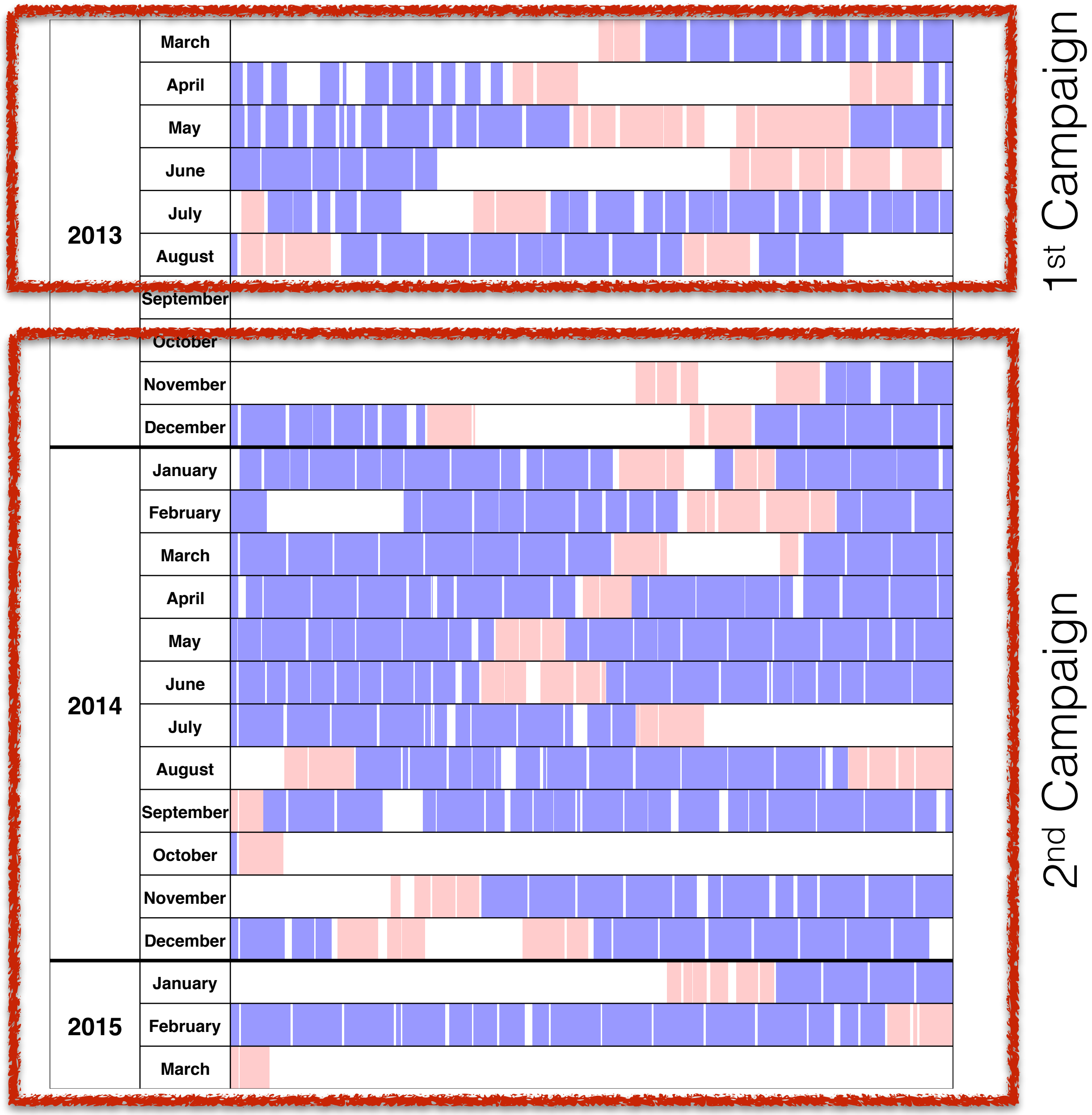

Calibration data taking

Physics data taking

- Detector assembled in Spring 2012.
- First successful cooldown in March 2013.
- One heater connection lost during the cooldown
  - 51/52 NTD connected
  - 50/52 heater connected
- 2-3 days per months are devoted to ^{232}Th calibrations
- Time between calibrations was devoted to physics data taking, and used for 0vDBD decay search

Exposure overview

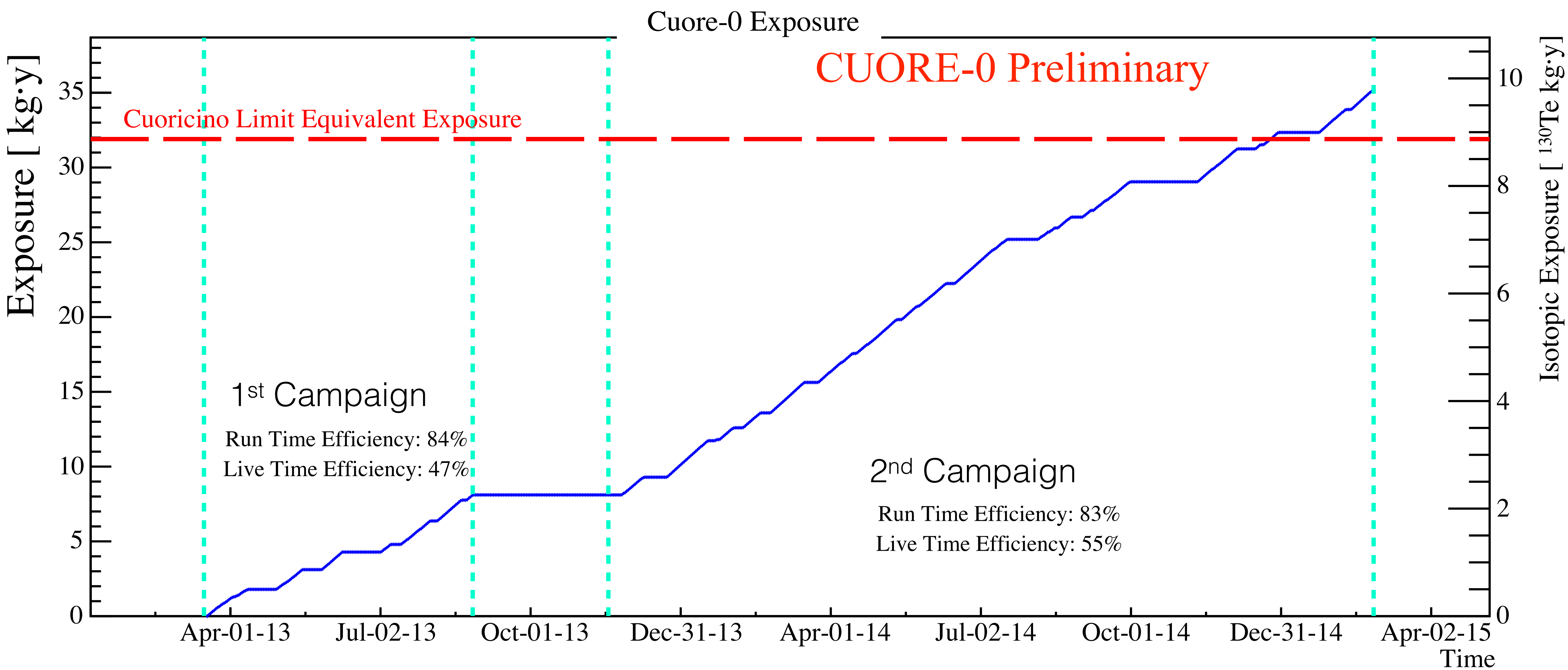

- Acquired statistic for 0vDBD decay search:
  - 35.2 kg·yr TeO_2
  - 9.8 kg·yr ^{130}Te

Detector stability

- We measure the resistance of each bolometer daily, to monitor the detector stability over time

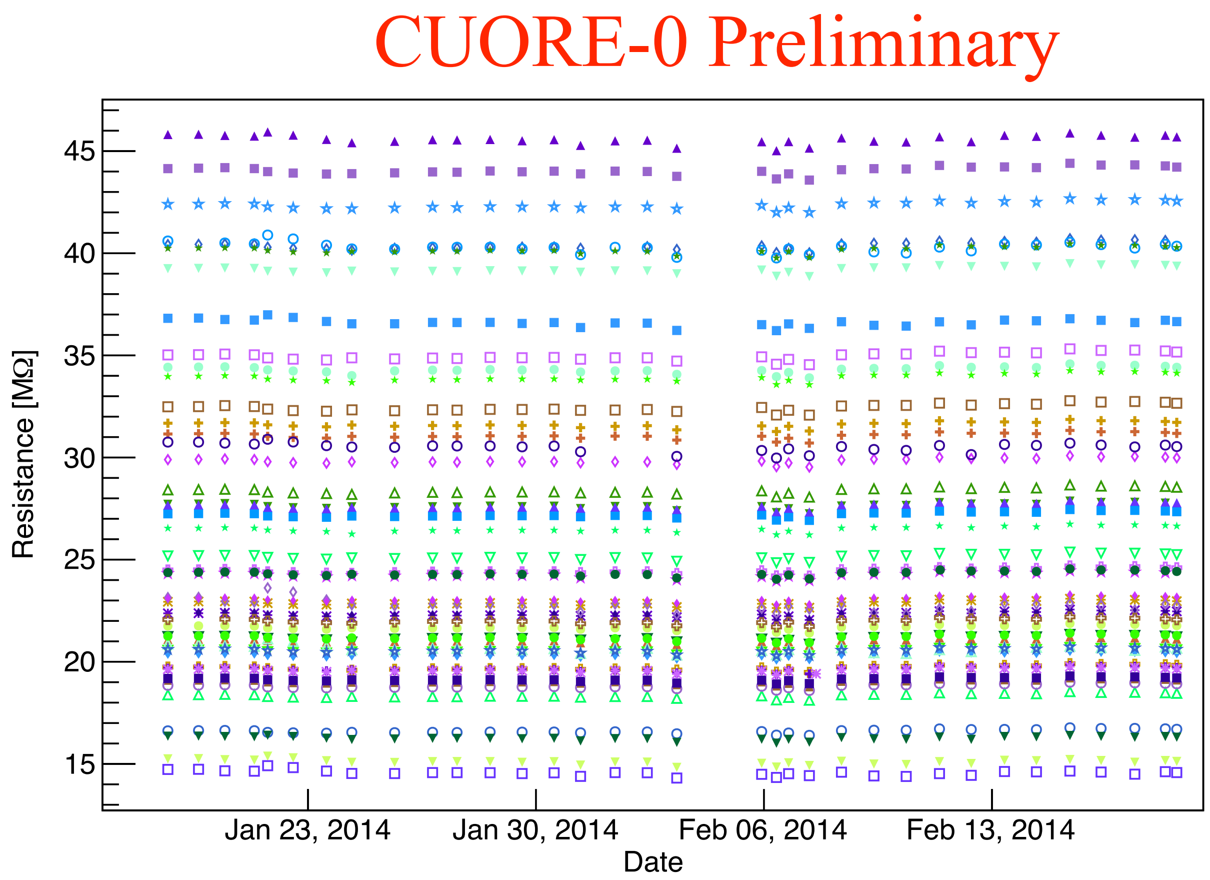

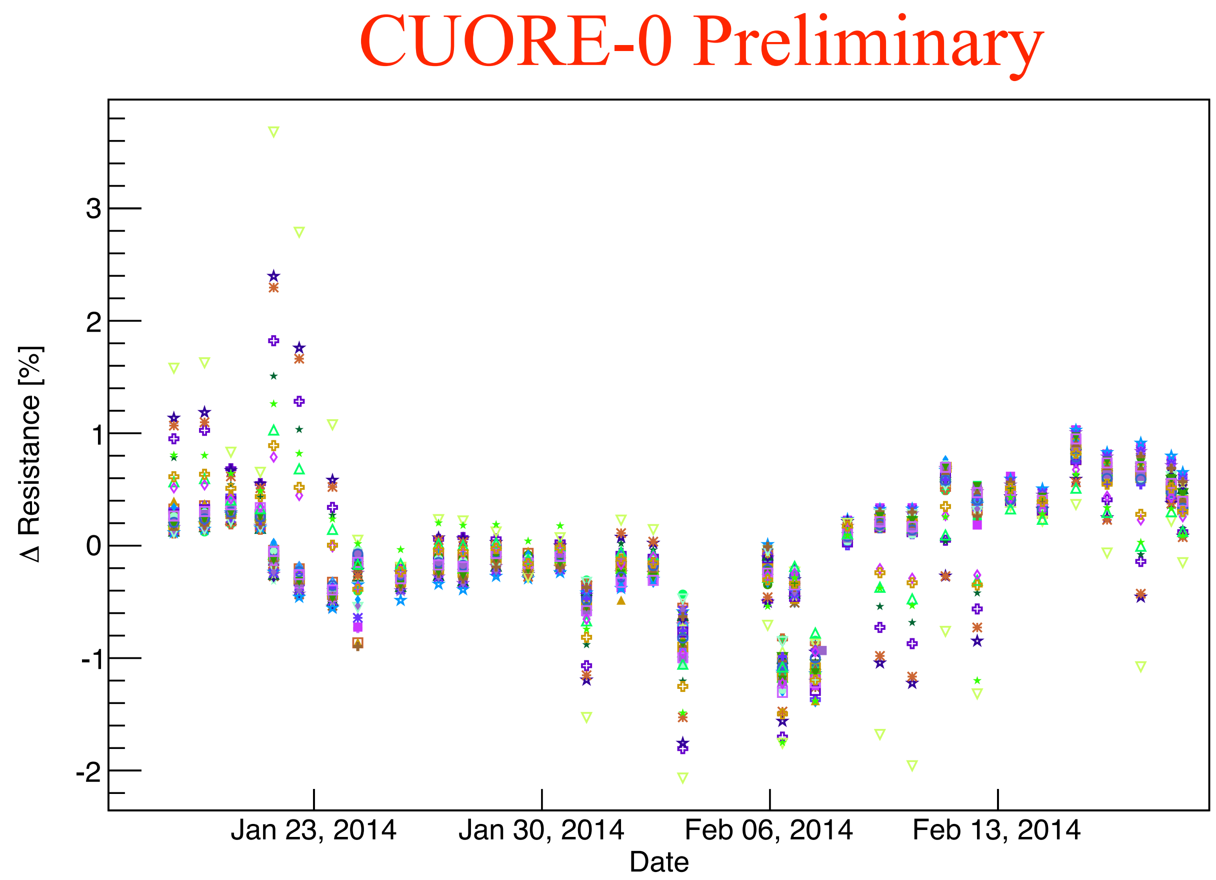

- The resistance of the bolometers are within a factor of 3

- The bolometers are stable within ~3% over a month timescale

Detector uniformity

- One of the main goal of CUORE-0 was to verify the improvements and the level of reproducibility in the bolometric performance achieved with the new CUORE assembly line.
- We evaluated the distribution of the thermistors temperatures once the detector has been cooled to base temperature and we compared to the Cuoricino one.

$$R(T)=R_0 \exp\left[\frac{T_0}{T}\right]^{1/2}$$

↓

$$T(R)= T_0\, ln^2\left[\frac{R}{R_0}\right]$$

The narrower distribution of CUORE-0 temperatures compared to Cuoricino shows the **improvement in the reproducibility of the detector construction**

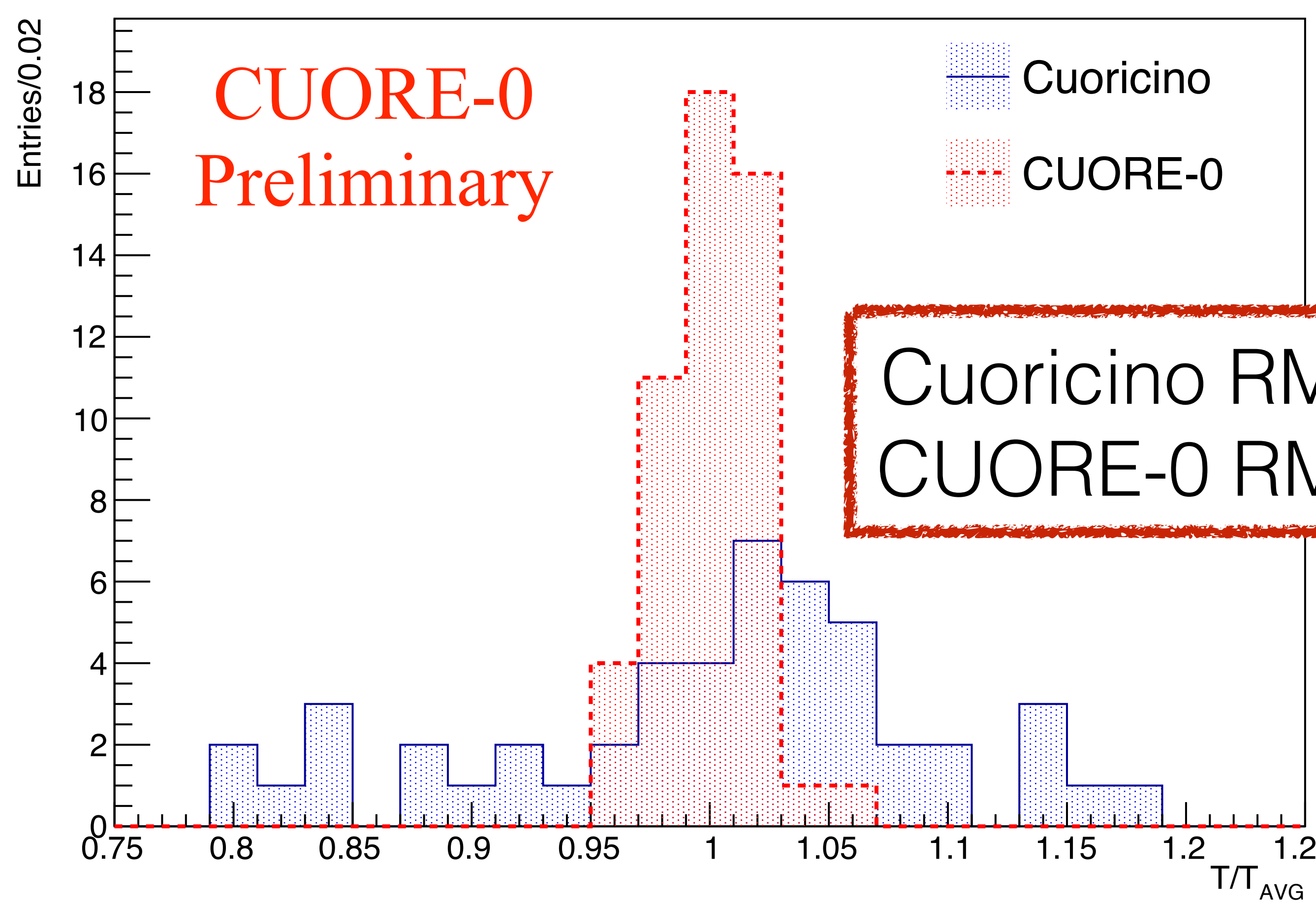

Cuoricino RMS: 9%
CUORE-0 RMS: 2%

Calibration spectra

CUORE-0 total calibration energy spectrum

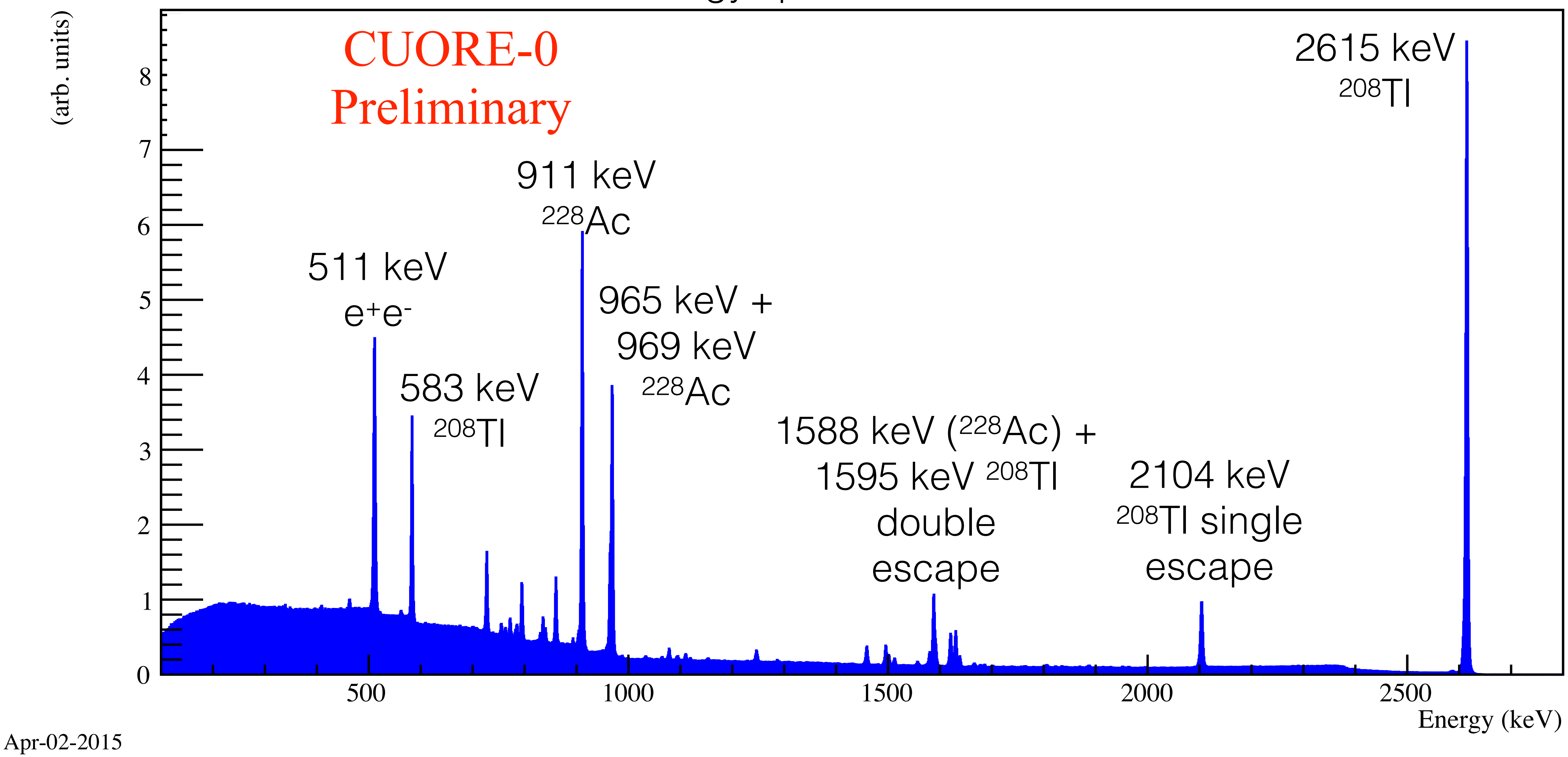

- We calibrate the detector using two thoriated tungsten wires source placed in between the outermost cryostat shield and the external lead shield.

Energy resolution

Total fit on the 2615 keV line

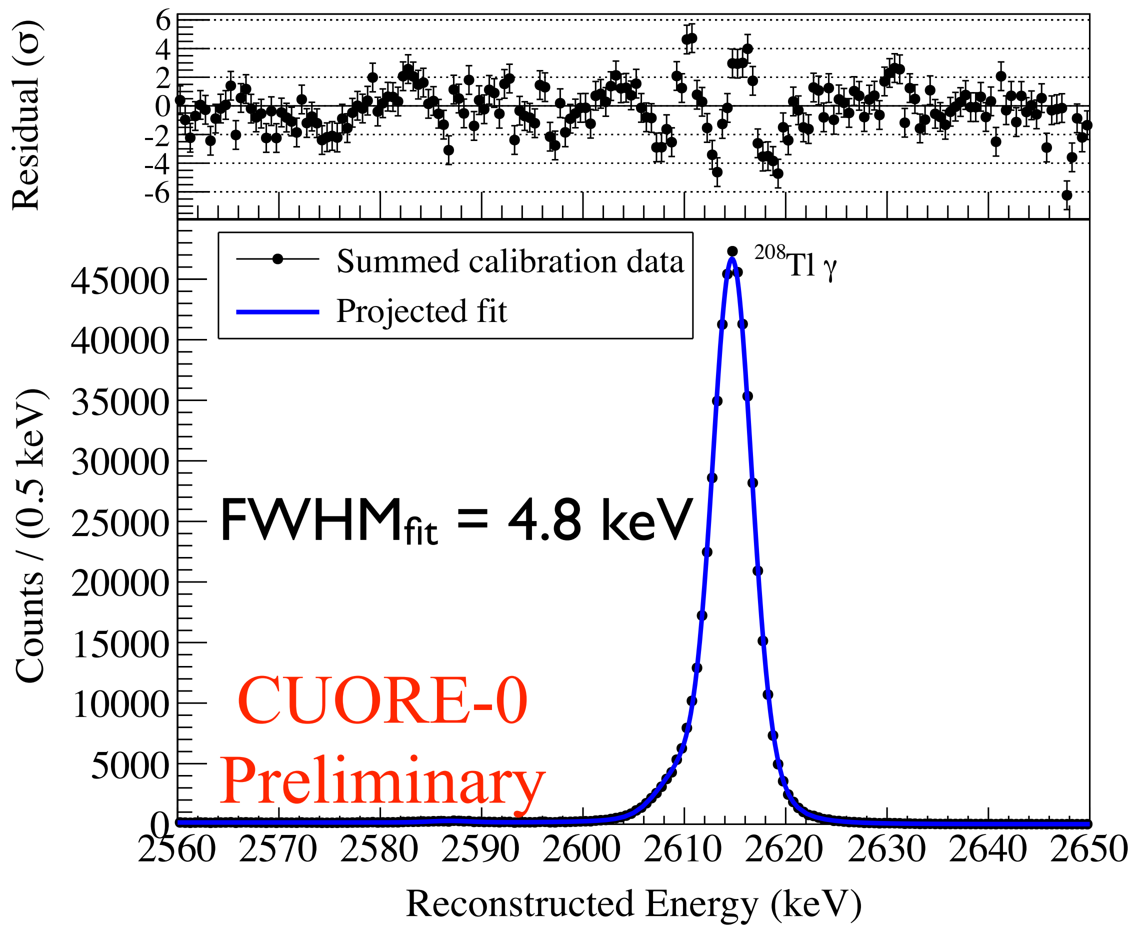

Distribution of energy resolution @ 2615 keV

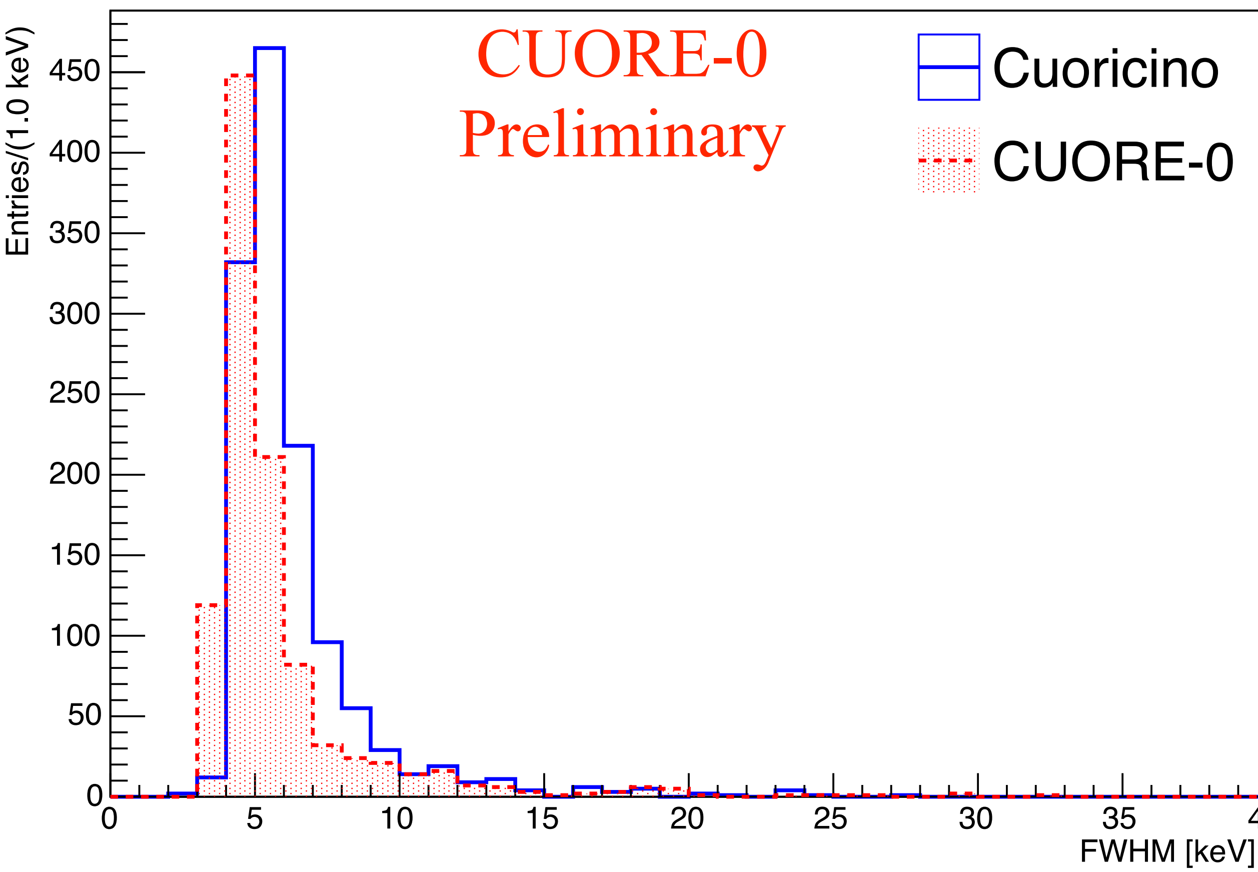

The 5 keV CUORE goal has been reached

Physics-exposure-weighted harmonic mean

	Average FWHM [keV]	RMS of FWHM [keV]
Cuoricino	5.8	2.1
CUORE-0	4.9	2.9

Background reduction

Comparison of the total background spectrum in CUORE-0 and Cuoricino

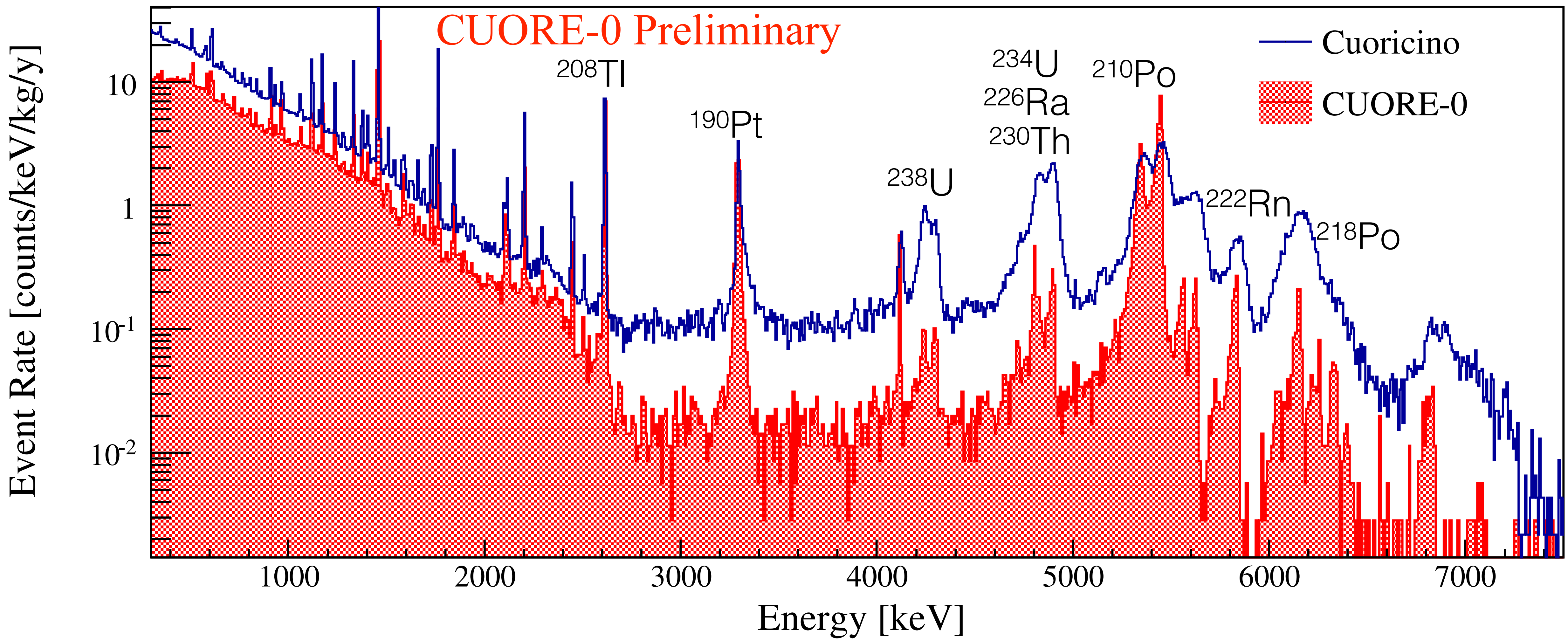

- ^{238}U and ^{232}Th α lines reduced thanks to the new detector surface treatment.
- ^{238}U γ lines reduced by a factor 2 (better radon control)
- ^{232}Th γ lines not reduced (originate from the cryostat).

Dedicated paper on background model is in preparation

Alpha background rate

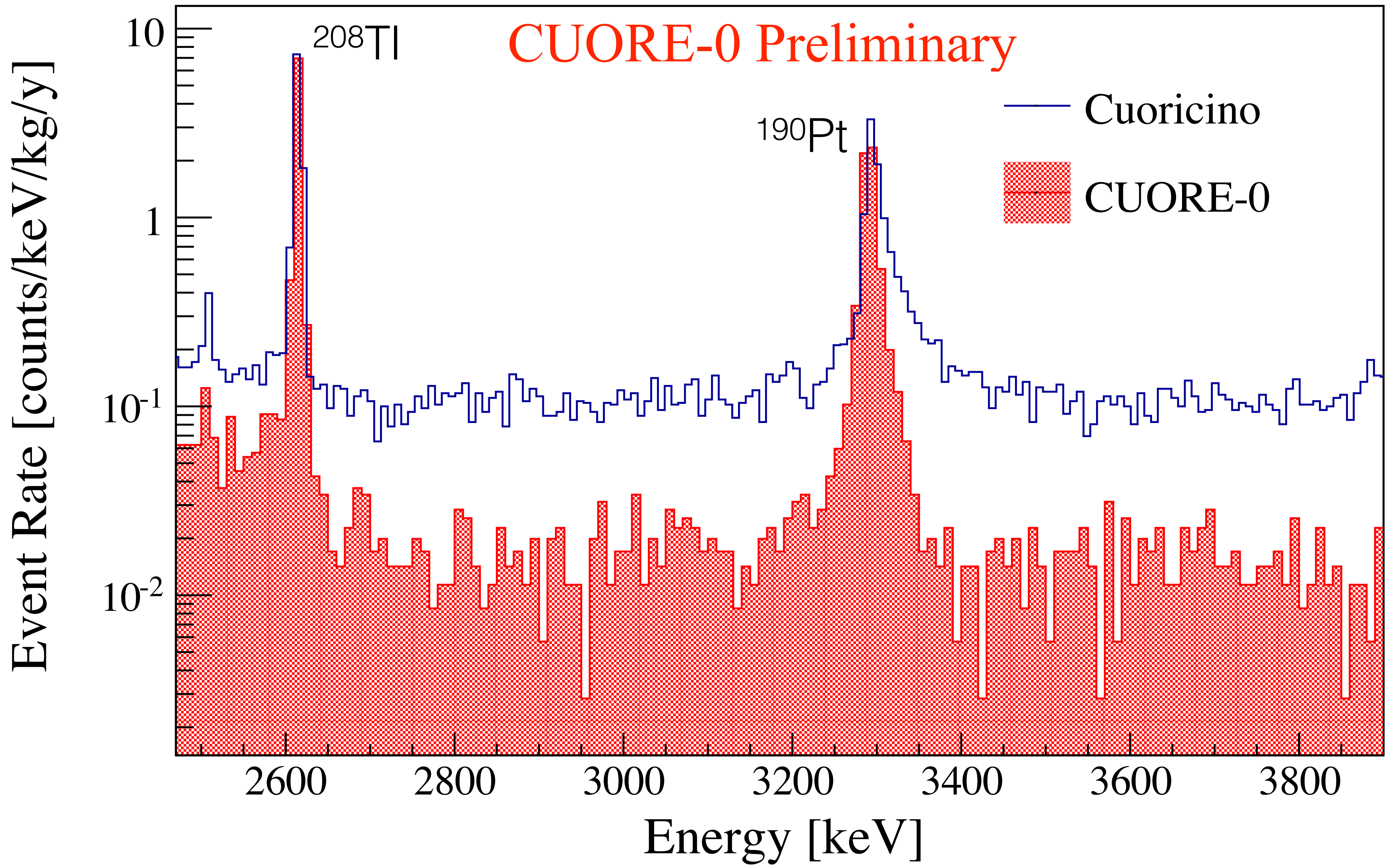

	2.7-3.9 MeV	eff
CUORE-0	0.016 ± 0.001	81 ± 1
Cuoricino	0.110 ± 0.001	83 ± 1

- x6 reduction in the alpha continuum region

Outline

- Double beta decay physics
- Thermal detectors
- History of ^{130}Te double beta decay experiments
- **CUORE-0 results**
  - Detector performance
  - **Neutrinoless double beta decay analysis**

Analysis technique

- Acquisition of triggered signals
- Data preprocessing: estimation of raw parameters
- Pulse filtering
- Thermal Gain Stabilization (TGS)
- Energy calibration
- Particle event selection
- Energy spectrum

Analysis technique

- Acquisition of triggered signals

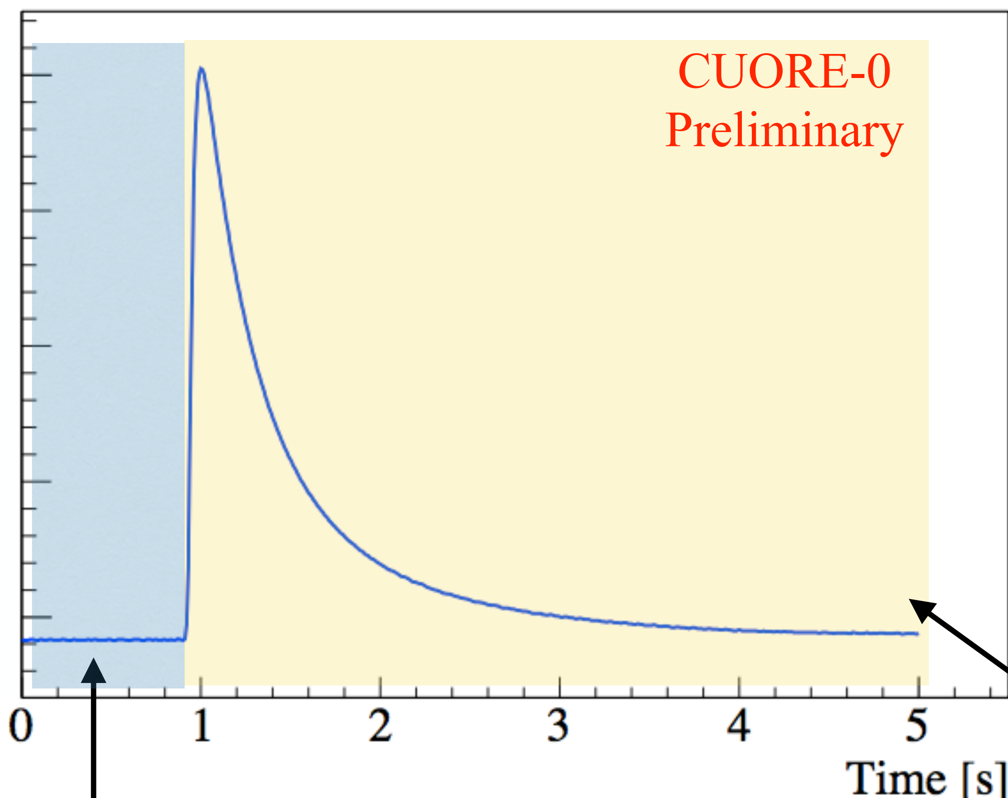

- Each thermistor voltage is continuously sampled at 125Hz
- Once triggered, a 5 sec window is selected for further study of the waveform

The pre trigger voltage is a good proxy for the bolometer temperature before the event

The following 4 sec are analysed to determine the pulse amplitude and to study the pulse shape parameters

Analysis technique

- Acquisition of triggered signals
- Data preprocessing: estimation of raw parameters
  - Raw waveform parameters: baseline, baseline RMS, raw pulse amplitude
  - rejection of noisy time intervals

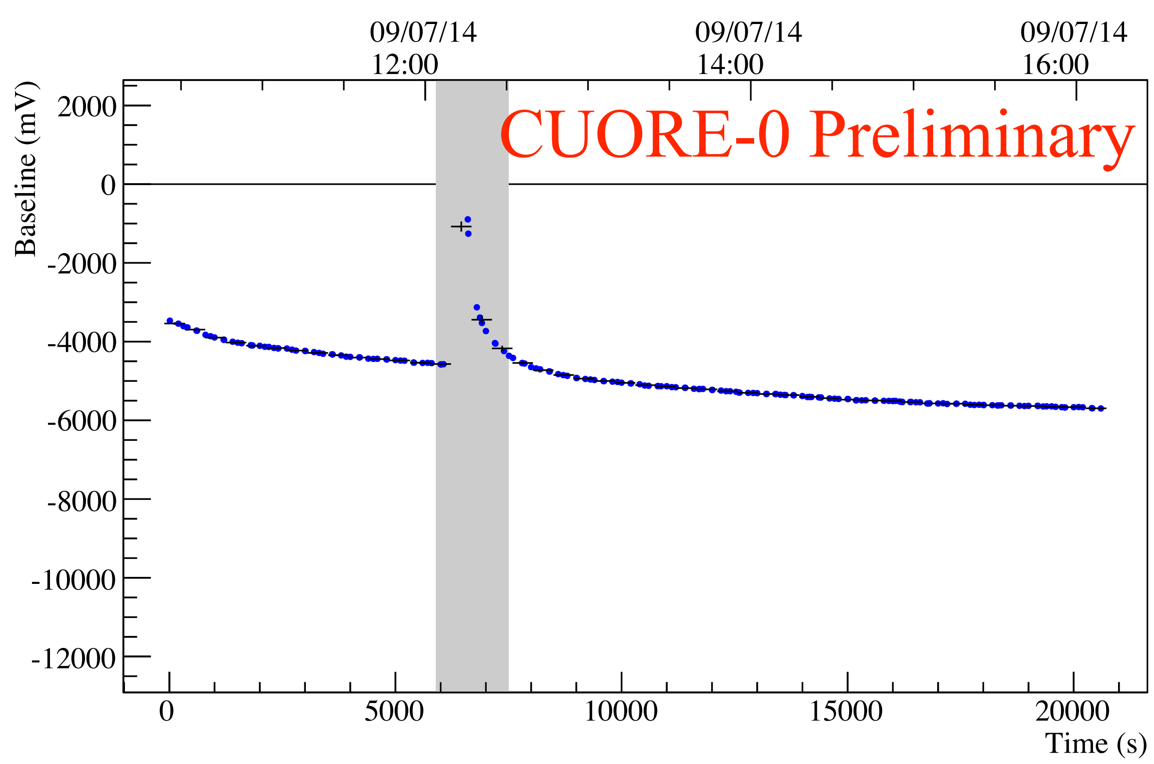

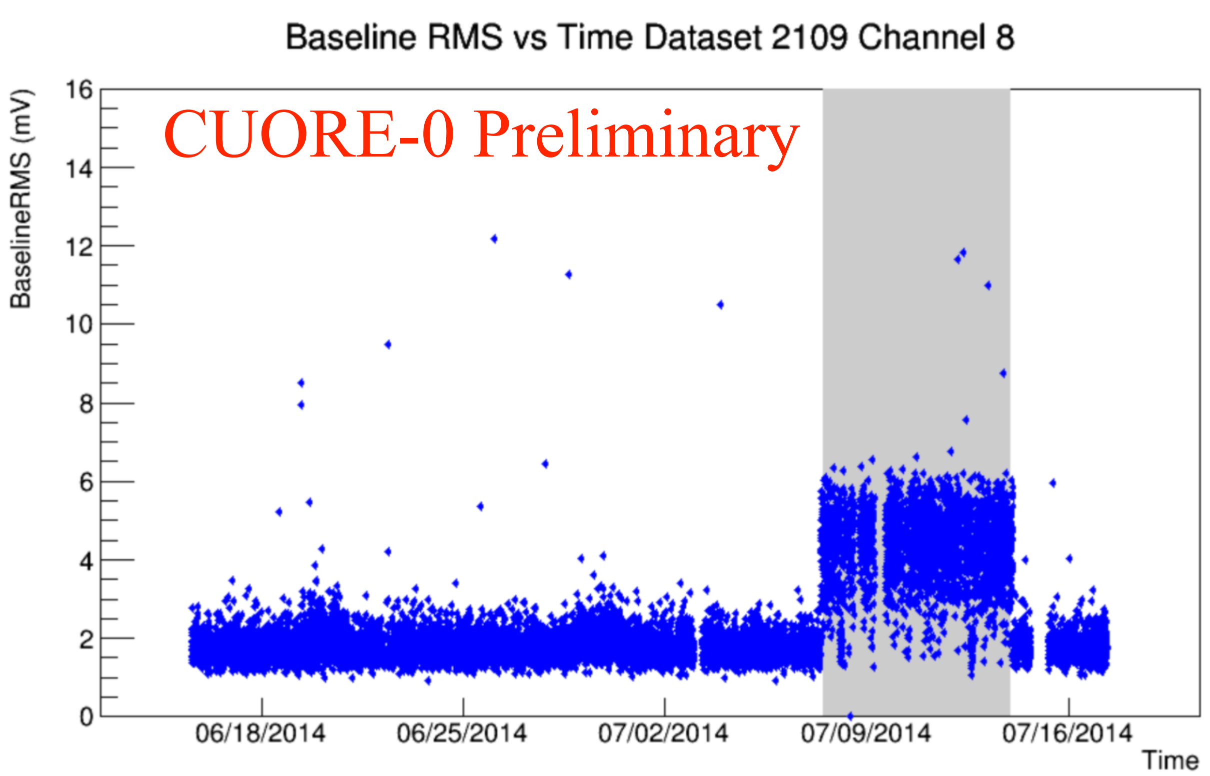

Analysis technique

- Acquisition of triggered signals
- Data preprocessing: estimation of raw parameters
- Pulse filtering
  - **Optimal Filter**: we require that the waveform is consistent with an average reference waveform template. We can optimise energy resolution by exploiting differences in the frequency characteristic of signal and noise events.
  - **Decorrelated Optimal Filter**: reduces the correlated noise between adjacent crystals in the array.

Signal and noise power spectrum

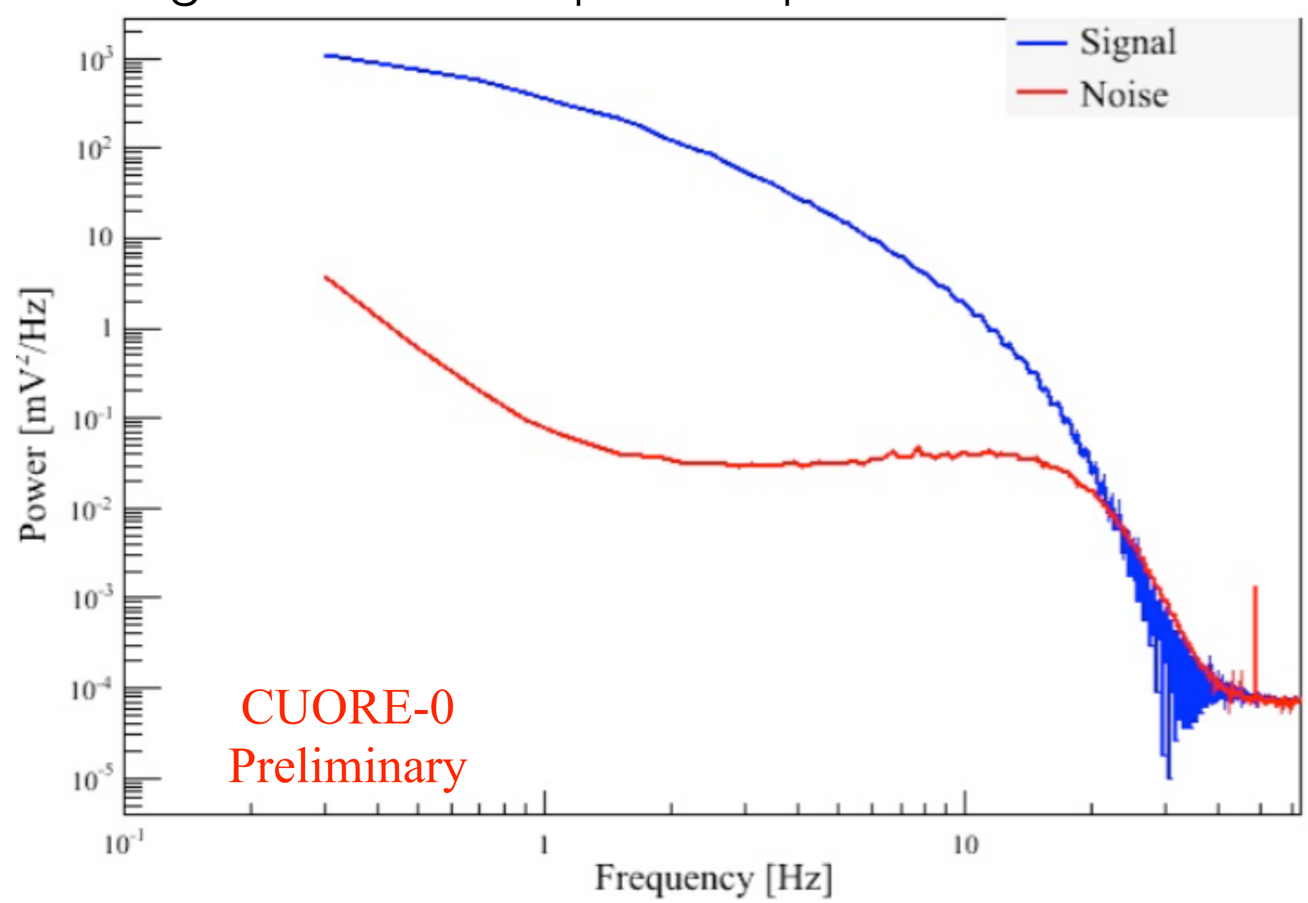

New technique developed for CUORE-0 analysis

Analysis technique

- Acquisition of triggered signals
- Data preprocessing: estimation of raw parameters
- Pulse filtering
- Thermal Gain Stabilization (TGS)
    - We need to correct the filtered pulse amplitude for small changes in the energy-to-amplitude response of the bolometer:
        - **heater-TGS**: uses as input the mono-energetic heater pulse
        - **calibration-TGS**: uses the 2.6 MeV line from calibration runs, to correct for the electronic parameters that can affect the bolometers response (drift in amplifier gain or DC offset).

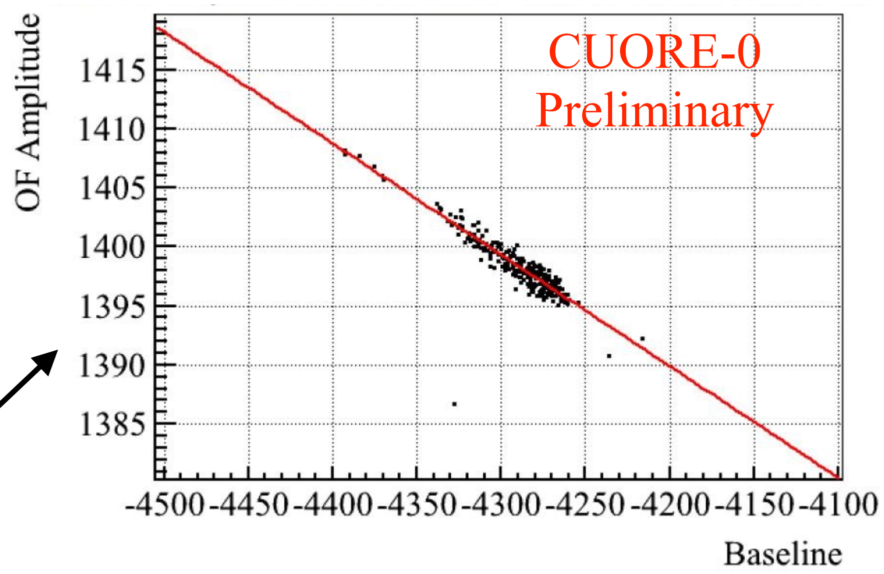

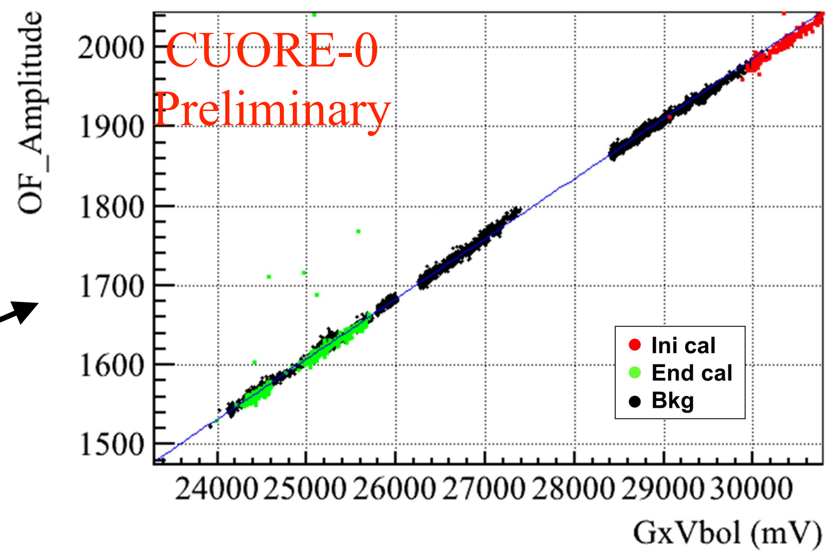

New technique developed for CUORE-0 analysis. We were able to recover the two channels without active heater

Analysis technique

- Acquisition of triggered signals
- Data preprocessing: estimation of raw parameters
- Pulse filtering
- Thermal Gain Stabilization (TGS)
- Energy calibration
  - Each stabilised amplitude is fitted with a gaussian peak and a polynomial function in the region of the peak.
  - We fit a quadratic function with zero intercept to the stabilized pulse amplitude vs know energy to determine the calibration function

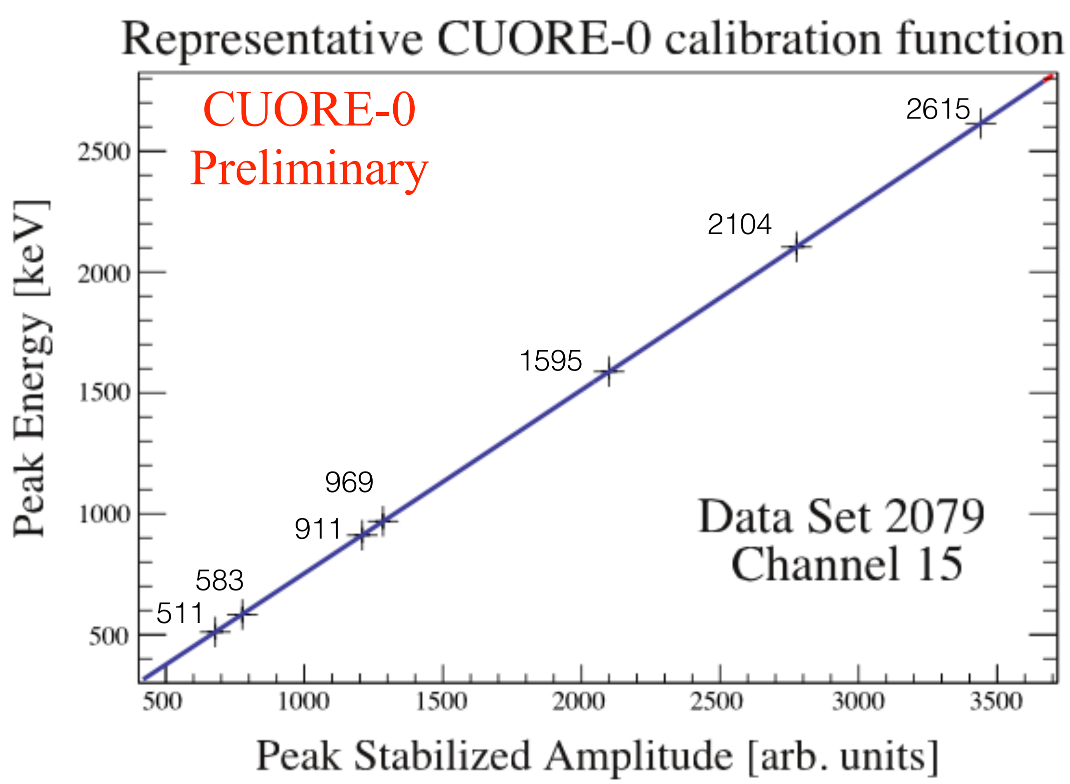

$$E(StabAmpl) = \mathrm{a}\cdot StabAmpl + \mathrm{b}\cdot StabAmpl^2$$

Analysis technique

- Acquisition of triggered signals
- Data preprocessing: estimation of raw parameters
- Pulse filtering
- Thermal Gain Stabilization (TGS)
- Energy calibration
- Particle event selection
  - **Cuts on the Pulse Shape parameters**
  - **Anticoincidence cut**

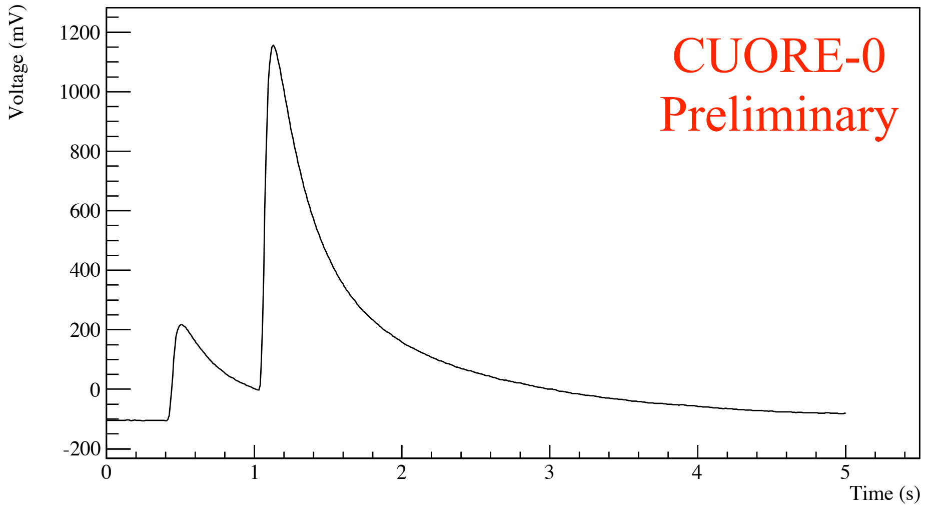

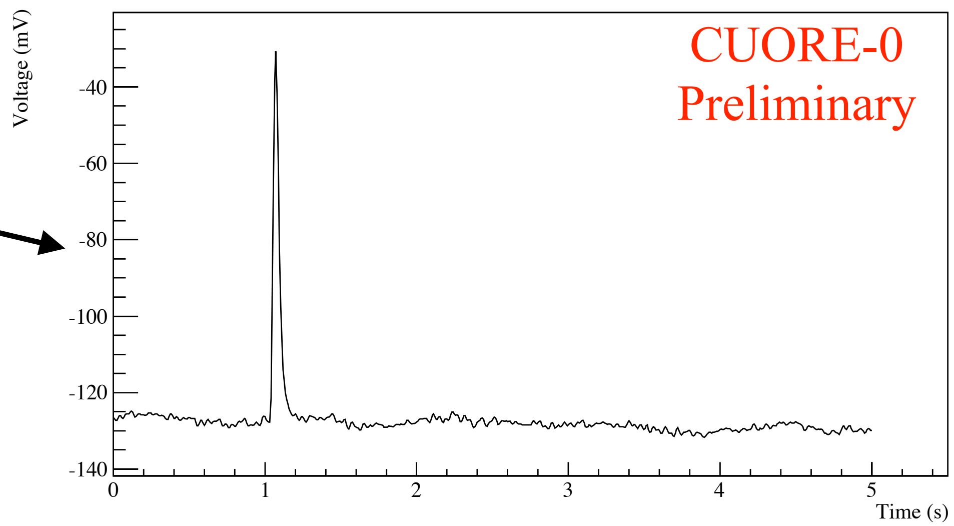

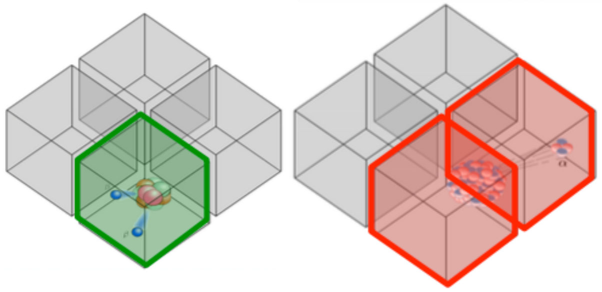

Exclude multi-site events

Analysis technique

- Acquisition of triggered signals
- Data preprocessing: estimation of raw parameters
- Pulse filtering
- Thermal Gain Stabilization (TGS)
- Energy calibration
- Particle event selection
- Energy spectrum

- For each channel and dataset we choose the best performing energy estimator to draw the energy spectrum

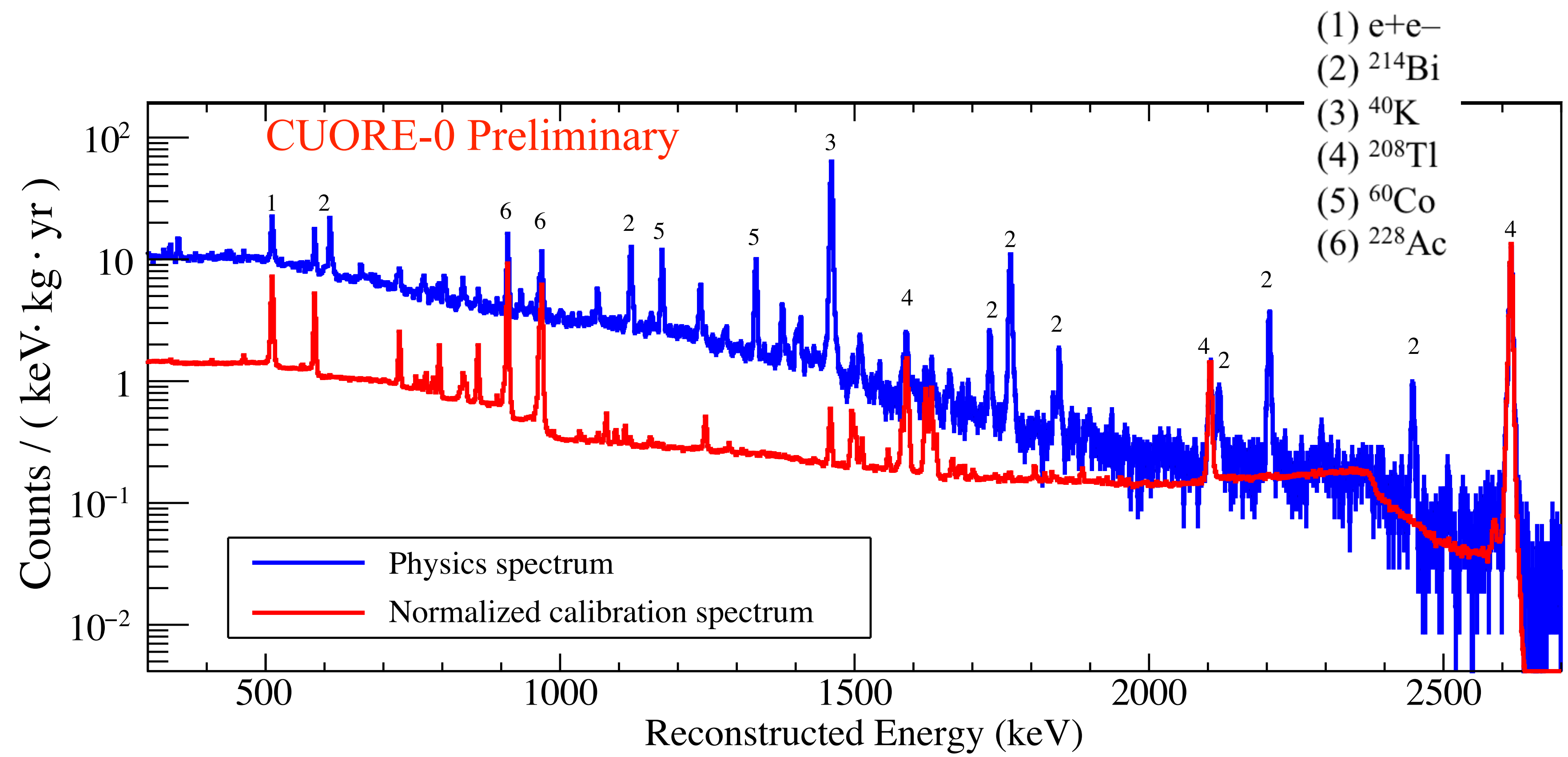

Efficiency of event selection

- Remove events from periods of low-quality data (total exposure reduced of 7%).

CUORE-0 Preliminary	efficiency [%]	error [%]
Trigger	98,529	0,004
Pile-up and PSA	93,7	0,7
Event containment	88,4	0,09
Accidental coincidence	99,64	0,10

- The total selection efficiency is: **(81,3 ± 0,6)%**

Blinded spectrum

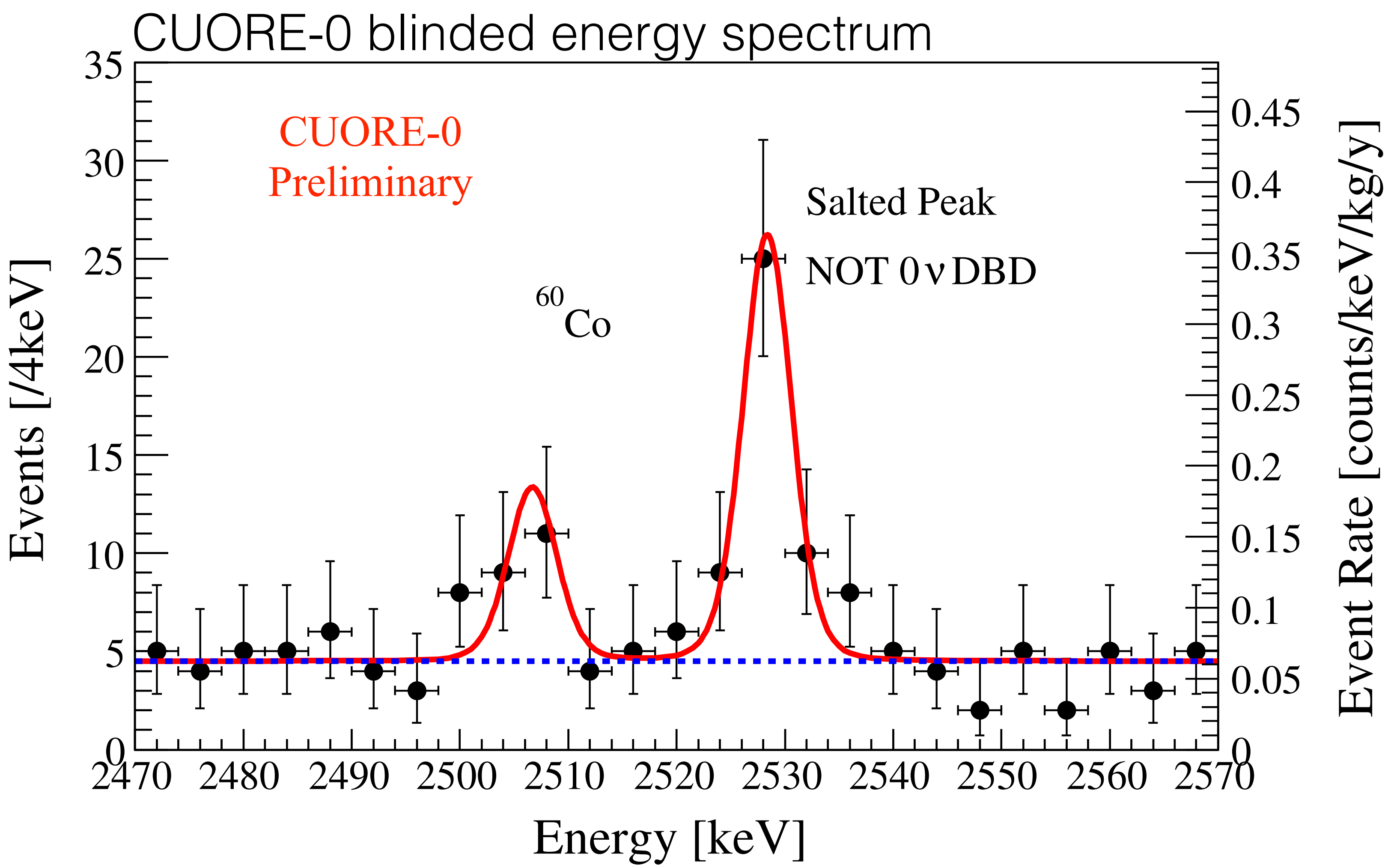

- To blind our data we randomly move a blinded fraction of events within ±10 keV of the 2615 keV γ-ray peak with events within ±10 keV of the 0vDBD Q-value.

- The blinding algorithm produces an artificial peak around the 0vDBD Q-value and blinds the real 0vDBD rate of ^{130}Te.

- This method of blinding the data preserves the integrity of the possible 0vDBD events while maintaining the spectral characteristics with measured energy resolution and introducing no discontinuities in the spectrum.

Before the unblinding

- We studied, discussed and froze the analysis methods prior to un-blinding:
    - Exposure to be collected
    - Energy reconstruction approach
    - Pulse shape cuts
    - Efficiency calculation approach
    - Detector response model
    - Fitting function in the region of interest

Unblinding

- We unblinded our data in of February 2015, once we surpassed the Cuoricino equivalent sensitivity.

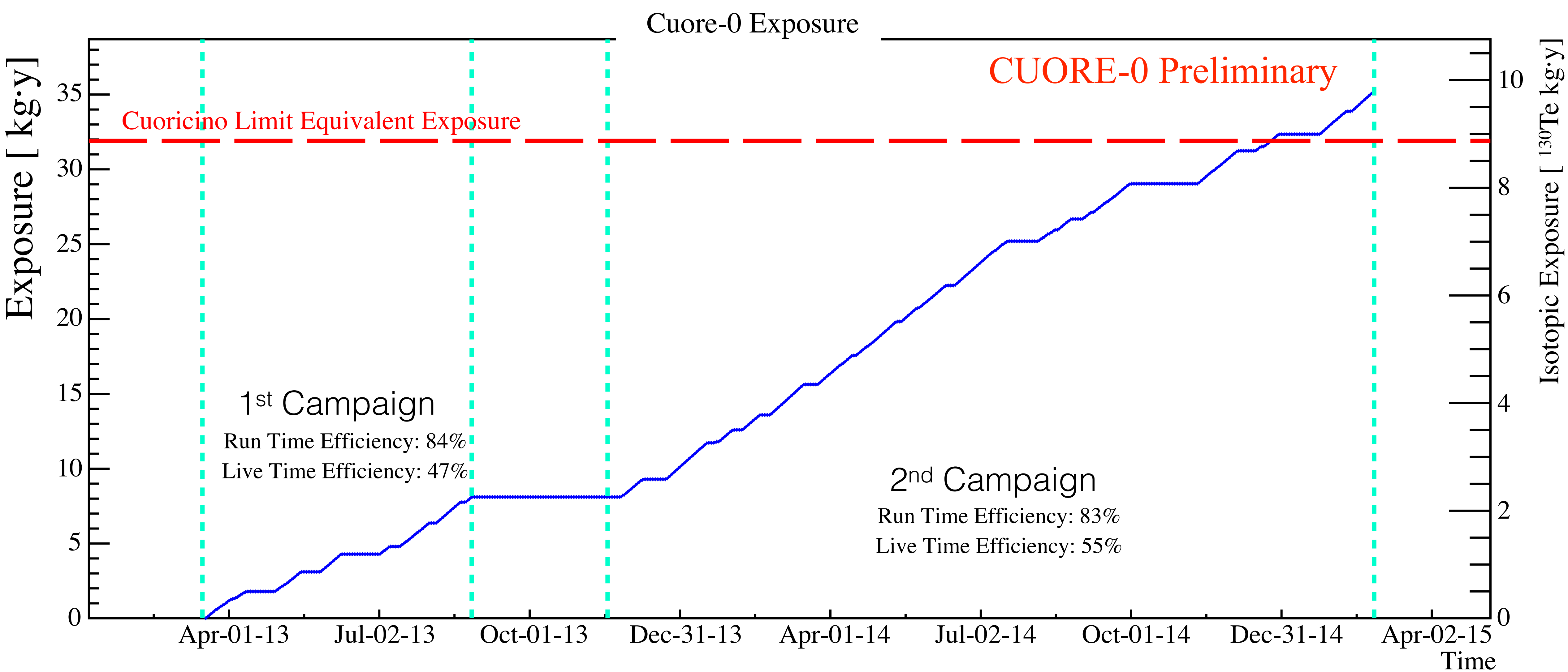

Unblinded spectrum

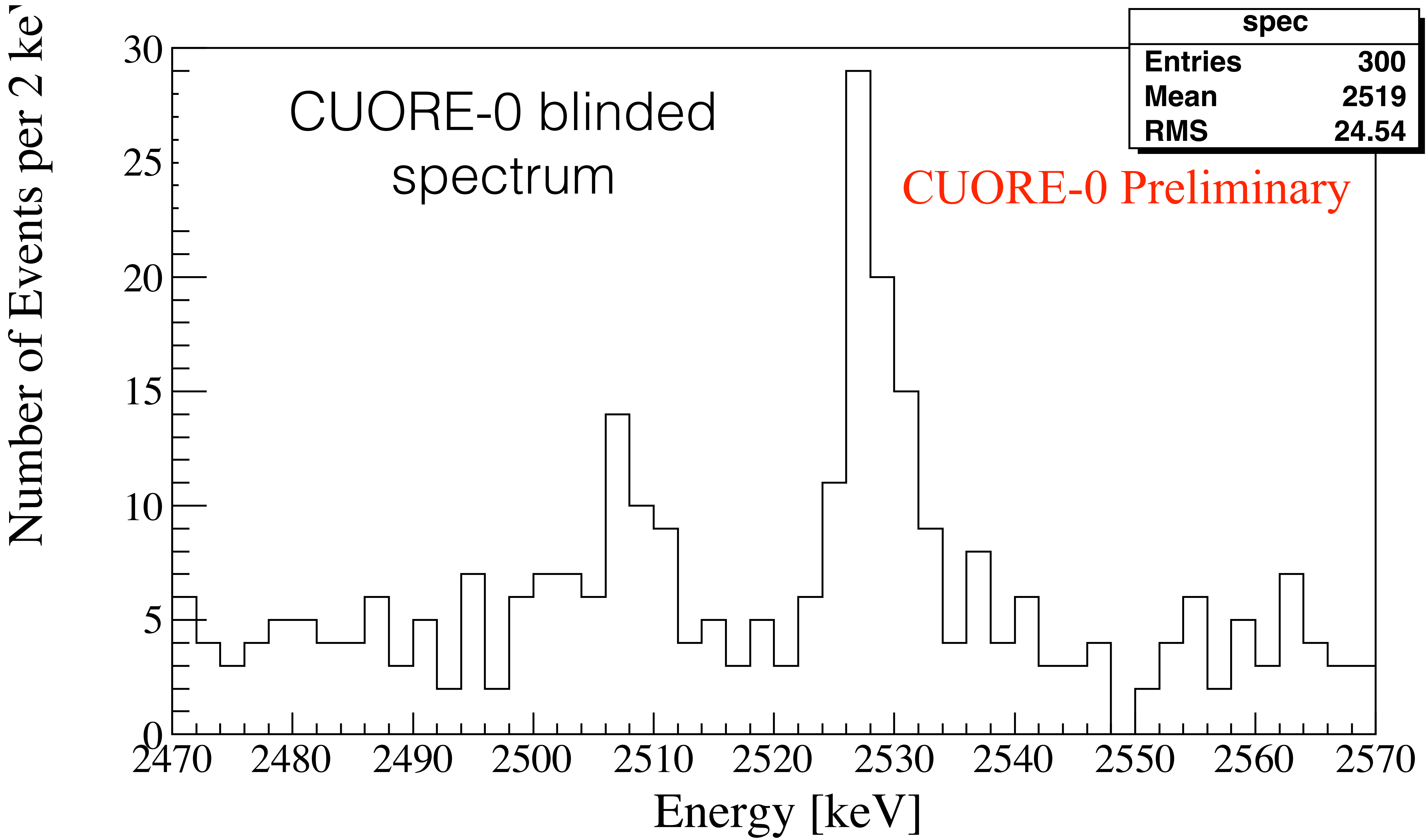

Unblinded spectrum

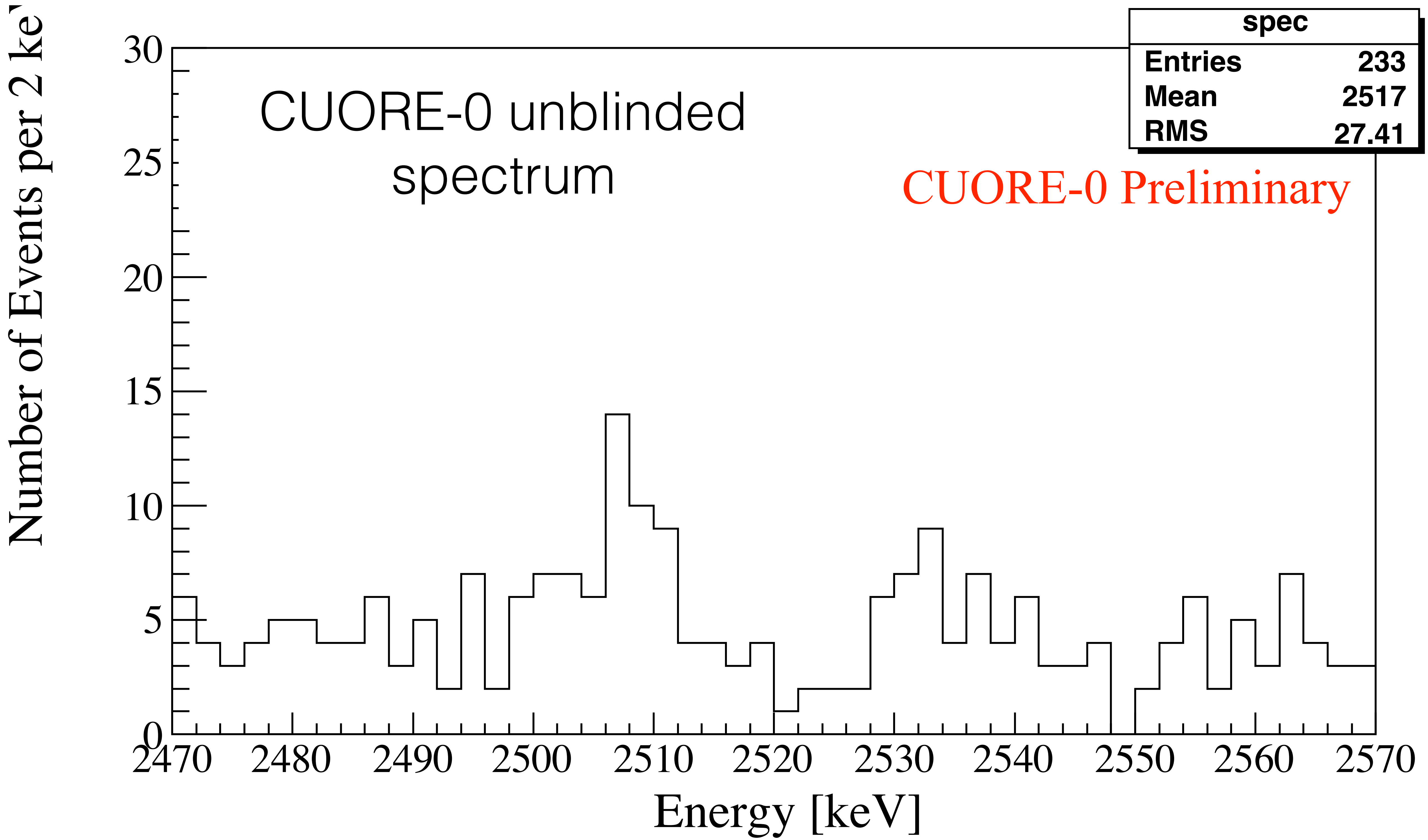

Fit in the ROI

- We determined the yield of 0vDBD events by performing a simultaneous UEML fit in the energy region 2470-2570 keV
- The fit has 3 components:
  - a posited peak at the Q-value of ^{130}Te
  - a peak at 2507 keV, attributed to the double gamma events from ^{60}Co in the nearby copper
  - a smooth continuum background, attributed to multi scatter Compton events from ^{208}Tl and surface alpha events

Fit in the ROI

- The best fit value of the 0vDBD decay rate is

$$\Gamma_{0\nu} = 0.01 \pm 0.12\,(\mathrm{stat.}) \pm 0.01\,(\mathrm{syst.}) \times 10^{-24}\mathrm{yr}^{-1}$$

- The background index in the ROI is:

$$0.058 \pm 0.004\,(\mathrm{stat.}) \pm 0.002\,(\mathrm{syst.})\ \mathrm{c/keV/kg/yr}$$

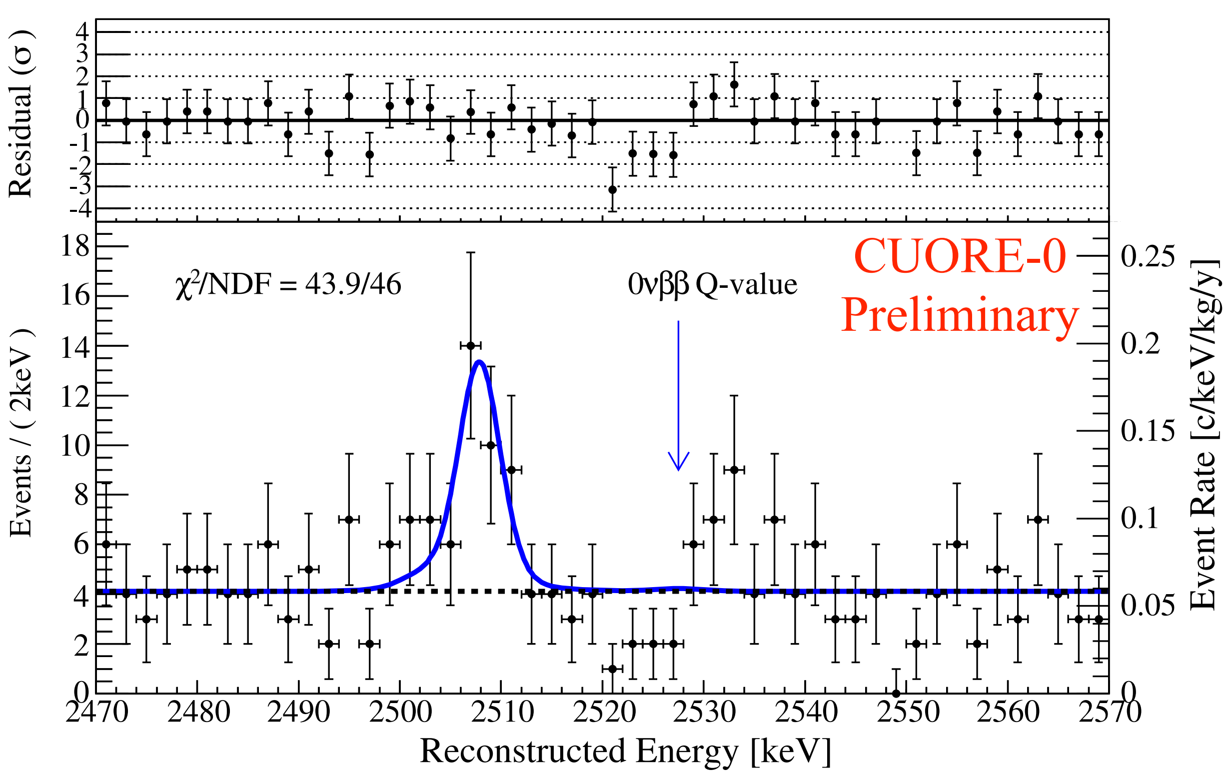

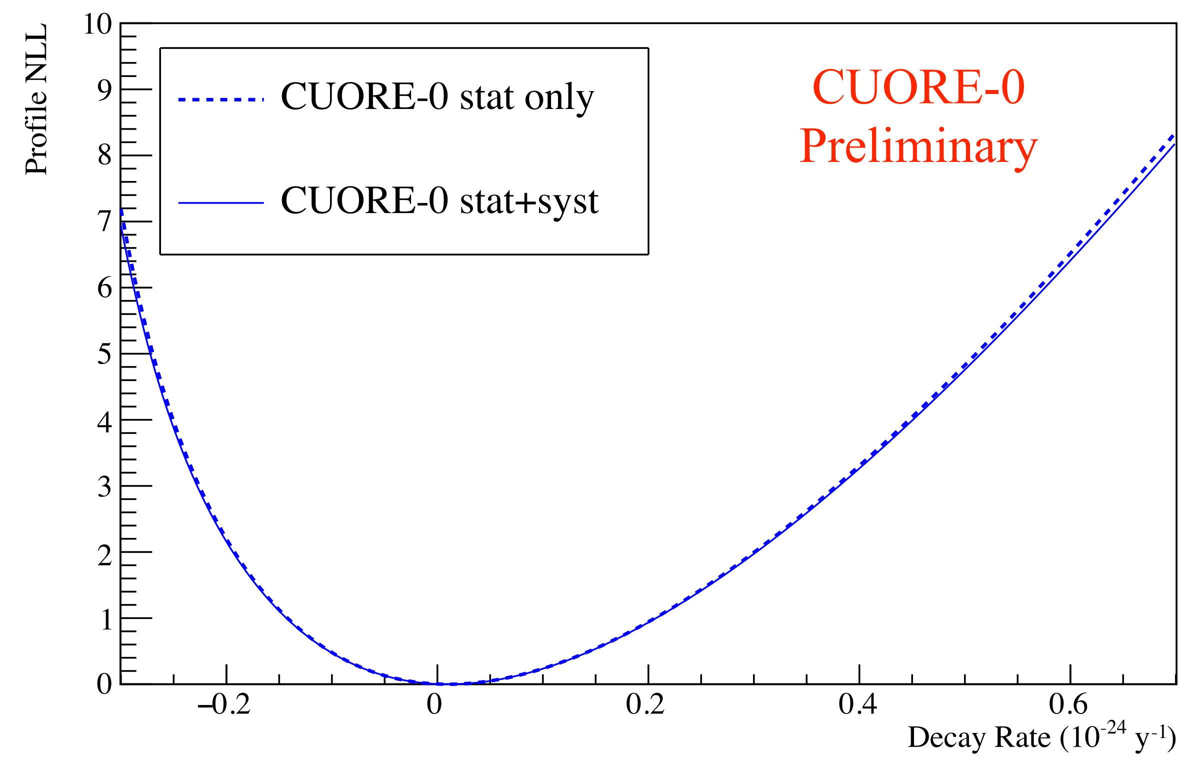

- We set a 90% C.L. Bayesian lower limit of: $\mathbf{T_{1/2} > 2.7 \times 10^{24}}$ **yr**.

Statistical fluctuations

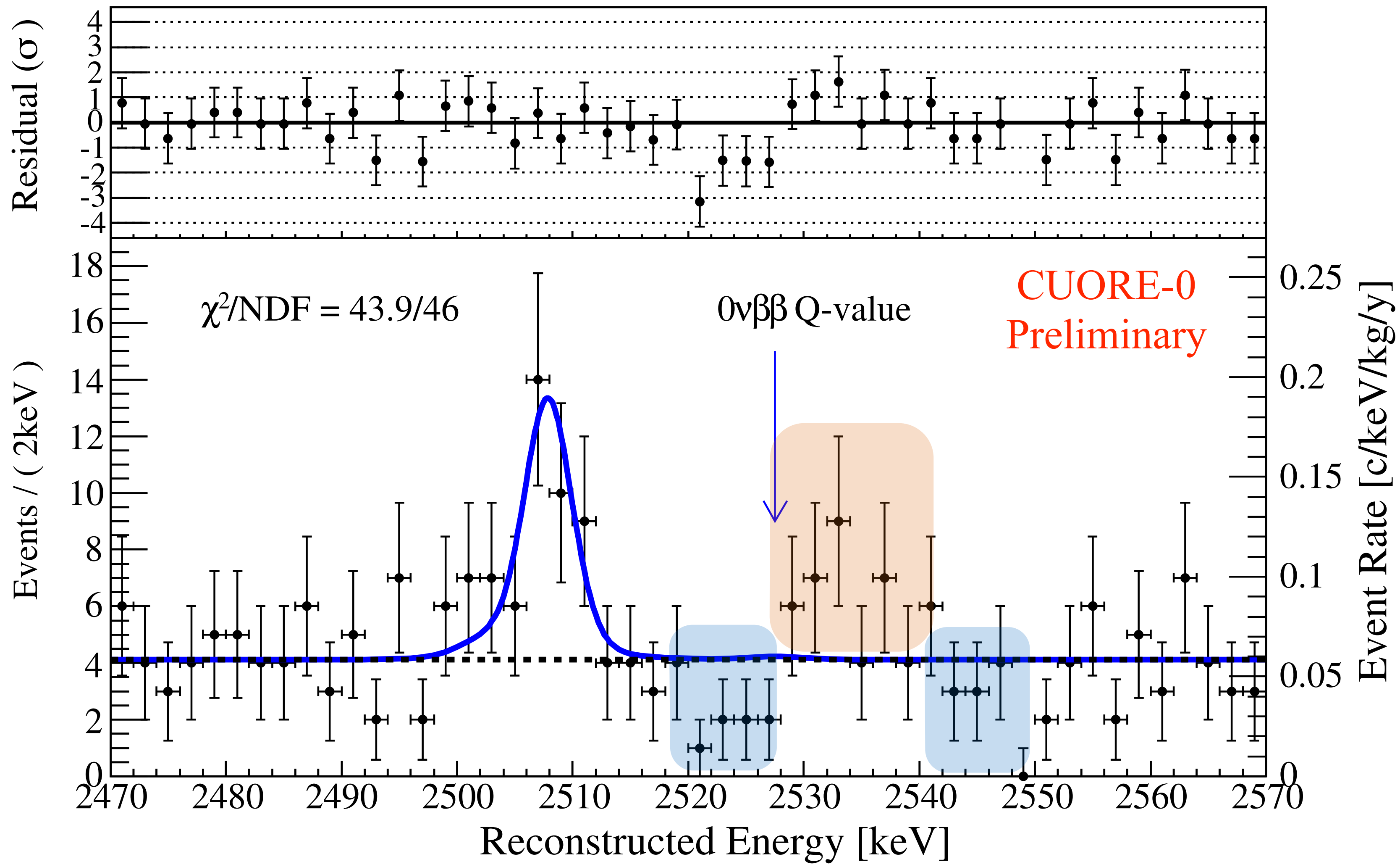

- We evaluated the statistical properties of the data (event excess above $Q\beta\beta$, dips below and above $Q\beta\beta$).

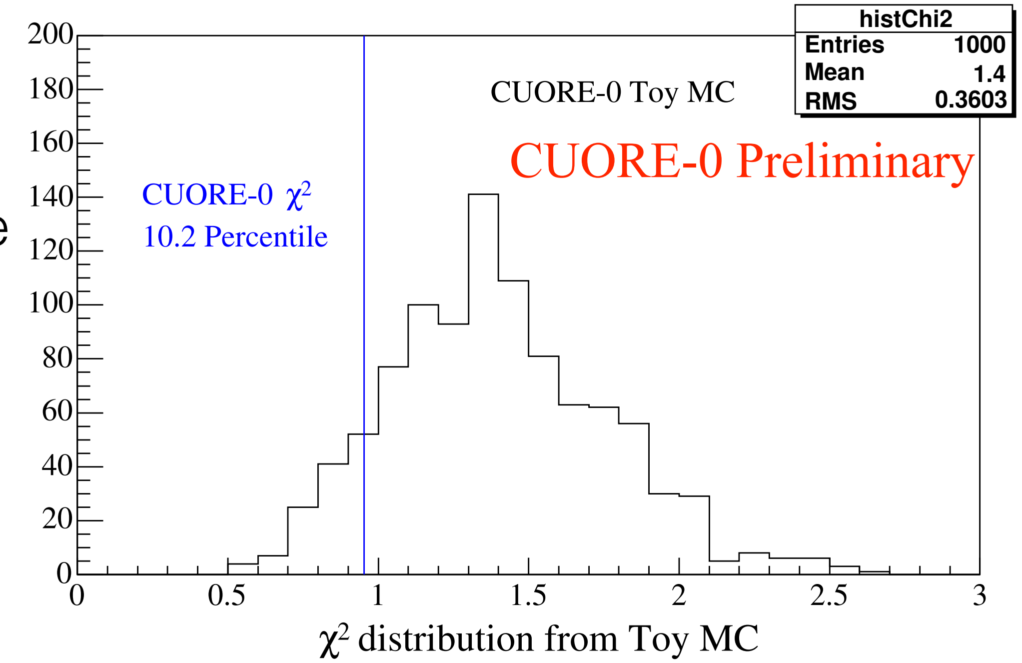

- A Kolmogorov-Smirnov test shows the data is consistent with the null hypothesis (i.e., the best-fit model but with $\Gamma_{0\nu}$ fixed to zero).
- We compared the value of the binned χ^2 with the distribution from a large set of Toy MC. The 90% of such experiments return a value of $\chi^2 > 43.9$.

Systematics errors

- For each systematic, we run toy MC experiments to evaluate bias on fitted 0vDBD decay rate. We parametrize the bias as p0 (additive) +p1· $\Gamma_{0\nu}$ (scaling)
- **Signal Lineshape**: used variety of different line shapes to model signal.
- **Energy resolution and scale**: we varied the resolution up to 10% of calibration-derived values and we propagated the uncertainties at the Q-value energy.
- **Fit bias:** We evaluated the bias on fitted 0vDBD decay rate as a function of a simulated rate.
- **Bkg function**: we treated the choice of 0-, 1-, or 2-order polynomial for the continuum background as a discrete nuisance parameter.

	Additive (10^{-24} y^{-1})	Scaling (%)
Lineshape	0.007	1.3
Energy resolution	0.006	2.3
Fit bias	0.006	0.15
Energy scale	0.005	0.4
Bkg function	0.004	0.8
Signal normalization	0.7%	

Cuoricino combination

- We combine the CUORE-0 result with the existing 19.75 kg · yr of ^{130}Te exposure from Cuoricino
- The combined 90% C.L. limit is **$T_{0\nu} > 4.0 \times 10^{24}$ yr**.

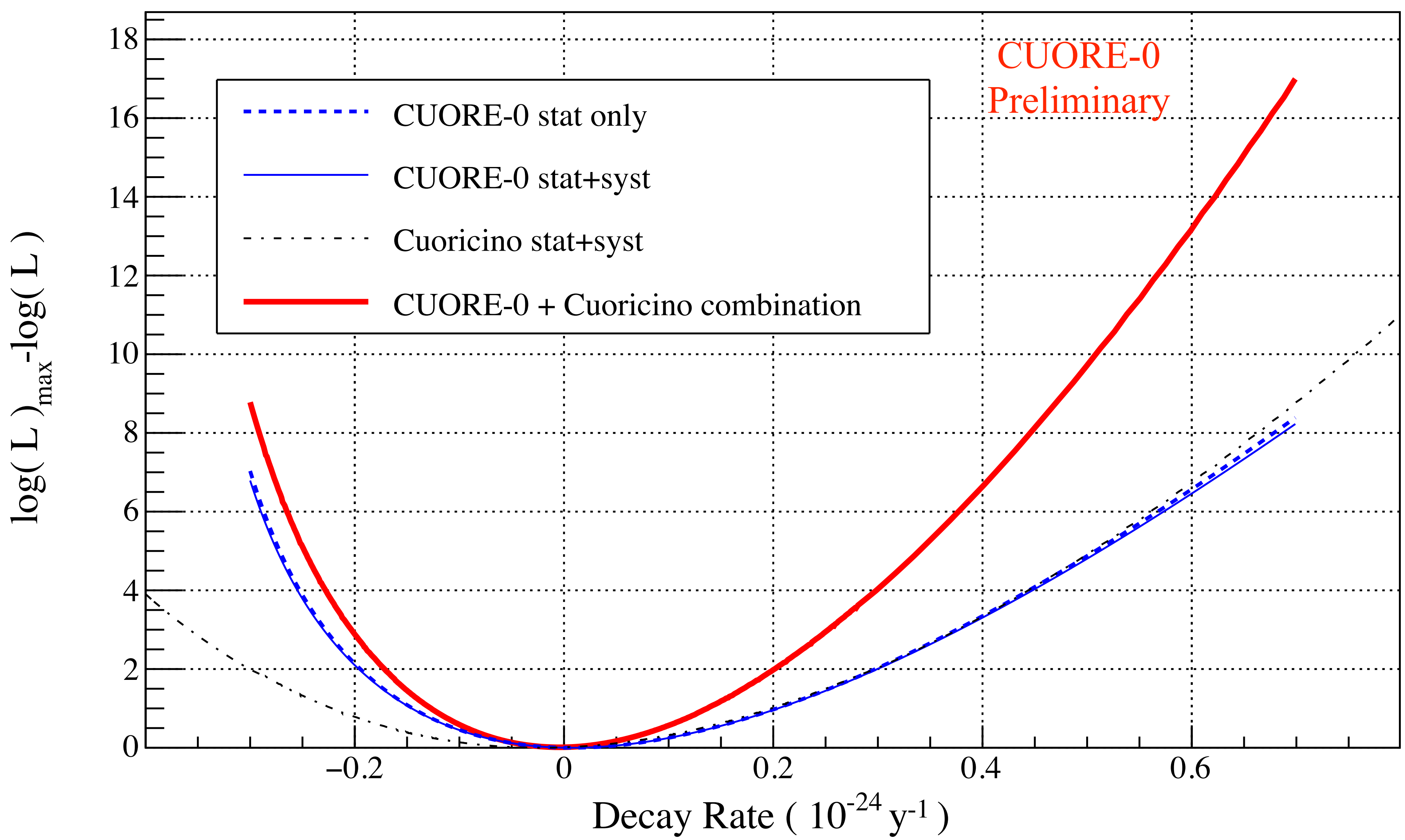

Limit on mbb

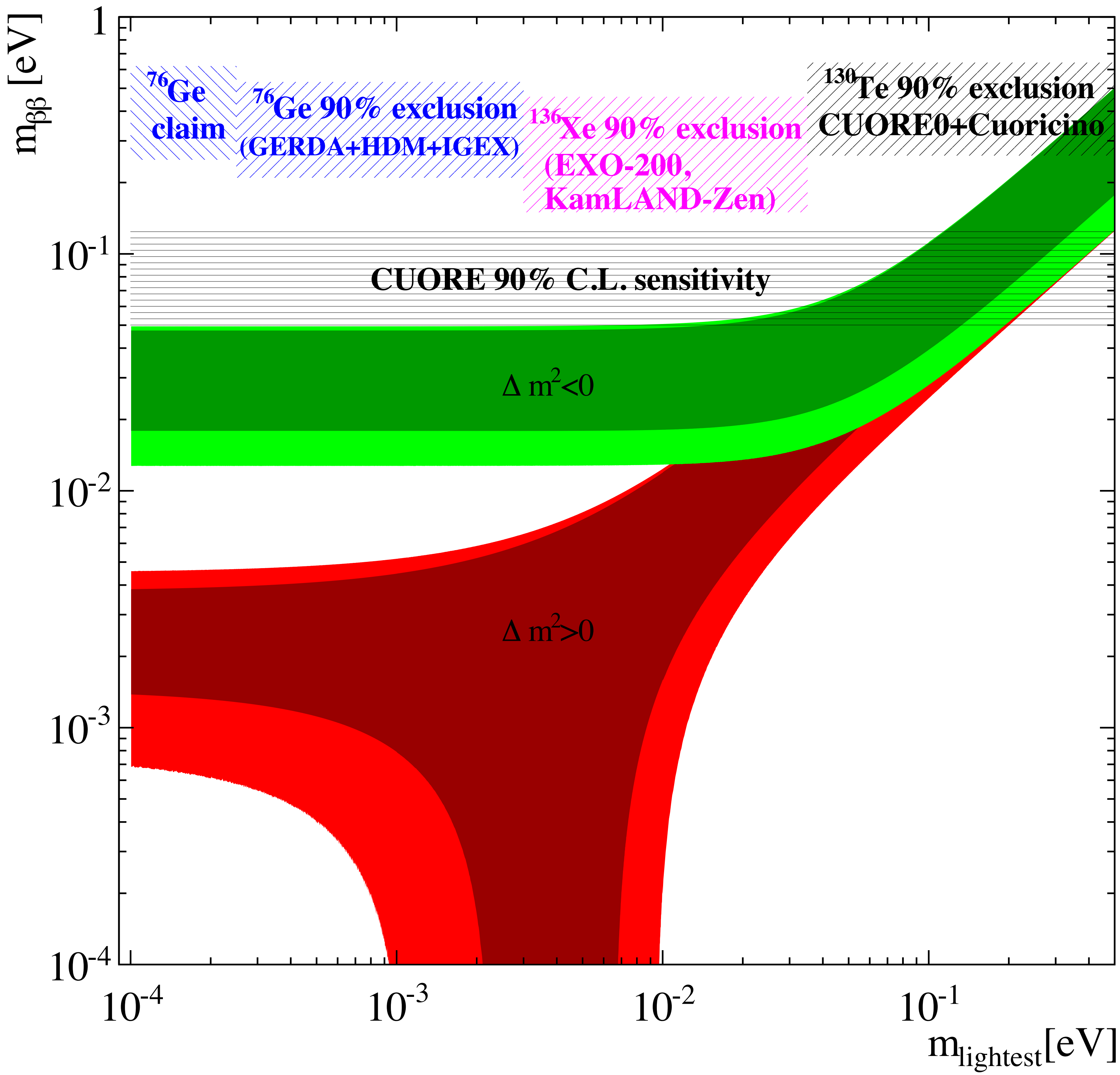

We interpret our combined Bayesian half-life result as a limit on the effective Majorana neutrino mass:

$m_{\beta\beta} < (270\text{-}650)$ meV

IBM-2 Phys. Rev. C 91, 034304 (2015)
QRPA-TU Phys. Rev. C 87, 045501 (2013)
pnQRPA Phys. Rev. C 91, 024613 (2015)
ISM Nucl. Phys. A 818, 139 (2009)
EDF Phys. Rev. Lett. 105, 252503 (2010)

Conclusions

- TeO2 bolometers offer a well-established, competitive technique in the search for 0vDBD decay
- CUORE-0
    - Achieved its energy resolution and background level objectives, surpassing the Cuoricino sensitivity in ~ half the time.
    - Did not find evidence of 0vDBD decay.
    - Indicated CUORE sensitivity goal is within reach.
    - We are going to post the paper to arXiv and to submit it to PRL. We have two more papers in preparation (detector and background).
- CUORE:
    - Assembly of the 19 CUORE towers is complete.
    - Commissioning of the cryogenic system and experimental infrastructure is in progress
    - Plan to start operations by end of 2015.

CUORE background budget

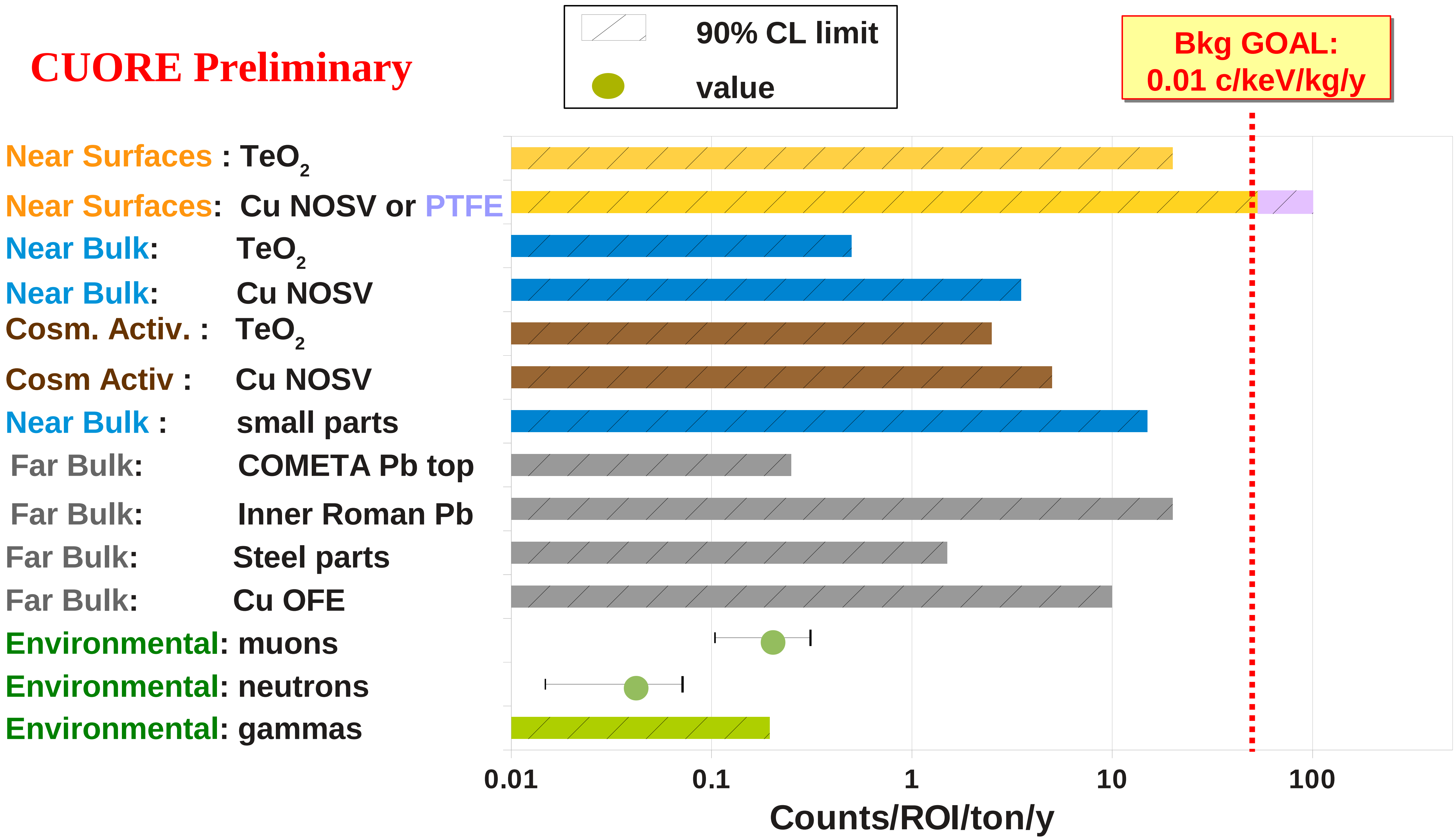

Energy spectra

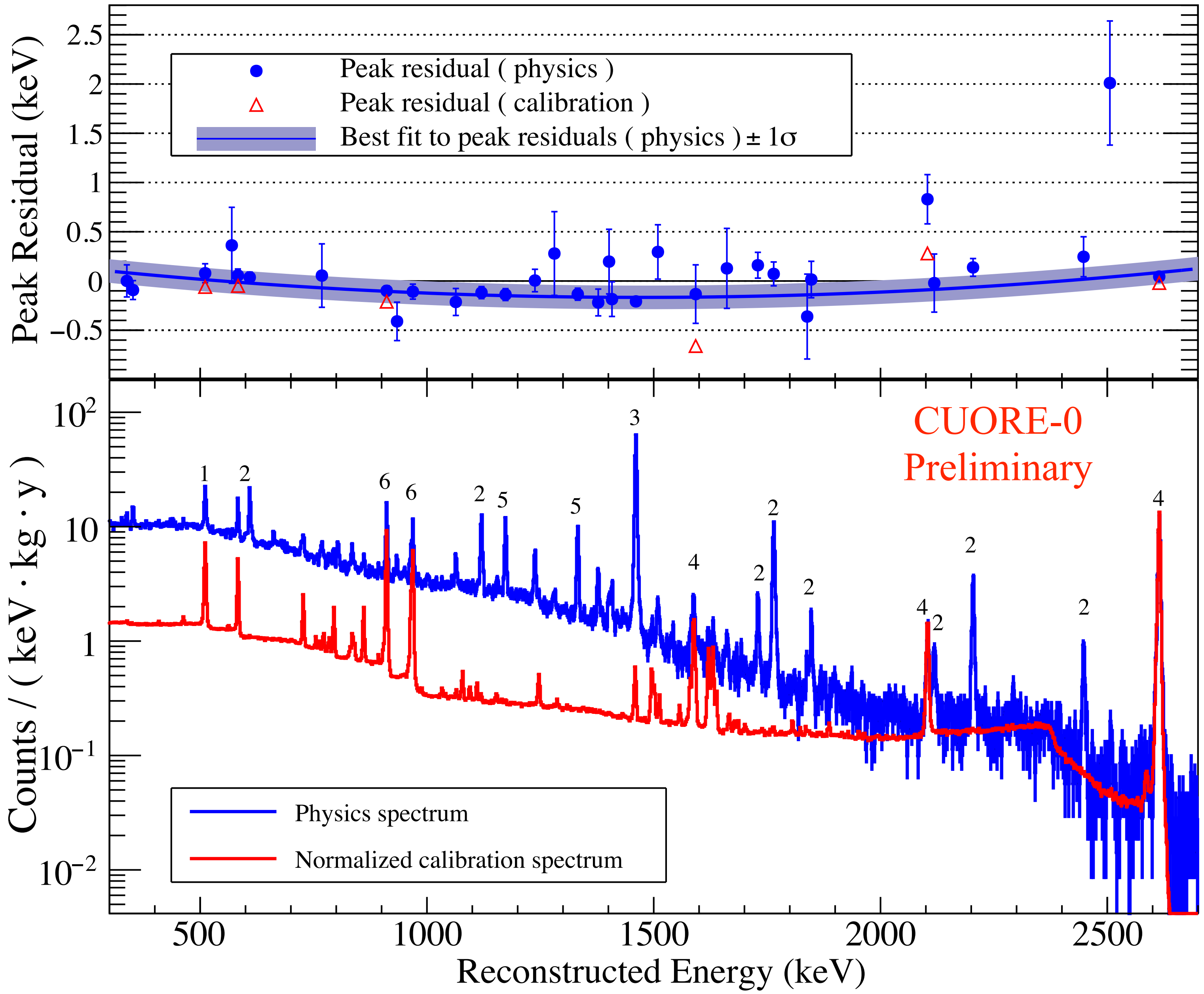

- Two outliers are:
  - ^{60}Co, which reconstruct at 2507±0.6 keV, 2.0±0.6 keV higher than the nominal value
  - ^{208}Tl single-escape line, which reconstruct 0.84±0.22 wrt the nominal value at 2103.51 keV.

- **We determined a global calibration offset function, by performing a parabolic fit to the peak residual (excluding the two outliers).**
- **We take the standard deviation of the fit residuals (0.12 keV) as a global systematic uncertainty on the reconstructed energy.**

2615 keV double escape reconstruction

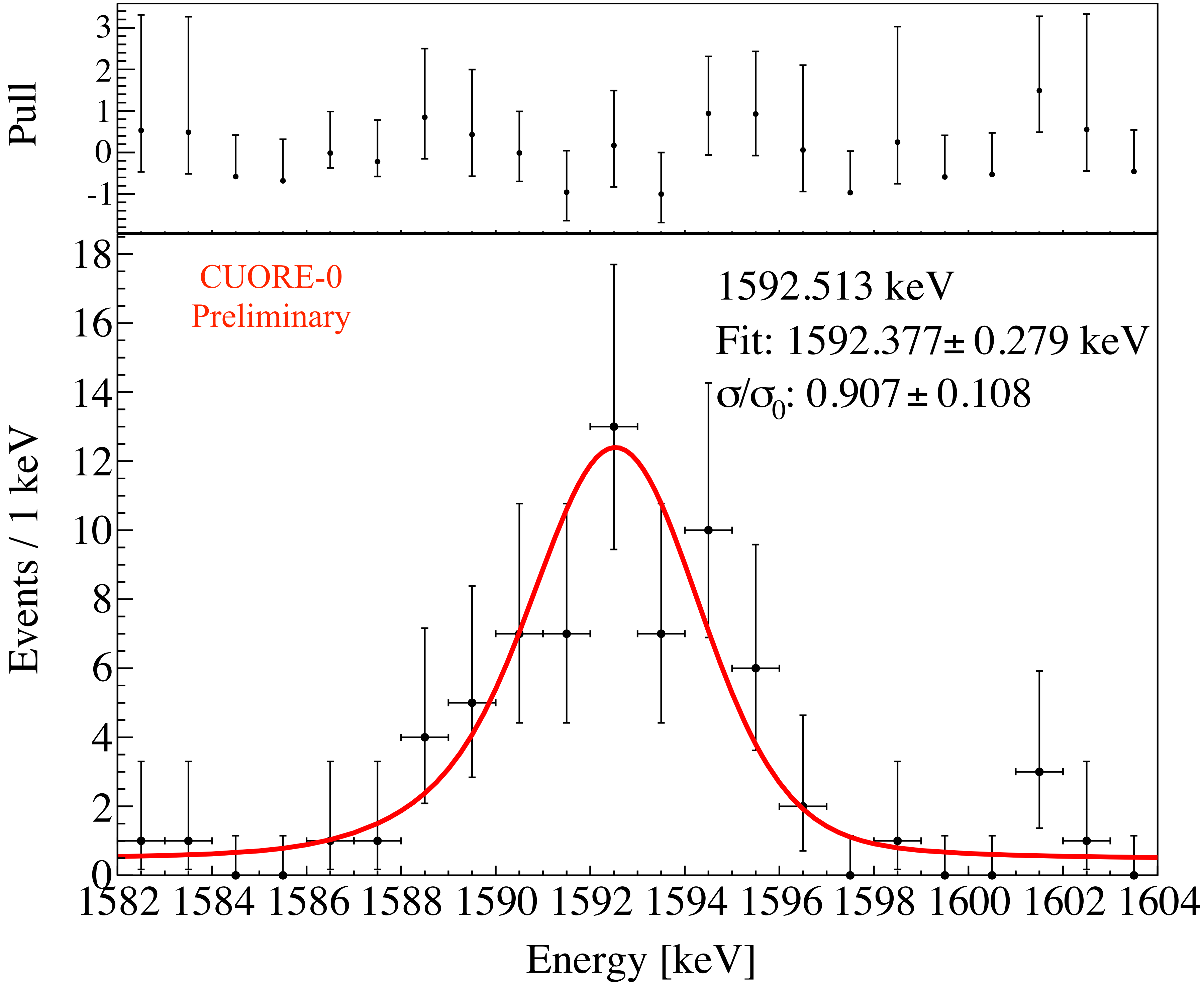

Cobalt calibration

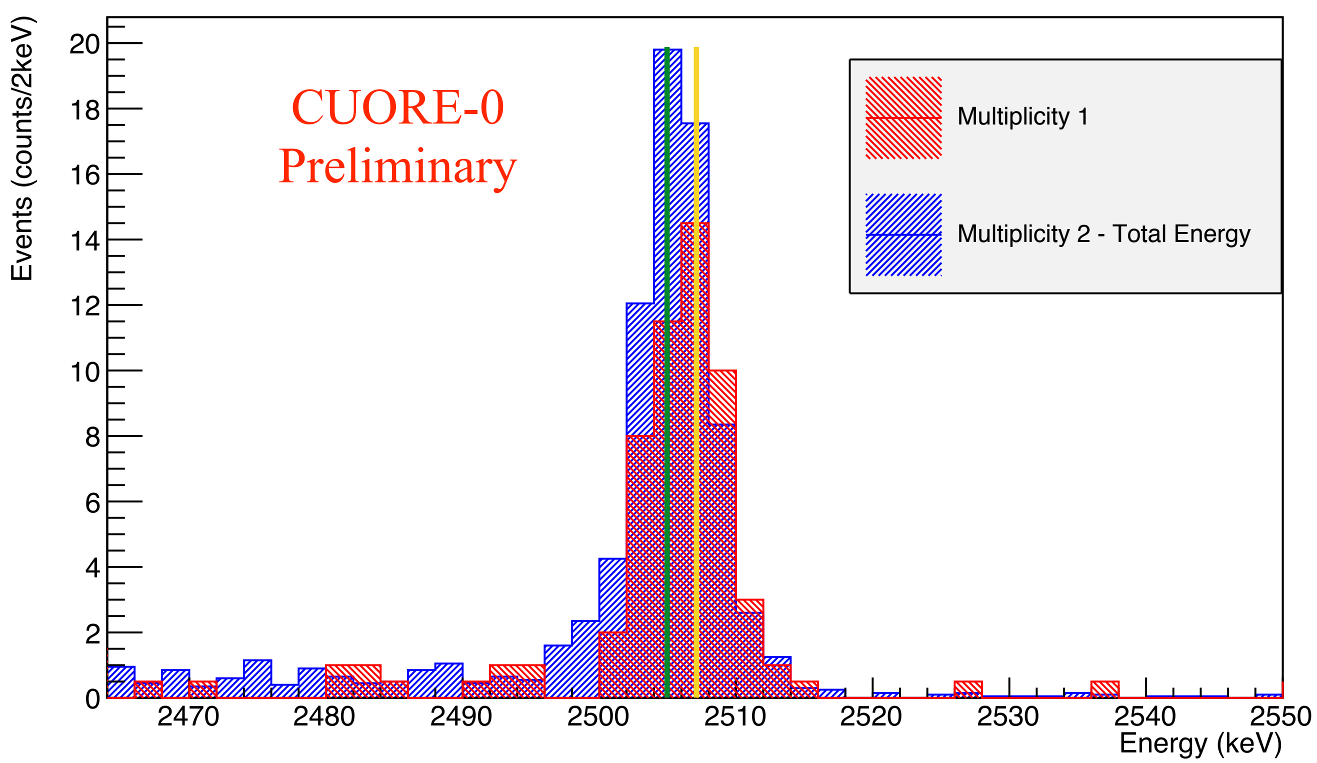

^{60}Co double-gamma events reconstructs at **2507.6 ± 0.7** keV, 1.9 ± 0.7 keV higher than the established value at **2505.6** keV

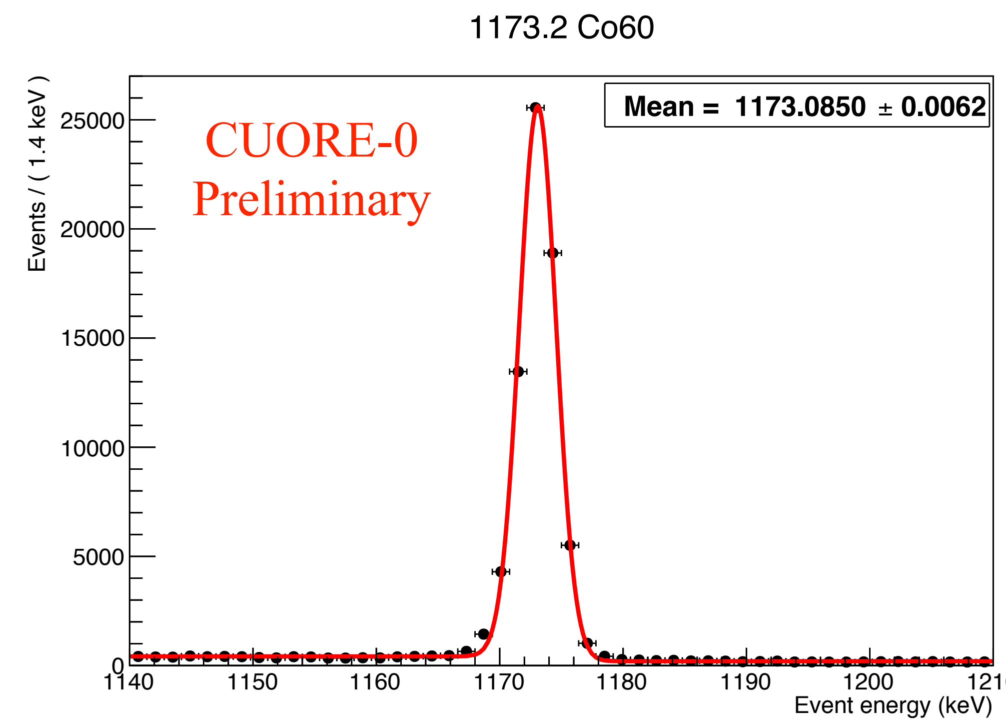

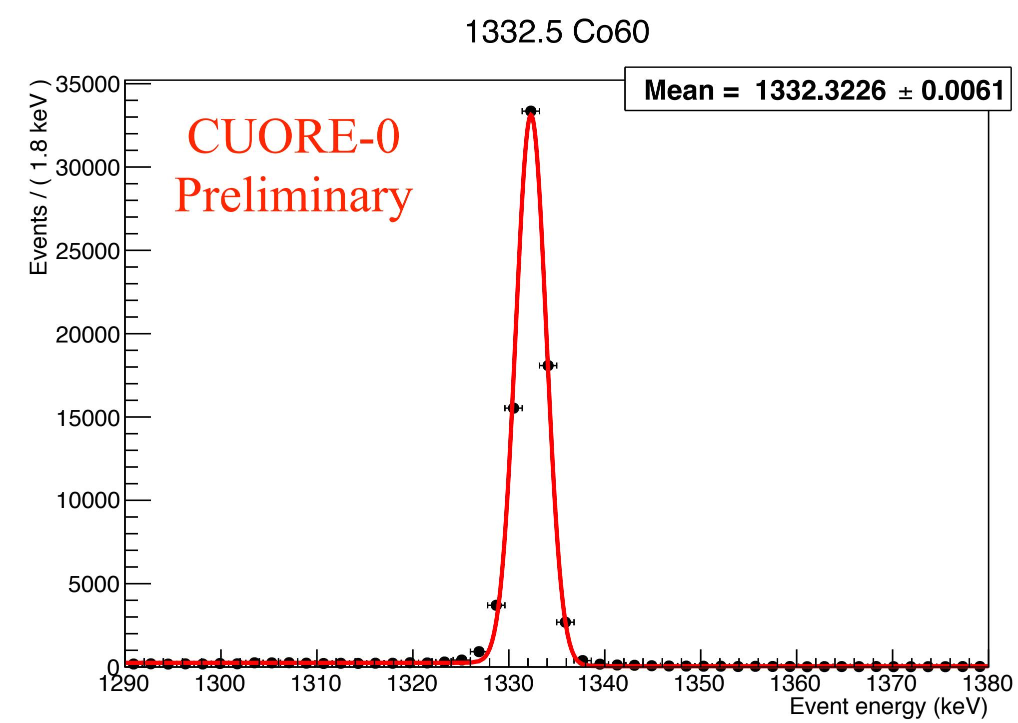

Signal lineshapes

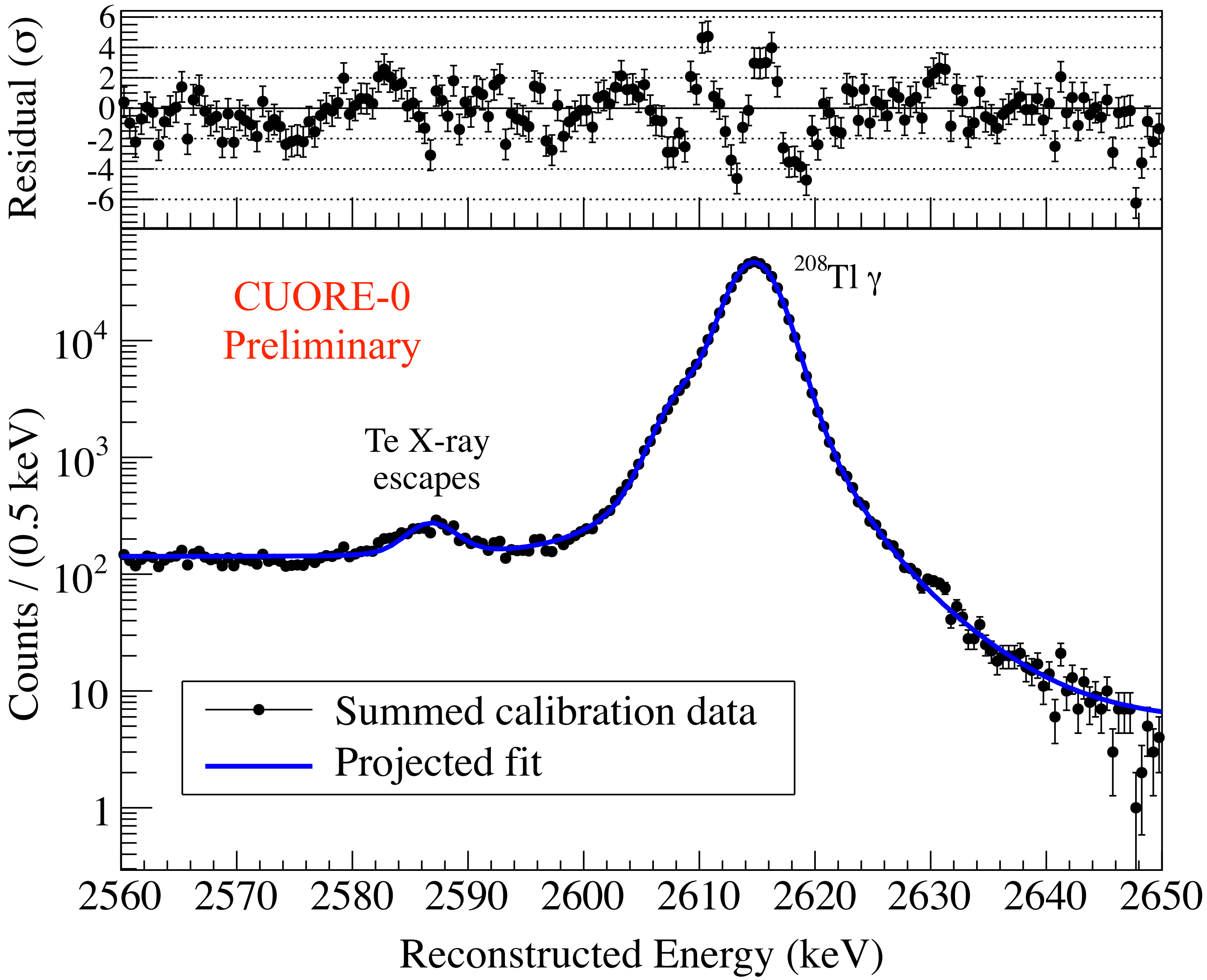

$$
\begin{aligned}
f_{\mathrm{Cal}}(E) = {} & n_0 \frac{1}{\sqrt{2\pi}\sigma} e^{-\frac{(E-E_0)^2}{2\sigma^2}} \\
& + n_1 \frac{1}{\sqrt{2\pi}\sigma} e^{-\frac{(E-E_1)^2}{2\sigma^2}} \\
& + n_2 \frac{1}{\sqrt{2\pi}\sigma} e^{-\frac{(E-E_2)^2}{2\sigma^2}} \\
& + n_3 \frac{1}{2} \mathrm{erfc}\left[\frac{E-E_0}{\sqrt{2}\sigma}\right] \\
& + n_4 \, .
\end{aligned}
$$

Bkg resolution scaling

- Background resolution as a function of energy
- Uncertainty shown in the plot is only from the fit.